Allosteric activation of periplasmic HtrA proteases

by

Anna Katherine de Regt

B.S., Engineering
Swarthmore College, 2009

Submitted to the Microbiology Graduate Program
in partial fulfillment of the requirements for the degree of

DOCTOR OF PHILOSOPHY

at the

MASSACHUSETTS INSTITUTE OF TECHNOLOGY

February 2015

Signature of Author _____
Anna K. de Regt
Microbiology Graduate Program
September 30, 2014

Certified by _____
Robert T. Sauer
Salvador E. Luria Professor of Biology
Thesis Supervisor

Accepted by _____
Michael T. Laub
Professor of Biology
Director, Microbiology Graduate Program

Allosteric activation of periplasmic HtrA proteases

by
Anna Katherine de Regt

Submitted to the Microbiology Graduate Program on September 26, 2014
in partial fulfillment of the requirements for the degree of Doctor of Philosophy

Abstract

Escherichia coli responds to outer-membrane stress using a signaling cascade initiated when DegS, an HtrA-family periplasmic protease, cleaves RseA, a transmembrane anti-sigma factor, causing downstream release of the σ^E sigma factor and transcription of stress-response genes. Each subunit of the DegS trimer contains a trypsin-like protease domain and a PDZ domain. In the absence of stress, autoinhibitory interactions stabilize an inactive conformation of DegS. Allosteric activation occurs as a consequence of the linked binding of unassembled outer-membrane proteins to the PDZ domains and RseA to the DegS active sites.

In Chapter 2, I probe the pathway of communication between the PDZ and protease domains and identify a set of residues crucial for signal propagation across the enzyme. This set of residues is conserved across the HtrA protease family, including orthologs linked to human disease, and thus a common mechanism of allosteric activation appears to function in all family members.

No satisfactory mechanism explains how OMP-peptide binding breaks autoinhibitory interactions. In Chapter 3, I present evidence that peptide binding initiates a steric clash between the side chains of a PDZ residue and an L3-loop residue that forces rearrangement of the loop and simultaneously breaks autoinhibitory interactions.

In *Pseudomonas aeruginosa*, a homologous signaling cascade controls the release of the transcription factor AlgU, which directs the production of alginate, an exopolysaccharide that protects the bacterium from antibiotics and the host immune system. The HtrA protease AlgW is activated by misfolded OMPs to cleave its transmembrane substrate MucA. In Chapter 4, I describe a collaboration that identifies the protein CupB5 as a novel regulator of this pathway. Peptides corresponding to a region of CupB5 needed for mucoidy activate AlgW in conjunction with OMPs to stimulate cleavage of MucA *in vitro*.

Finally, in Chapter 5, I summarize my findings on DegS and describe aspects of DegS activation that are yet to be resolved.

Thesis supervisor: Robert T. Sauer
Title: Salvador E. Luria Professor of Biology

Acknowledgements

Many people have supported me and helped me along in my graduate school adventure. First, I would like to thank my advisor, Bob Sauer, for his mentorship, his excitement about science and teaching, his open-door policy, and for striking the right balance between attention to detail and maintaining an appropriately messy bench and lab notebook. Thanks also to my co-advisor, Tania Baker, and my committee members, Leona Samson and Amy Keating, for always being there for me with advice on experiments, careers, or purple clothing - whatever I needed.

Thank you to my labmates both past and present, and especially my baymates, Steve and Ben, for making this such a fun, productive and unique place to do science. And thank you to my postdocs, J, Randall, Steve and Santiago, for teaching me so much and then leaving me, forcing me to grow up as a scientist.

A special thanks goes to my undergradute advisor, Stephen Miller, who taught me that there is nothing cooler in the world than protein mechanism and set me on the biochemical path.

My time in graduate school was profoundly enriched by my friends, particularly from sMITe, MIT's ultimate frisbee team, and MITOC, the outing club. They have kept me laughing, kept me challenged, kept me focused, and kept me out of lab. We have shared countless adventures that I will never forget.

And last but most importantly, unending thanks to my family, for their unconditional love and support. It has been incredible.

Table of Contents

Table of Figures and Tables

Chapter 1

Introduction:

The role of HtrA proteases in the outer-membrane stress response

Cellular proteolysis

The proteome of a cell is in constant flux, as proteins are continuously synthesized, modified, and degraded. Some regulatory proteins must have their numbers tightly controlled so that pathway flux and cellular homeostasis are properly maintained. Other regulatory proteins are degraded in response to stress signals, allowing changes in transcription or translation. Protein degradation allows amino acids to be recycled from unnecessary or damaged proteins and used to synthesize new proteins, helping cells adapt to quickly changing environmental and/or developmental challenges. Finally, misfolded or unfolded proteins often need to be degraded before they aggregate and cause cell dysfunction or disease. Cellular quality control systems must ensure that misfolded or damaged proteins are degraded efficiently without rogue degradation of incorrect substrates. In times of stress, quality control proteases must be precisely activated to ensure a timely stress response, but also must be tightly regulated such that the response ceases upon the removal of stress.

HtrAs

HtrA proteases represent a large family, with members in all domains of life. Each HtrA protease consists of an N-terminal localization domain that targets the enzyme to a cellular compartment, to a membrane, or to be secreted; a trypsin-like serine protease domain; and one or more C-terminal PDZ domains (Fig. 1.1). In some cases, additional functional domains are also present (Clausen *et al.*, 2002). PDZ domains are an abundant class of small globular domains found in a wide variety of multidomain proteins, in which they usually play a regulatory role (Wang *et al.*, 2010). The human genome appears to contain over 150 PDZ-containing proteins, with more than 250 non-redundant PDZ domains (Wang *et al.*, 2010). PDZ domains generally bind C-terminal

peptide sequences, although some can bind internal sequences as well (Stiffler *et al.*, 2007; Tonikian *et al.*, 2008). The basic unit of HtrA function is a trimer, some of which further assemble into higher-order oligomers as a regulatory mechanism (Li *et al.*, 2002; Walsh *et al.*, 2004; Krojer *et al.*, 2008; Kim *et al.*, 2011; Truebestein *et al.*, 2011).

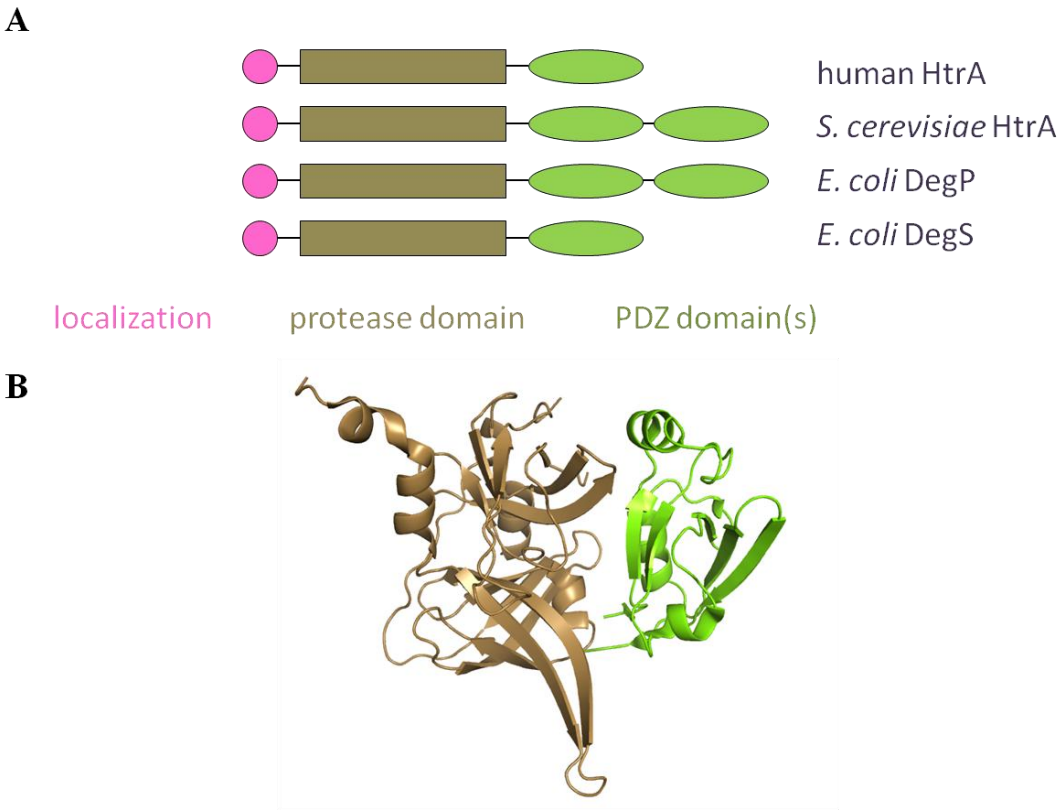

Fig. 1.1. The HtrA family of proteases. (A) Each HtrA subunit contains an N-terminal localization domain, a trypsin-like protease domain, and one or two C-terminal PDZ domains. (B) The structure of one subunit of human HtrA2 (PDB ID: 1LCY).

HtrA stands for high-temperature requirement A, which reflects the knockout phenotype of the first family member identified, an *Escherichia coli* protein that is often called DegP (Lipinska *et al.*, 1989). Subsequently, HtrA proteases have been identified in many single- and multi-cellular organisms, where they have roles in cell migration, cell-cycle regulation, bacterial virulence, and

protein quality control (Ades *et al.*, 1999; Huesgen *et al.*, 2009; Mahomedmohaideen *et al.*, 2008; Chien *et al.*, 2009; Patel *et al.*, 2014; Bakker *et al.*, 2014). Humans have four HtrA proteins, HtrA1-4. HtrA1 is a secreted enzyme, which cleaves fibronectin and activates matrix metalloproteases and has been implicated roles in a wide range of diseases, including gingivitis, osteoarthritis, Alzheimer's disease, and preeclampsia (Grau *et al.*, 2005; Grau *et al.*, 2006; Hara *et al.*, 2009; Lorenzi *et al.*, 2009; Lorenzi *et al.*, 2014). HtrA2, a mitochondrial protein, is the best-studied human HtrA. It was originally thought that its most important role is pro-apoptotic, as HtrA2 is released into the cytoplasm during stress, where it is processed into its active form and cleaves anti-apoptotic proteins (Suzuki *et al.*, 2001; Cilenti *et al.*, 2004). More recently, however, the focus has shifted to a role in cellular quality control, as HtrA2 can cleave the β-amyloid precursor protein (Gray *et al.*, 2000; Huttenen *et al.*, 2007; Park *et al.*, 2006; Li *et al.*, 2010). HtrA2 knockout mice have a neurodegenerative parkinsonian phenotype, and some Parkinson's Disease patients have mutations in the *htrA2* gene (Jones *et al.*, 2003; Martins *et al.*, 2004; Strauss *et al.*, 2005). HtrA3 is associated with many pregnancy- and cancer-related processes, such as placental development, endometrial cancer, ovarian cancer, and lung cancer, but almost nothing is known about its substrates or mechanism (Nie *et al.*, 2003; Bowden *et al.*, 2006; Nie *et al.*, 2006; Narkiewicz *et al.*, 2008; Narkiewicz *et al.*, 2009; Beleford *et al.*, 2010). HtrA4, the least-studied human family member, has high homology to HtrA1 and has also been suggested to be involved in preeclampsia (Wang *et al.*, 2012).

Little detailed structural or mechanistic information is available for any of the human HtrA enzymes. Inactive and active crystal structures have been solved for HtrA1, and limited mutagenesis studies have been performed, revealing that neither the substrates tested, the PDZ

domain, nor the N-terminal domain seem to regulate enzyme activity (Truebestein *et al.*, 2011; Eigenbrot *et al.*, 2012). A crystal structure of HtrA2 in an inactive conformation has been solved, revealing a domain arrangement in which the PDZ domain packs against active site (Li *et al.*, 2002). This arrangement suggests a regulatory mechanism in which activation induces a large conformational change in which the PDZ domain shifts away from the protease domain, but mutations that disrupt the protease-PDZ interface resulted in a decrease in proteolytic activity (Li *et al.*, 2002). A crystal structure and an NMR structure of the PDZ domain of HtrA3 have been solved (Appleton *et al.*, 2007). There are no structures of HtrA4.

At present, much of our understanding of HtrA proteolysis comes from studies of the structure and mechanism of two *E. coli* family members, the periplasmic proteases DegP and DegS. Together with a third family member, DegQ, these bacterial proteases are involved in protein quality control in the periplasm and in responding to stresses that affect the outer cell envelope.

Outer-membrane protein quality control

Gram negative outer envelope

Gram-negative bacteria have an envelope consisting of an outer membrane (OM), the periplasmic compartment, and an inner membrane (IM). A thin peptidoglycan layer runs through the periplasm, anchoring the OM and giving the cell its shape and rigidity. The OM serves as a protective barrier and problems with OM assembly or integrity serve as an important marker for environmental stress. Each face of the OM is chemically distinct, phospholipids comprising the inner leaflet and glycolipids comprising the outer leaflet. The glycolipids are overwhelmingly lipopolysaccharide (LPS), which consists of a glucosamine disaccharide with acyl chains

extending into the bilayer, a polysaccharide core, and the O-antigen, a long polysaccharide chain protruding to the outside of the cell (Raetz and Whitfield, 2002). LPS biogenesis begins on the cytoplasmic face of the inner membrane, and the full molecule is transported by a series of seven proteins across the IM, though the periplasm, and finally into the OM (Silhavy *et al.*, 2010).

Outer-membrane proteins (OMPs), mostly transmembrane β-barrel porins, are the principal non-lipid component of the OM. These OMPs are tasked with controlling the permeability of the OM. Some are simple porins that enable passive diffusion of small molecules, whereas others allow passage only of specific substrates. The porins are mostly trimeric and are arranged such that their C-terminal tails are packed at the oligomeric interfaces and occluded from solvent (Cowan *et al.*, 1992; Cowan *et al.*, 1995). OMPs are synthesized in the cytoplasm, translocated across the IM, associate with periplasmic chaperones as they pass through this compartment, and are finally inserted into the OM by a complex protein machine (Silhavy *et al.*, 2010; Hagan *et al.*, 2011). The OM is essential, and Gram-negative bacteria have evolved methods to monitor its health and to respond to OM stress. As discussed below, these systems require the sensing of OM-specific signals in the periplasm and communication of this information across the inner membrane to the cytoplasm.

Signal transmission across membranes

Cells employ diverse systems for propagating external signals across a membrane to the cytoplasm. In eukaryotes, G-coupled protein receptors, transmembrane proteins located at the plasma membrane, bind extracellular small molecules, causing a conformational change that allows a partnered G-protein on the cytoplasmic face to hydrolyze GTP and initiate a signaling

cascade (Wettschureck and Offermanns, 2005). Many bacteria utilize two-component regulatory systems, in which a cytoplasmic domain of a transmembrane histidine kinase is autophosphorylated in response to an external signal and then transfers that phosphate to an associated response regulator, resulting in a conformational change in the response regulator that allows it to up- or down-regulate relevant genes (Mascher *et al.*, 2006). Regulated membrane proteolysis (RIP), in which a transmembrane protein is sequentially cleaved by two proteases, resulting in the release of a cytoplasmic signal, is also widely used to propagate diverse signals across membranes (Ades 2008). For example, in the human sterol-sensing system, site-1-protease (S1P) and site-2-protease (S2P) in the Golgi membrane sequentially cleave a transmembrane protein in response to low-sterol conditions, releasing transcription factors that promote biosynthesis of sterols and fatty acids (Chen and Zhang, 2010). In *E. coli* and some other Gram-negative bacteria, a RIP cascade is used to sense and respond to OM stress.

σ^E pathway

When *E. coli* are exposed to environmental conditions that threaten the OM, a RIP system propagates a periplasmic stress signal across the IM to the cytoplasm (Fig. 1.2). In the absence of stress, OMPs and LPS molecules undergo normal biogenesis, passing through the periplasm on their way to the OM; the alternative sigma factor σ^E is sequestered against the IM by the cytoplasmic domain of RseA, a transmembrane anti-sigma factor (De Las Peñas *et al.*, 1997; Missiakas *et al.*, 1997); RseB, a periplasmic protein with homology to members of the lipid-binding family, binds the periplasmic domain of RseA and protects it from proteolysis (Cezairliyan and Sauer, 2007); and DegS protease, which is anchored to periplasmic face of the IM, waits in a catalytically inactive state.

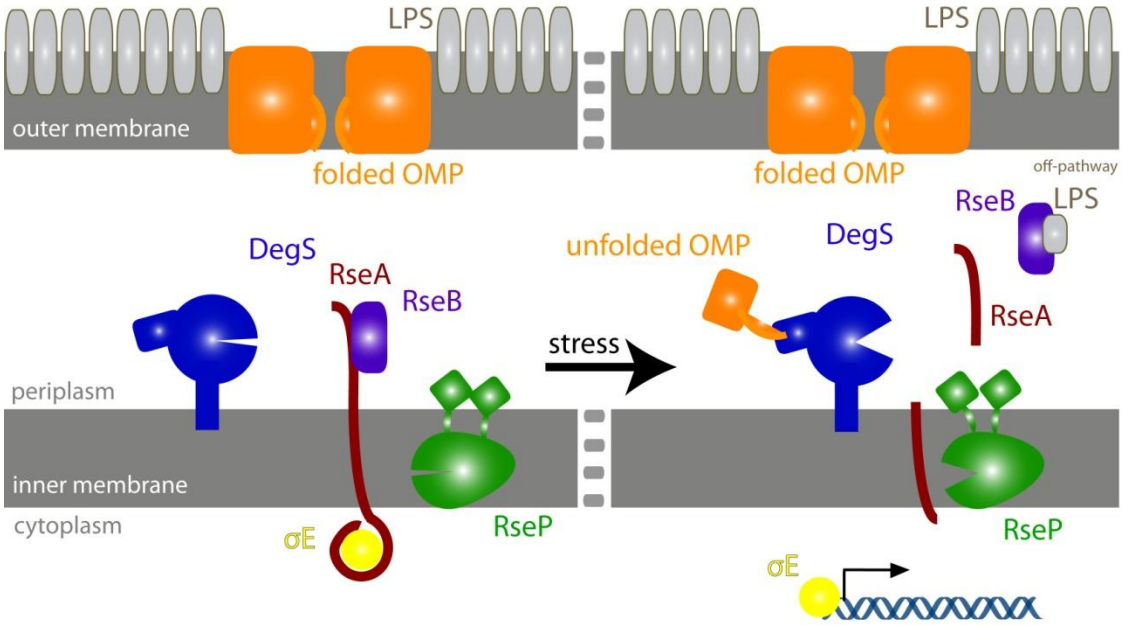

Fig. 1.2: The *E. coli* periplasmic stress response. In the absence of stress, σ^E is sequestered by RseA. Under stress conditions, unassembled OMPs bind and activate DegS, and periplasmic LPS binds RseB, releasing it from RseA. These dual signals induce cleavage of RseA and initiate a proteolytic cascade that frees σ^E and results in transcription of stress-response genes.

When OM biogenesis pathways are disrupted by stress, unassembled OMPs and intermediates in LPS biogenesis accumulate in the periplasm (Mecsas *et al.*, 1993; Tam *et al.*, 2005; Klein *et al.*, 2009). The exposed C-termini of the unassembled periplasmic OMPs bind to the PDZ domains of DegS, activating its proteolytic activity (Walsh *et al.*, 2003). Periplasmic LPS molecules compete for binding RseB with RseA, freeing the site-1 cleavage sequence (Lima *et al.*, 2013). Activated DegS then cleaves the unprotected periplasmic domain of RseA at site 1, which initiates a proteolytic cascade. Site-1 cleavage of RseA by DegS recruits the integral-membrane RseP protease, which cleaves RseA at site 2 within the IM. This site-2 cleavage releases the inhibited complex of σ^E bound to the cytoplasmic domain of RseA from the inner membrane (Alba *et al.*, 2002; Kanehara *et al.*, 2002). σ^E is then released to up-regulate stress-response genes when cytoplasmic AAA+ proteases, such as ClpXP, unfold and degrade the cytoplasmic domain

of RseA (Chaba *et al*., 2007). σ^E regulates transcription of diverse genes relevant to cell-envelope health, including σ^E itself, RseA, RseB, the periplasmic DegP protease, periplasmic chaperones (*skp*, *dsbC*, *fkpA*), and biogenesis genes for LPS, phospholipids, and IM and OM proteins (Rouviere *et al.*, 1995; Raina *et al.*, 1995; Dartigalongue *et al.*, 2001; Raivio *et al.*, 2001; Rezuchova *et al.*, 2003).

The DegS protease

DegS allostery

As the site-1 protease, DegS is the gatekeeper for the OM-stress response. It must remain largely inactive in the absence of stress but cleave RseA when periplasmic OMPs accumulate. Like other HtrA proteases, DegS is a trimer. Proteolytic activation can be modeled by classic Monod-Wyman-Changeux (MWC) allostery, in which periplasmic OMPs and RseA bind more tightly to active than inactive DegS trimers and thus increase the equilibrium population of active enzymes (Monod *et al.*, 1965; Sohn and Sauer, 2009). Both binding events are positively cooperative, allowing the switch to be ultra-sensitive with respect to OMP and RseA concentration (Sohn *et al.*, 2007).

Most *E. coli* OMPs have a YxF motif at the C terminus, where Y is tyrosine, x is any amino acid, and F is phenylalanine (Struyve et al., 1991). Peptides with C-terminal YxF sequences were initially found to bind to the PDZ domain of DegS and to active cleavage of RseA (Walsh et al., 2003). The identity of the "x" position affects the strength of binding to DegS, but saturating concentrations of peptide differing only at this penultimate position activate DegS cleavage to very similar extents (Sohn et al., 2007). Interestingly, OMP peptides with the same C-terminal

YxF tripeptide but with different lengths or N-terminal sequences have different affinities for active and inactive trimers of DegS and therefore activate the enzyme to different maximal extents (Sohn and Sauer, 2009). A YYF tripeptide is the most potent activator of DegS yet to be identified, and saturating concentrations increase DegS activity ~1000-fold over the basal cleavage rate (Sohn and Sauer, 2009). The detailed mechanism by which OMP-peptide binding to the PDZ domain activates DegS has been controversial, as discussed below, but studies of hybrid enzymes show that OMP-peptide binding to one PDZ domain activates both *cis* and *trans* protease domains (Mauldin and Sauer, 2012). Moreover, the peptide-free PDZ domain appears to inhibit DegS protease activity, as deletion of the PDZ domains results in a variant ($DegS^{\Delta PDZ}$) with increased protease activity *in vitro* and *in vivo* (Walsh et al., 2003; Sohn et al., 2007).

DegS crystal structures

Crystal structures of DegS trimers in an OMP-free inactive conformation and an OMP-bound active state established the overall architecture of the enzyme and revealed subtle but important differences between the two states (Wilken *et al.*, 2004; Zeth, 2004). In both structures, the protease domains of DegS pack together in the center of the trimer with the PDZ domains on the outside (Fig. 1.3A). However, OMP-bound active DegS has a properly formed active-site oxyanion hole and thus is capable of stabilizing a tetrahedral intermediate and catalyzing proteolysis, whereas rotation about the 198-199 peptide bond in the inactive OMP-free structure destroys the oxyanion hole (Fig. 1.3B).

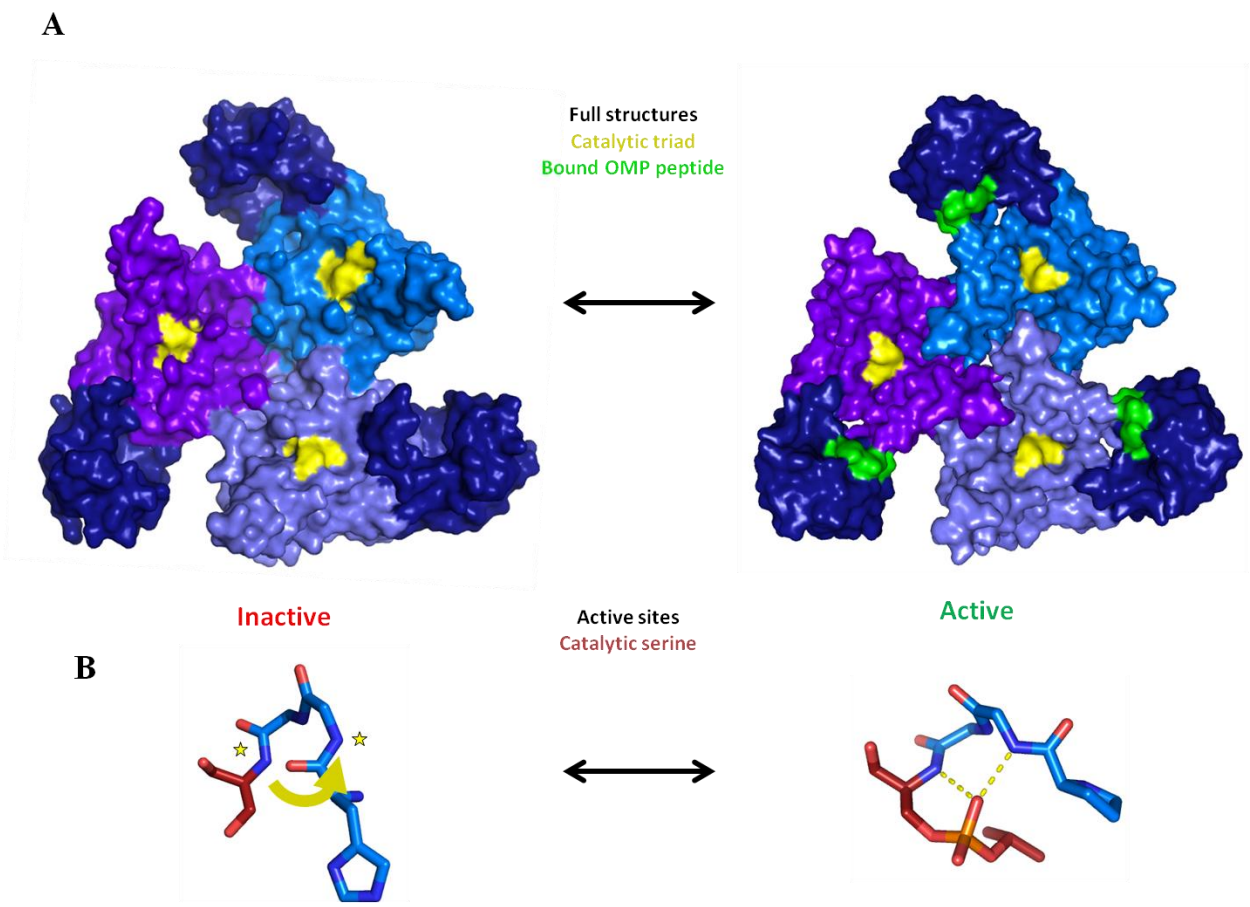

Fig. 1.3. Allosteric activation of DegS. (A) In inactive (1SOT) and active (3GDS) DegS, the protease domains (light colors) pack together to stabilize the trimer and the PDZ domains (dark blue) are on the periphery. The catalytic triad is shown in yellow. OMP peptides (green) are bound to the PDZ domains of active DegS. (B) Structures of residues 198-201 (catalytic Ser^{201} is red) in inactive and active DegS. A functional oxyanion hole is absent in inactive DegS. In active DegS, rotation of the peptide backbone between residue 198 and 199 creates a functional oxyanion hole. In the active structure, which also harbors the H198P mutation, the active site serine is modified with isopropyl-fluorophosphate and mimics a tetrahedral degradation intermediate.

Importantly, crystal structures predicted interactions that could be broken or introduced to bias the allosteric equilibrium in a particular direction and thereby increase or decrease DegS activity, many of which have been subsequently tested by mutational studies. For example, His^{198} lies near the catalytic site and its backbone atoms must be properly oriented to form a functional oxyanion hole and support catalysis. The His_{198}→Pro mutation allows the mutant side chain, to pack favorably against the neighboring Tyr^{162} side chain, stabilizing the functional conformation

of DegS (Fig. 1.4). DegS^{H198P} has higher basal and peptide-stimulated activity than wild-type DegS *in vitro* and results in higher σ^E activity *in vivo* (Sohn *et al.*, 2009; Chaba *et al.*, 2011).

Mutations can also bias the equilibrium in the inactive direction. In active DegS, the hydroxyl group of the Tyr^{162} side chain makes a hydrogen bond with the side chain of Asn^{197}. When Tyr^{162} is mutated to alanine, this interaction is abolished and the resulting Y162A enzyme has extremely low degradation activity both in the absence and presence of OMP peptide (Sohn *et al.*, 2007). Tellingly, neither adding in the activating H198P mutation nor deleting the PDZ domain can activate the Y162A variant, and both Y162A DegS$^{\Delta PDZ}$ and H198P/Y162A DegS$^{\Delta PDZ}$ crystallize in the inactive conformation (Sohn *et al.*, 2010).

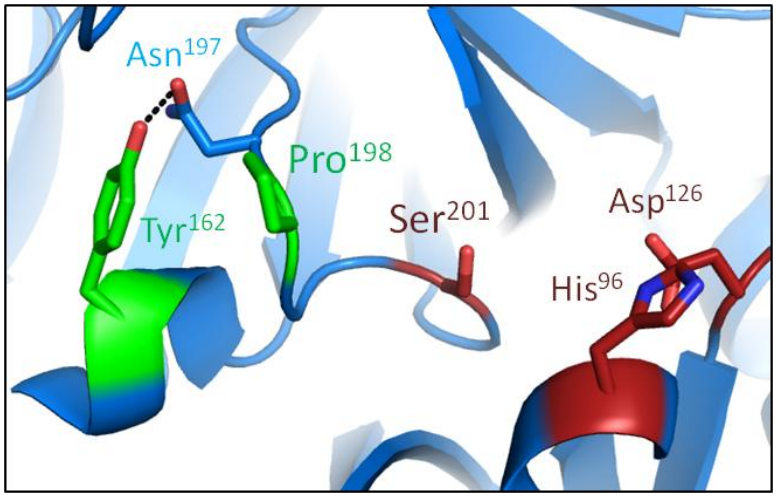

Fig. 1.4. Residues important for stabilizing active versus inactive conformations of DegS. The catalytic triad is shown in red and sites of relevant mutations in green. The H198P mutation stabilizes the functional conformation of the oxyanion hole by introducing Pro^{198}, which packs against the neighboring Tyr^{162}. This conformation is also stabilized in wild type DegS by the hydrogen bond between the side chains of Tyr^{162} and Asn^{197}, an interaction that is absent the Y162A mutant.

A large collection of crystal structures of full-length DegS or the ΔPDZ variant with different mutations and bound to various OMP peptides provide support for a two-state allosteric model.

All structures contain a set of "triangular base" residues in the protease domain that assume the same conformation in active and inactive structures (Sohn *et al.*, 2010). Another set of protease-domain residues assume one conformation in active structures and another conformation in inactive structures.

DegS activation via OMP-peptide binding

Two models have been suggested for the mechanism of enzyme activation by OMP-peptide binding (Fig. 1.5). Both models involve the L3 loop (residues 176–189), which extends from the protease domain towards the PDZ domain and assumes different conformations in active versus inactive DegS. In the peptide-activation model, the penultimate residue of PDZ-bound OMP peptide makes specific activating contacts with the L3 loop that stabilize the active conformation of the protease domain (Wilken et al., 2004; Hasselblatt et al., 2007). Depending on the identity of the penultimate residue and its interactions, the protease domain assumes one of many different conformations that can vary from somewhat active to very active. However, in crystal structures of peptide-bound DegS, no consistent contacts between bound OMP peptide and the L3 loop of the protease domain are observed (Sohn *et al.*, 2009). Furthermore, changing the penultimate residue of the OMP peptide affects its affinity for DegS but has little effect on the maximal level of DegS activation at peptide saturation (Sohn *et al.*, 2009). As previously mentioned, DegS crystal structures also reveal two basic conformations. Although there are small differences in surface loops and side-chain conformations among each class of structures, there is no evidence for the proposed multitude of somewhat-active states with uniquely-tuned active sites of differing activity.

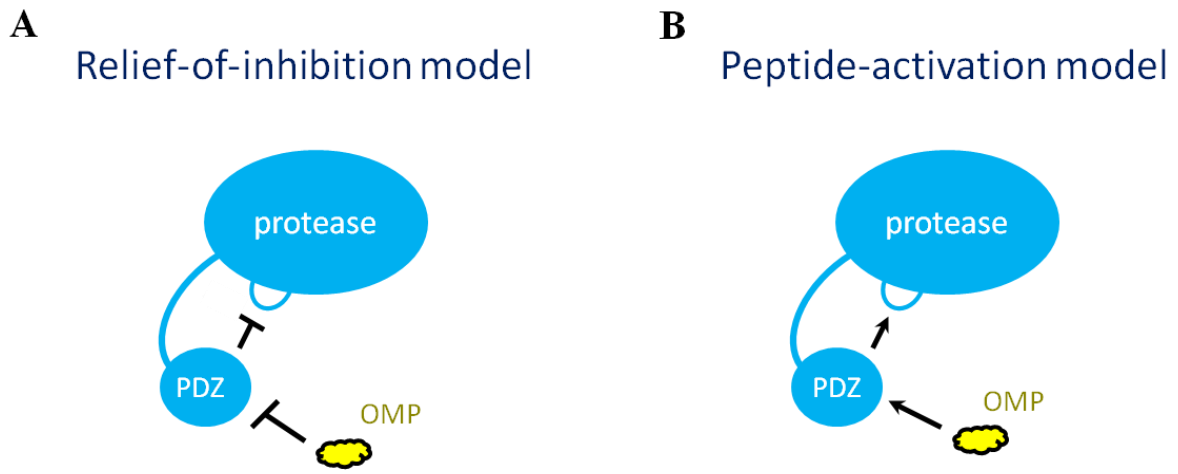

Fig. 1.5. Two models for activation of DegS by OMP peptides. In the relief-of-inhibition model, OMP binding to the PDZ domain breaks inhibitory interactions made by the L3 loop on the protease domain. The peptide-activation model posits that OMP peptide bound to the PDZ domain makes specific activating contacts with the L3 loop.

The relief-of-inhibition model for OMP-peptide activation is an extension of the two-state model and posits that inhibitory contacts between the unliganded PDZ domain and the L3 loop stabilize inactive DegS, with peptide binding breaking or destabilizing inhibitory interactions (Walsh et al., 2003; Sohn et al., 2007; Sohn and Sauer, 2009). The simplest evidence for this model is that deleting the entire PDZ domain or making mutations that remove inter-domain contacts that are observed in inactive but not active DegS results in enzyme activation (Sohn *et al.*, 2007; Sohn *et al.*, 2009; Sohn *et al.*, 2010).

DegS binding to RseA substrate

The RseA substrate also allosterically activates DegS, but much less is known about how RseA interacts with DegS than about how OMP peptides bind. The periplasmic domain of RseA (residues 120-216) is an intrinsically disordered polypeptide that is cleaved by DegS between Val^{148} and Ser^{149}. However, an RseA peptide (residues 143-152) that contains the scissile peptide bond is cleaved by DegS far more slowly than the full periplasmic domain, indicating that RseA

residues distant from the cleavage site, called exosites, are important for tight binding and/or efficient cleavage by DegS. A potential RseA exosite (residues 160-189) that also binds the inhibitor RseB has been identified, but one or more additional sites probably exist (Cezairliyan and Sauer, 2007). Several glutamine-rich regions of RseA appear to inhibit cleavage of full-length RseA by RseP, but mutating these regions did not significantly affect DegS cleavage (Kanehara *et al.*, 2003). An RseA peptide spanning residues 135-185, which includes the RseB interaction site, binds DegS very similarly to full-length periplasmic RseA and is efficiently cleaved by DegS (A.K. de Regt, unpublished). Further studies will be required to map the exosites of RseA and determine how they bind DegS and contribute to allosteric activation.

The DegP protease

Studies of DegS have led to improved understanding of *E. coli* DegP, another periplasmic HtrA protease with a more complicated activation mechanism. DegP differs from DegS in having no membrane anchor and two PDZ domains per subunit instead of one (Waller and Sauer, 1996; Ponting, 1997). Like all HtrA proteases, DegP trimers appear to be the basic unit of function but can assemble into higher-order oligomers. For example, DegP forms inactive hexamers in which trimers pack face-to-face, but addition of protein or peptide substrates results in formation of catalytically active 12-, 18-, or 24-mer cages stabilized by interactions between the PDZ1 and PDZ2 domains (Fig. 1.6; Kim *et al.*, 2012; Krojer et al., 2002; Jiang et al., 2008; Krojer et al., 2008). An allosteric model also describes DegP activity well, with substrate binding cooperatively and stabilizing the active conformation of trimers, which can then assemble into cages (Kim *et al.*, 2011). The best DegP substrates contain a hydrophobic C-terminal residue that

binds to the PDZ1 domain of DegP and a small hydrophobic residue at the P1 position that binds to the active-site cleft (Krojer *et al.*, 2008; Kim *et al.*, 2011).

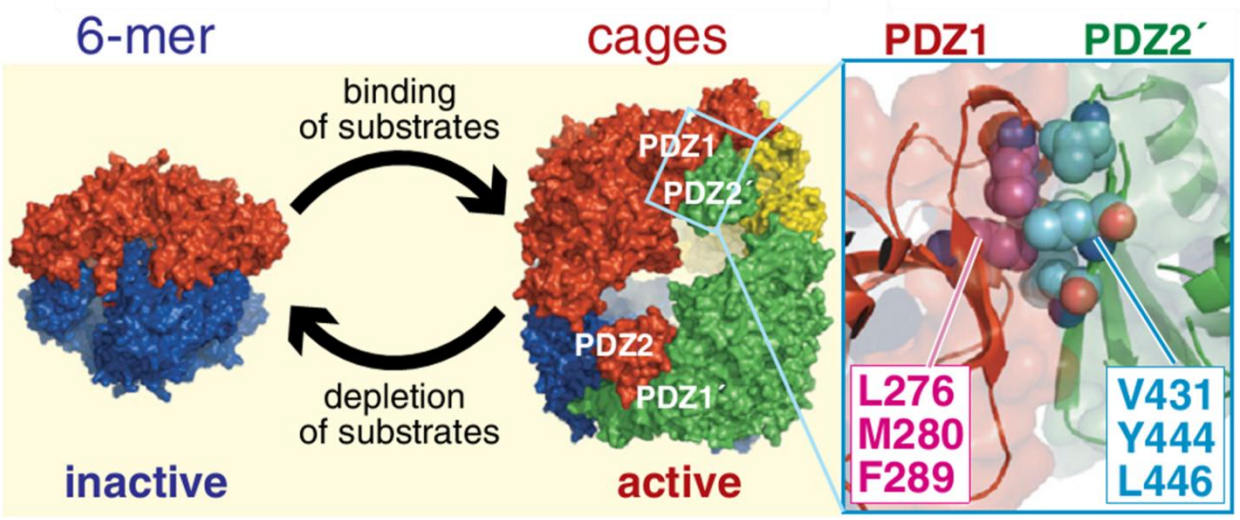

Fig. 1.6. Inactive DegP hexamers assemble into higher-order cages upon substrate binding. Cages are mediated by interactions between PDZ1 and PDZ2 and disassemble when substrate is depleted. (from Kim *et al.*, 2012).

In wild type DegP, substrate binding is linked not only to proteolytic activation and formation of a functional oxyanion hole but also to cage formation, although these processes can be uncoupled by mutations, and substrate binding but not cage formation is required for protease activation (Kim *et al.*, 2011; Kim and Sauer, 2012). DegP cages stay assembled until the concentration of intact substrates has been depleted, at which point they disassemble and revert back to inactive trimers or hexamers (Kim *et al.*, 2011). This regulation of DegP activity is essential for cell viability, as DegP variants carrying double mutations that stabilize the active form and abolish cage formation are lethal to the cell (Kim and Sauer, 2014). Thus HtrA proteases have evolved a variety of mechanisms to regulate their activities.

The AlgU RIP pathway in *P. aeruginosa*

In *Pseudomonas aerguinosa*, a RIP system homologous to the *E. coli* σ^E pathway controls the release of AlgU, a stress-response transcription factor homologous to σ^E (Erickson and Gross, 1989; DeVries and Ohman, 1994; Rouvier *et al.*, 1995; Ades, 2008). AlgW, which shares 44% sequence identity with DegS, is the site-1 protease, and MucA, a transmembrane anti-sigma factor with 34% sequence identity to RseA, is its substrate (Schurr *et al.*, 1996; Cezairliyan and Sauer, 2009). The RseB homolog in the *P. aeruginosa* system is called MucB, and its inhibition of MucA cleavage by AlgW can be also be relieved by binding LPS (Cezairliyan and Sauer, 2007; Lima *et al.*, 2013). A peptide corresponding to the C-terminus of MucE, a *P. aeruginosa* OMP, activates AlgW cleavage activity by binding to its PDZ domains (Cezairliyan and Sauer, 2009).

In addition to up-regulating stress-response genes, AlgU also directs transcription of the AlgD transcription factor, which in turn promotes transcription of genes for the biogenesis of alginate, an exopolysaccharide that renders the bacterium resistant to many antibiotics as well as to the human immune system (Govan and Deretic, 1996; Martin *et al.*, 1993; Wood *et al.*, 2006). For patients with cystic fibrosis, the production of alginate is a particular problem because their mucus-filled lungs have difficulty clearing chronic infections of *P. aeruginosa* (Folkesson *et al.*, 2012). Over 80% of the alginate-producing clinical strains of *P. aeruginosa* have mutations in their *mucA* genes that cause constitutive activation of the AlgU pathway (Boucher *et al*., 1997).

Thesis overview

I have presented an introduction to the outer-membrane stress response in Gram-negative bacteria and to allostery in the *E. coli* DegS protease. In the following chapters, I further examine the activation mechanism of DegS and its homolog, *P. aeruginosa* AlgW. In Chapter 2, I examine the allosteric pathway for communication between the site of OMP peptide binding and the catalytic active site. Using mutagenesis and sequence alignments, I establish a network of conserved interactions that promote inter-subunit communication and stabilize the active conformation of DegS. Chapter 3 describes experiments seeking to understand the molecular mechanism by which OMP peptide activates DegS. I find that peptide binding causes a steric clash between a PDZ domain residue and a residue on the L3 loop, which forces the L3 loop to rearrange, breaking autoinhibitory interactions and activating the protease. In Chapter 4, I investigate a new protein activator of AlgW, periplasmic CupB5. I find that peptides corresponding to the activation signal on CupB5 bind to AlgW and stabilize the active form in conjunction with OMP peptide bound to the PDZ domain, a novel activation mechanism for this protein family. Finally, I conclude in chapter 5 with suggestions for further experiments to elucidate the activation mechanism of DegS.

References

Ades SE, Connolly LE, Alba BM, Gross CA. (1999). The *Escherichia* coli sigma(E)-dependent extracytoplasmic stress response is controlled by the regulated proteolysis of an anti-sigma factor. Genes Dev *13*, 2449-61.

Ades SE. Regulation by destruction: design of the σ^E envelope stress response.(2008). Curr Opin Microbiol *11*, 535-40.

Alba BM, Leeds JA, Onufryk C, Lu CZ, Gross CA. (2002). DegS and YaeL participate sequentially in the cleavage of RseA to activate the σ^E-dependent extracytoplasmic stress response. Genes Dev *16*, 2156-2168.

Appleton BA, Wiesmann C. (2007). Structural and functional analysis of the PDZ domains of human HtrA1 and HtrA3. Protein Sci *16*, 2454-2471.

Bakker D, Buckley AM, de Jong A, van Winden VJ, Verhoeks JP, Kuipers OP, Douce GR, Kuijper EJ, Smits WK, Corver J. (2014). The HtrA-like protease CD3284 modulates virulence of Clostridium difficile. Infect Immun 02336-14.

Beleford D, Liu Z, Rattan R, Quagliuolo L, Boccellino M, Baldi A, Maguire J, Staub J, Molina J, Shridhar V. (2010). Methylation induced gene silencing of HtrA3 in smoking-related lung cancer. Clin Cancer Res *16*, 398–409.

Boucher JC, Yu H, Mudd MH, Deretic V. (1997) Mucoid *Pseudomonas aeruginosa* in cystic fibrosis: Characterization of *muc*mutations in clinical isolates and analysis of clearance in a model of respiratory infection. Infect Immun *65*, 3838–3846.

Bowden MA, Di Nezza-Cossens LA, Jobling T, Salamonsen LA, Nie G. (2006). Serine proteases HTRA1 and HTRA3 are down-regulated with increasing grades of human endometrial cancer. Gynecol Oncol *103*, 253–60.

Cezairliyan BO, Sauer RT. (2007). Inhibition of regulated proteolysis by RseB. Proc Natl Acad Sci U S A *104*, 3771-6.

Cezairliyan BO, Sauer RT. (2009). Control of *Pseudomonas aeruginosa* AlgW protease cleavage of MucA by peptide signals and MucB. Mol Microbiol *72*, 368-79.

Chaba R, Alba BM, Guo MS, Sohn J, Ahuja N, Sauer RT, Gross CA. (2011). Signal integration by DegS and RseB governs the σ^E-mediated envelope stress response in *Escherichia* coli. Proc Natl Acad Sci USA *108*, 2106-11.

Chaba R, Grigorova IL, Flynn JM, Baker TA, Gross CA. (2007). Design principles of the proteolytic cascade governing the sigmaE-mediated envelope stress response in *Escherichia coli*: keys to graded, buffered, and rapid signal transduction. Genes Dev *21*, 124-36.

Chen G, Zhang X. (2010). New insights into S2P signaling cascades: regulation, variation, and conservation. Protein Sci *19*, 2015-30.

Chien J, Ota T, Aletti G, Shridhar R, Boccellino M, Quagliuolo L, Baldi A, Shridhar V. (2009). Serine protease HtrA1 associates with microtubules and inhibits cell migration. Mol Cell Biol *29*, 4177–4187.

Cilenti L, Soundarapandian MM, Kyriazis GA, Stratico V, Singh S, Gupta S, Bonventre JV, Alnemri ES, Zervos AS. (2004).Regulation of HAX-1 anti-apoptotic protein by Omi/HtrA2 protease during cell death. J Biol Chem *279*, 50295–50301.

Clausen T, Southan C, Ehrmann M. (2002). The HtrA family of proteases: implications for protein composition and cell fate. Mol Cell *10*, 443-55.

Cowan SW, Garavito RM, Jansonius JN, Jenkins JA, Karls-son R, Konig N, Pai EF, Pauptit RA, Rizkallah PJ, Rosenbusch JP, Rummel G, Schirmer T. (1995). The structure of OmpF porin in a tetragonal crystal form. Structure *3*, 1041–1050.

Cowan SW, Schirmer T, Rummel G, Steiert M, Ghosh R, Pauptit RA, Jansonius JN, Rosenbusch JP. (1992). Crystal structures explain functional properties of two *E. coli* porins. Nature *358*, 727-733.

Dartigalongue C, Missiakas D, Raina S. (2001). Characterization of the *Escherichia coli* σ^E regulon. J Biol Chem. *276*, 20866–20875.

De Las Peñas A, Connolly L, Gross CA. (1997). σ^E is an essential sigma factor in *Escherichia* coli. J Bacteriol *179*, 6862–6864.

DeVries CA, and Ohman DE. (1994). Mucoid-to-nonmucoid conversion in alginate-producing *Pseudomonas* aeruginosa often results from spontaneous mutations in algT, encoding a putative alternative sigma factor, and shows evidence for autoregulation. J Bacteriol *176*, 6677–6687.

Eigenbrot C, Ultsch M. (2012). Structural and functional analysis of HtrA1 and its subdomains. Structure *20*, 1040-1050.

Erickson JW, and Gross CA. (1989). Identification of the σ^E subunit of *Escherichia coli* RNA polymerase: a second alternate s factor involved in high-temperature gene expression. Genes Dev *3*, 1462–1471.

Folkesson A, Jelsbak L, Yang L, Johansen HK, Ciofu O, Hoiby N, Molin S. (2012). Adaptation of *Pseudomonas aeruginosa* to the cystic fibrosis airway: an evolutionary perspective. *Nat Rev* Microbiol *10*, 841-851.

Govan JRW, and Deretic V. (1996). Microbial pathogenesis in cystic fibrosis: mucoid *Pseudomonas aeruginosa* and *Burkholderia cepacia*. Microbiol Rev *60*, 539–574.

Grau S, Baldi A, Bussani R, Tian X, Stefanescu R, Przybylski M, Richards P, Jones SA, Shridhar V, Clausen T, Ehrmann M.. (2005). Implications of the serine protease HtrA1 in amyloid precursor protein processing. Proc Natl Acad Sci USA 1026021–6026.

Grau S, Richards PJ, Kerr B, Hughes C, Caterson B, Williams AS, Junker U, Jones SA, Clausen T, Ehrmann M. (2006). The role of human HtrA1 in arthritic disease. J Biol Chem 2816124–6129.

Gray CW, Ward RV, Karran E, Turconi S, Rowles A, Viglienghi D, Southan C, Barton A, Fantom KG, West A, Savopoulos J, Hassan NJ, Clinkenbeard H,Hanning C, Amegadzie B, Davis JB, Dingwall C, Livi GP, Creasy CL. (2000).Characterization of human HtrA2, a novel serine protease involved in the mammalian cellular stress response. Eur J Biochem *267*, 5699–5710 .

Hagan CL, Silhavy TJ, Kahne D. (2011). β-Barrel membrane protein assembly by the Bam complex. Annu Rev Biochem *80*, 189-210.

Hara K, Shiga A, Fukutake T, Nozaki H, Miyashita A, Yokoseki A, Kawata H, Koyama A, Arima K, Takahashi T, Ikeda M, Shiota H, Tamura M, Shimoe Y,Hirayama M, Arisato T, Yanagawa S, Tanaka A, Nakano I, Ikeda S, Yoshida Y, Yamamoto T, Ikeuchi T, Kuwano R, Nishizawa M, Tsuji S, Onodera O. (2009). Association of HTRA1 mutations and familial ischemic cerebral small-vessel disease. N Engl J Med 360, 1729–1739.

Hasselblatt H, Kurzbauer R, Wilken C, Krojer T, Sawa J, Kurt J, Kirk R, Hasenbein S, Ehrmann M, and Clausen T. (2007). Regulation of the sigmaE stress response by DegS: how the PDZ domain keeps the protease inactive in the resting state and allows integration of different OMP-derived stress signals upon folding stress. Genes Dev. *21*, 2659-2670.

Huesgen PF, Schuhmann H, Adamska I. (2009). Deg/HtrA proteases as components of a network for photosystem II quality control in chloroplasts and cyanobacteria. Res Microbiol *160*, 726–732.

Huttunen HJ, Guénette SY, Peach C, Greco C, Xia W, Kim DY, Barren C, Tanzi RE, Kovacs DM. (2007). HtrA2 regulates β-amyloid precursor protein (APP) metabolism through endoplasmic reticulum-associated degradation. J Biol Chem *282*, 28285–28295

Jiang J, Zhang X, Chen Y, Wu Y, Zhou ZH, Chang Z, Sui SF. (2008). Activation of DegP chaperone-protease via formation of large cage-like oligomers upon binding to substrate proteins. Proc Natl Acad Sci USA *105*, 11939–11944.

Jones JM, Datta P, Srinivasula SM, Ji W, Gupta S, Zhang Z, Davies E, Hajnóczky G, Saunders TL, Van Keuren ML, Fernandes-Alnemri T, Meisler MH, Alnemri ES. (2003). Loss of Omi mitochondrial protease activity causes the neuromuscular disorder of *mnd2* mutant mice. *Nature 425*, 721–727.

Kanehara K, Ito K, Akiyama Y. (2002). YaeL (EcfE) activates the σ^E pathway of stress response through a site-2 cleavage of anti-σ^E, RseA. Genes Dev *16*, 2147-2155.

Kanehara K, Ito K, Akiyama Y. (2003). YaeL proteolysis of RseA is controlled by the PDZ domain of YaeL and a Gln-rich region of RseA. EMBO J *22*, 6389-98.

Kim S, Grant RA, Sauer RT. (2011) .Covalent linkage of distinct substrate degrons controls assembly and disassembly of DegP proteolytic cages.Cell *145*, 67–78.

Kim S, Sauer RT. (2012). Cage assembly of DegP protease is not required for substrate-dependent regulation of proteolytic activity or high-temperature cell survival. Proc Natl Acad Sci USA *109*, 7263-8.

Kim S, Sauer RT. (2014). Distinct regulatory mechanisms balance DegP proteolysis to maintain cellular fitness during heat stress. Genes Dev *28*, 902-11.

Klein G, Lindner B, Brabetz W, Brade H, Raina S. (2009). *Escherichia* coli K-12 Suppressor-free Mutants Lacking Early Glycosyltransferases and Late Acyltransferases: minimal lipopolysaccharide structure and induction of envelope stress response. J Biol Chem *284*, 15369-89.

Krojer T, Garrido-Franco M, Huber R, Ehrmann M, Clausen T. Crystal structure of DegP (HtrA) reveals a new protease-chaperone machine. (2002). Nature *416*, 455-9.

Krojer T, Sawa J, Schäfer E, Saibil HR, Ehrmann M, Clausen T. (2008). Structural basis for the regulated protease and chaperone function of DegP. Nature *453*, 885–890.

Li W, Srinivasula SM, Chai J, Li P, Wu JW, Zhang Z, Alnemri ES, Shi Y. (2002). Structural insights into the pro-apoptotic function of mitochonrial serine protease HtrA2/Omi. Nat Struc Biol *9*, 436-441.

Lima S, Guo MS, Chaba R, Gross CA, Sauer RT. (2013). Dual molecular signals mediate the bacterial response to outer-membrane stress. Science *340*, 837-41.

Lipinska B, Fayet O, Baird L, Georgopoulos C. (1989). Identification, characterization, and mapping of the *Escherichia coli htrA* gene, whose product is essential for bacterial growth only at elevated temperatures. J Bacteriol 171, 1574–1584.

Lorenzi T, Marzioni D, Giannubilo S, Quaranta A, Crescimanno C, De Luca A, Baldi A, Todros T, Tranquilli AL, Castellucci M. (2009). Expression patterns of two serine protease HtrA1 forms in human placentas complicated by preeclampsia with and without intrauterine growth restriction. Placenta 3035–40.

Lorenzi T, Niţulescu EA, Zizzi A, Lorenzi M, Paolinelli F, Aspriello SD, Baniţă M, Crăiţoiu S, Goteri G, Barbatelli G, Lombardi T, Di Felice R, Marzioni D, Rubini C, Castellucci M. (2014). The novel role of HtrA1 in gingivitis, chronic and aggressive periodontitis. PLoS One. *9*, 96978.

Martin DW, Holloway BW, and Deretic V. (1993). Characterization of a locus determining the mucoid status of *Pseudomonas aeruginosa*: AlgU shows sequence similarities with a Bacillus sigma factor. J Bacteriol *175*, 1153-1164.

Martins LM, Morrison A, Klupsch K, Fedele V, Noisoi N, Tesmann P, Abuin A, Grau E, Greppert M, Livi GP, Creasy CL, Martin A, Hargreaves I, Heales SJ, Okada H, Brandner S, Schulz JB, Mak T, Downward J. (2004). Neuroprotective role of the Reaper-related serine protease HtrA2/Omi revealed by targeted deletion in mice. Mol Cell Biol *24*, 9848–9862.

Mascher T, Helmann JD, Unden G. (2006). Stimulus perception in bacterial signal-transducing histidine kinases. Microbiol Mol Biol Rev *70*, 910-38.

Mauldin RV, and Sauer RT. (2013). Allosteric regulation of DegS protease subunits though a shared energy landscape. Nat. Chem. Biol. *9*, 90-96.

Mecsas J, Rouviere PE, Erickson JW, Donohue TJ, Gross CA. (1993). The activity of sigma E, an *Escherichia* coli heat-inducible sigma-factor, is modulated by expression of outermembrane proteins. Genes Dev *7*, 2618-28.

Missiakas, D., M. Lemaire, M. Mayer, C. Georgopoulos, and S. Raina. (1997). Modulation of the *Escherichia coli* σ^E (RpoE) heat shock transcription factor activity by the RseA, RseB, and RseC proteins. Mol Microbiol *24*, 355–372.

Monod J, Wyman J, Changeux JP. (1965). On the nature of allosteric transitions: A plausible model. J Mol Biol *12*, 88-118.

Narkiewicz J, Klasa-Mazurkiewicz D, Zurawa-Janicka D, Skorko-Glonek J, Emerich J, Lipinska B. (2008). Changes in mRNA and protein levels of human HtrA1, HtrA2 and HtrA3 in ovarian cancer. Clin Biochem *41*, 561–9.

Narkiewicz J, Lapinska-Szumczyk S, Zurawa-Janicka D, Skorko-Glonek J, Emerich J, Lipinska B. (2009). Expression of human HtrA1, HtrA2, HtrA3 and TGF-beta1 genes in primary endometrial cancer. Oncol Rep *21*, 1529–37.

Nie G, Li Y, Hale K, Okada H, Manuelpillai U, Wallace EM, Salamonsen LA. (2006). Serine peptidase HTRA3 is closely associated with human placental development and is elevated in pregnancy serum. Biol Reprod *74*, 366–74.

Nie GY, Li Y, Minoura H, Batten L, Ooi GT, Findlay JK, Salamonsen LA. (2003). A novel serine protease of the mammalian HtrA family is up-regulated in mouse uterus coinciding with placentation. Mol Hum Reprod *9*, 279–90.

Park HJ, Kim SS, Seong YM, Kim KH, Goo HG, Yoon EJ, Min do S, Kang S, Rhim H.. (2006). β-amyloid precursor protein is a direct cleavage target of HtrA2 serine protease. Implications for the physiological function of HtrA2 in the mitochondria. J Biol Chem *281*, 34277–34287

Patel P, De Boer L, Timms P, Huston WM. (2014). Evidence of a conserved role for Chlamydia HtrA in the replication phase of the chlamydial developmental cycle. Microbes Infect S1286-4579.

Ponting CP. (1997). Evidence for PDZ domains in bacteria, yeast, and plants. Protein Science *6*, 464-468.

Raetz CR, Whitfield C. (2002). Lipopolysaccharide endotox-ins. Annu Rev Biochem *71*, 635-700.

Raina S, Missiakas D, Georgopoulos C. (1995). The *rpoE* gene encoding the σ^E (σ^{24}) heat shock sigma factor of *Escherichia coli*. EMBO J. *14*, 1043–1055.

Raivio TL, Silhavy TJ. (2001). Periplasmic stress and ECF sigma factors. Annu Rev Microbiol *55*, 591–624.

Rezuchova B, Miticka H, Homerova D, Roberts M, Kormanec J. (2003). New members of the *Escherichia coli* σ^E regulon identified by a two-plasmid system. FEMS Microbiol Lett. *225*, 1-7.

Rouviere, PE, De Las Peñas A, Mecsas J, Lu CZ, Rudd KE, Gross CA. (1995). *rpoE*, the gene encoding the second heat-shock sigma factor, σ^E, in *Escherichia coli*. EMBO J. *14*, 1032–1042.

Schurr MJ, Yu H, Martinez-Salazar JM, Boucher JC, Deretic V. (1996). Control of AlgU, a member of the sigma E-like family of stress sigma factors, by the negative regulators MucA and MucB and *Pseudomonas aeruginosa* conversion to mucoidy in cystic fibrosis. J Bacteriol. *16*, 4997-5004.

Silhavy TJ, Kahne D, Walker S. The bacterial cell envelope. (2010). Cold Springs Harb Perspect Biol *5*, 414.

Sohn J, Grant RA, Sauer RT. (2007). Allosteric activation of DegS, a stress sensor PDZ protease. Cell *131*, 572-83.

Sohn J, Grant RA, Sauer RT. (2009). OMP peptides activate the DegS stress-sensor protease by a relief of inhibition mechanism. Structure *17*, 1411-21.

Sohn J, Grant RA, Sauer RT. (2010). Allostery is an intrinsic property of the protease domain of DegS: implications for enzyme function and evolution. J Biol Chem *285*, 34039-47.

Sohn J, Sauer RT. (2009). OMP peptides modulate the activity of DegS protease by differential binding to active and inactive conformations. Mol Cell *33*, 64-74.

Stiffler MA, Chen JR, Grantcharova VP, Lei Y, Fuchs D, Allen JE, Zaslavskaia LA, MacBeath G. (2007). PDZ domain binding selectivity is optimized across the mouse proteome. Science *317*, 364–369.

Strauss KM, Martins LM, Plun-Favreau H, Marx FP, Kautzmann S, Berg D, Gasser T, Wszolek Z, Müller T, Bornemann A, Wolburg H, Downward J, Riess O,Schulz JB, Krüger R. (2005). Loss of function mutations in the gene encoding Omi/HtrA2 in Parkinson's disease. Hum Mol Genet *14*, 2099–2111.

Struyve M, Moons M, and Tommassen J. (1991). Carboxy-termi-nal phenylalanine is essential for the correct assembly of a bacterial outer membrane protein. J Mol Biol *218*, 141–148.

Suzuki Y, Imai Y, Nakayama H, Takahashi K, Takio K, Takahashi R. (2001). Serine protease, HtrA2, is released from the mitochondria and interacts with XIAP, inducing cell death. Mol Cell *8*, 613–621

Tam C, Missiakas D. (2005). Changes in lipopolysaccharide structure induce the sigma(E)-dependent response of *Escherichia* coli. Mol Microbiol *55*, 1403-12.

Tonikian R, Zhang Y, Sazinsky SL, Currell B, Yeh JH, Reva B, Held HA, Appleton BA, Evangelista M, Wu Y, Xin X, Chan AC, Seshagiri S, Lasky LA, Sander C, Boone C, Bader GD, Sidhu SS. (2008). A specificity map for the PDZ domain family. PLoS Biol *6*, e239.

Truebestein L, Tennstaedt A, Hauske P, Krojer T, Kaiser M, Clausen T, Ehrmann M. (2011). Substrate-induced remodeling of the active site regulates human HTRA1 activity. Nat Struct Mol Biol. *18*, 386-388.

Waller PR, Sauer RT. (1996). Characterization of *degQ* and *degS, Escherichia coli* genes encoding homologs of the DegP protease. J Bacteriol *178*, 1146-53.

Walsh NP, Alba BM, Bose B, Gross CA, Sauer RT. (2003). OMP peptide signals initiate the envelope-stress response by activating DegS protease via relief of inhibition mediated by its PDZ domain. Cell *113*, 61-71.

Wang CK, Pan L, Chen J, Zhang M. (2010). Extensions of PDZ domains as important structural and functional elements. Protein Cell *1*, 737-51.

Wang LJ, Cheong ML, Lee YS, Lee MT, Chen H. (2012). High-temperature requirement protein A4 (HtrA4) suppresses the fusogenic activity of syncytin-1 and promotes trophoblast invasion. Mol Cell Biol *32*, 3707-17

Wilken C, Kitzing K, Kurzbauer R, Ehrmann M, Clausen T. (2004). Crystal structure of the DegS stress sensor: How a PDZ domain recognizes misfolded protein and activates a protease. Cell *117*, 483-94.

Wood LF, Leech AJ, and Ohman DE. (2006). Cell wall-inhibitory antibiotics activate the alginate biosynthesis operon in *Pseudomonas aeruginosa*: roles of σ^{22} (AlgT) and the AlgW and Prc proteases. Mol Microbiol *62*, 412-426.

Wettschureck N, Offermanns S. (2005). Mammalian G proteins and their cell type specific functions. Physiol Rev *85*, 1159-204.

Zeth K. (2004). Structural analysis of DegS, a stress sensor of the bacterial periplasm. FEBS Lett *569*, 351-8.

Chapter 2

Conserved pathways of allosteric communication in HtrA-family proteases

This work has been submitted to *Structure* as de Regt AK, Kim S, Sohn J, Grant RA, Baker TA, Sauer RT.

A.K.D. and J.S. purified and expressed recombinant proteins. A.K.D. performed all experiments involving DegS and wrote the initial manuscript. S.K. performed all experiments with DegP. R.A.G and R.T.S. re-refined the crystal structures.

Abstract

Escherichia coli responds to outer-membrane stress using a signaling cascade initiated when DegS, an HtrA-family periplasmic protease, cleaves RseA, a transmembrane anti-sigma factor, causing downstream release of the σ^E sigma factor and transcription of stress-response genes. Each subunit of the DegS trimer contains a trypsin-like protease domain and a PDZ domain. The trimeric protease domain is normally inactive because of intrinsic conformational preferences and autoinhibition mediated in part by the unliganded PDZ domains. Allosteric activation of RseA cleavage occurs as a consequence of the binding of unassembled outer-membrane proteins (OMPs) to the PDZ domains. Here, we identify a set of DegS residues that cluster together at subunit-subunit interfaces in the trimer, link the active sites and substrate-binding sites, and are crucial for stabilizing the active enzyme conformation in response to OMP signaling. These residues are conserved across the HtrA-protease family, including orthologs linked to human disease, and thus a common mechanism of allosteric activation in response to signaling appears to function in all family members. Indeed, mutation of residues at homologous positions in the DegP quality-control protease also eliminates allosteric activation.

Introduction

Allostery, a shift between distinct molecular structures, controls the biological activities of many enzymes, including proteases. In the periplasm of *Escherichia coli*, for example, heat and other environmental stresses allosterically activate the DegS protease, which is anchored to the inner membrane, and initiate an intramembrane proteolytic cascade that results in transcription of stress-response genes in the cytoplasm (Ades, 2008). DegS is a trimeric HtrA-family protease, in which each subunit contains a trypsin-like protease domain and a regulatory PDZ domain (Fig. 2.1A). The trimer is stabilized by packing between the protease domains. The principal substrate of DegS is the periplasmic domain of RseA, a transmembrane protein also containing a cytoplasmic domain that binds and inhibits the σ^E transcription factor (Alba and Gross, 2004). Two stress-induced molecular signals are required for DegS cleavage of RseA *in vivo*. First, unassembled outer-membrane proteins (OMPs) accumulate in the periplasm during stress, and Tyr-Xxx-Phe (YxF) peptides at the C termini of these OMPs bind to the PDZ domains of DegS and stimulate proteolytic activity (Walsh et al., 2003). Second, lipopolysaccharides bind the RseB regulatory protein, releasing it from RseA, which allows cleavage of RseA at a single site by OMP-activated DegS (Lima et al., 2013). This initial cleavage event results in subsequent cleavage of RseA by other proteases, freeing σ^E to activate transcription of stress-response genes (Ades et al., 1999; Kanehara et al., 2002; Akiyama et al., 2004; Flynn et al., 2004; Chaba *et al*., 2007; Li et al., 2009).

In the absence of stress, DegS cleaves RseA at a low rate *in vivo* (Ades, 2008). Similarly, in the absence of OMP peptides *in vitro*, DegS cleaves the periplasmic domain of RseA much more slowly (>100-fold) than in their presence (Walsh *et al*. 2003; Sohn *et al*., 2007; Sohn and Sauer, 2009). Crystal structures of DegS or DegS$^{\Delta PDZ}$ trimers show two distinct conformations, one

inactive because of a malformed oxyanion hole and one with a functional His-Asp-Ser catalytic triad and oxyanion hole (Wilken *et al*., 2004; Zeth, 2004; Hasselblatt et al., 2007; Sohn et al., 2007; 2009; 2010). The PDZ domain has two major roles, keeping OMP-free DegS in an autoinhibited state ($DegS^{\Delta PDZ}$ has robust protease activity) and binding OMP peptide to allow activation. In structures of active DegS, the PDZ-bound OMP peptide is ~25 Å from the closest active site in the trimer. Allosteric activation over this distance is partially explained by remodeling of the protease-domain L3 loop, which is spatially adjacent to bound OMP peptide. This remodeling breaks autoinhibitory interactions between the L3 loop and the PDZ domain and allows formation of alternative contacts that appear to stabilize active DegS. Experiments using hybrid DegS enzymes with mixtures of full-length and ΔPDZ subunits show that all subunits in the trimer experience a strongly coupled energetic landscape, with peptide binding to a single PDZ domain stimulating proteolytic cleavage both in the attached protease domain and in neighboring domains (Mauldin and Sauer, 2013).

Proteolytic activation of DegS largely conforms to a two-state model of MWC allostery, in which the preferential binding of RseA substrates and OMP peptides to active DegS provides ~2.2 and ~4.4 kcal/mol of stabilization, respectively, relative to the inactive enzyme (Fig. 2.1B; Monod *et al*., 1965; Sohn and Sauer, 2009). Thus, only ~0.3% of substrate-saturated DegS assumes the active conformation, whereas ~83% of substrate-saturated and OMP-saturated DegS is active. $DegS^{\Delta PDZ}$ still behaves as an allosteric enzyme with respect to RseA cleavage (Sohn and Sauer, 2009; Sohn *et al*., 2007; 2010), indicating that the protease-domain trimer still adopts inactive and active conformations and thus contains the basic machinery required for allostery.

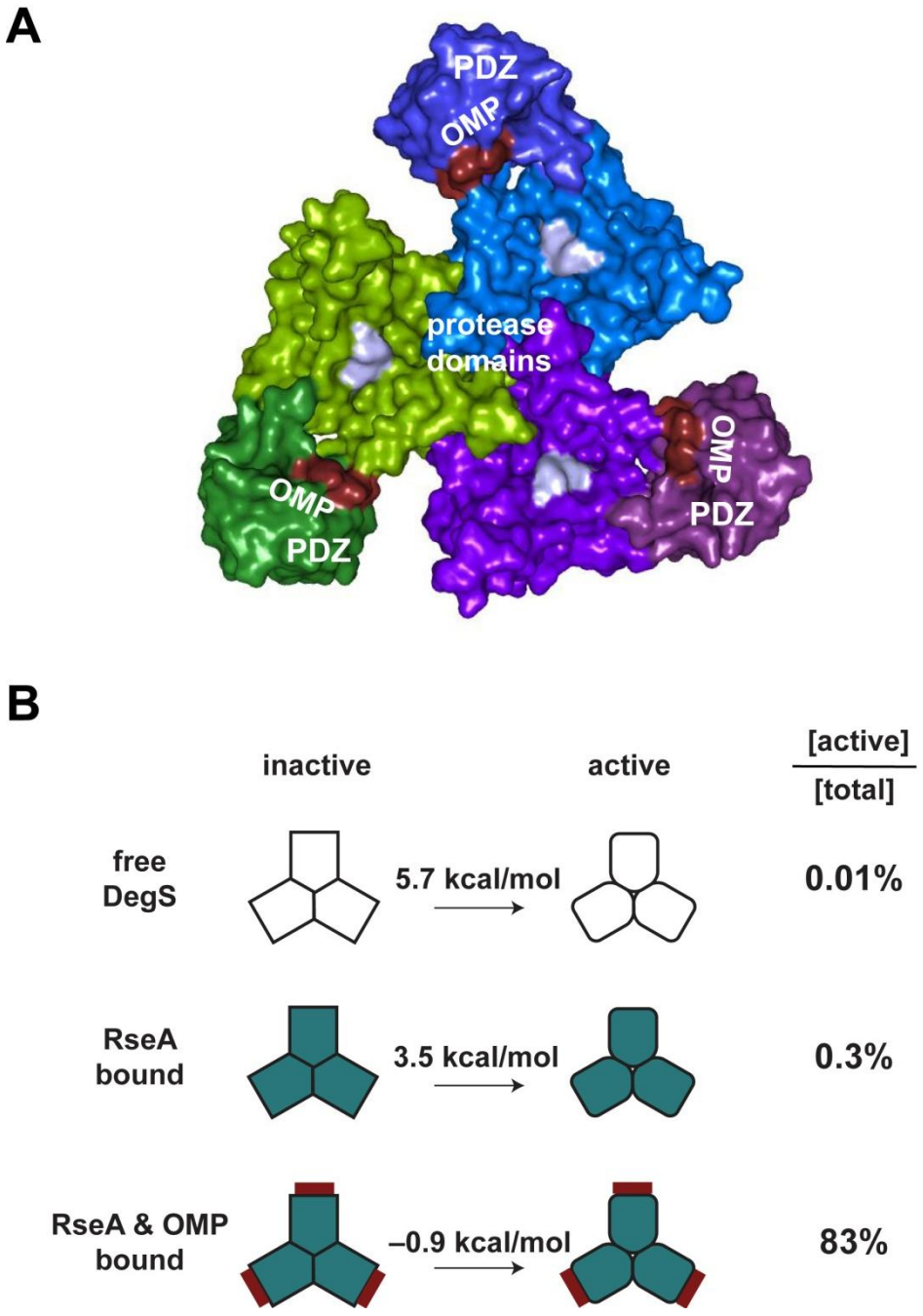

Fig. 2.1. The DegS trimer equilibrates between inactive and active structures. (A) Structure a DegS trimer in the active conformation with OMP peptides bound to the PDZ domains (pdb code 3GDS). Each DegS subunit (colored green, purple or blue) consists of a protease domain (lighter colors), which pack together to form the trimer, and a distal PDZ domain (darker colors). The catalytic triad is shown in light blue and YYF tripeptides bound to the PDZ domains are shown in red. (B) Free energies for conversion of inactive to active DegS in the free enzyme, the substrate-saturated enzyme, and the substrate and OMP-peptide saturated enzyme (Sohn and Sauer, 2009). These values would be decreased by ~4 kcal/mol for H198P DegS (Sohn et al., 2009; 2010). The column on the right lists the percentage of total DegS that assumes the active conformation for the unbound and ligand bound states.

Previous studies identified a handful of mutations that preferentially stabilize the inactive conformation compared to the active conformation of DegS or *vice versa*, and inspection of crystal structures suggested additional residues that may be involved in DegS allostery (Wilken *et al*., 2004; Hasselblatt et al., 2007; Sohn et al., 2007; 2010; Sohn and Sauer, 2009). However, there has been no comprehensive test of the importance of these residues in mediating the allosteric switch between DegS conformations. Here, we identify a critical set of amino acids needed for allosteric activation of DegS, providing a foundation for understanding regulation by substrate and OMP-peptide binding. These critical residues cluster at each subunit-subunit interface in the trimer and adjoin the active sites. Bound substrates would link these clusters and active sites around the trimer, providing a direct mechanism for allosteric activation. By contrast, bound OMP peptide appears to activate DegS indirectly by destabilizing autoinhibition. The cluster residues most important for DegS allostery are highly conserved within the HtrA-protease family, strongly suggesting that all of these enzymes function in similar fashions. Indeed, based on homology with DegS, we identify and characterize mutations that prevent allosteric activation of *E. coli* DegP, a trimeric HtrA quality-control protease that assembles into proteolytically active polyhedral cages in the presence of substrate proteins (Jiang et al. 2008; Krojer et al., 2008; Kim et al., 2011). These results have broad implications, as mutant forms of human HtrA homologs have been linked to cancer, vascular disease, arthritis, macular degeneration, and neurodegenerative disease (Grau *et al*., 2005; Coleman *et al*., 2008; Milner *et al*., 2008; Vande Walle *et al*., 2008; Chien *et al*., 2009; Hara *et al*., 2009; Bowden *et al*., 2010).

Results

Allosteric activation of DegS requires linkage between OMP-peptide binding to the PDZ domains, substrate binding to the protease domain, and the conformations of the active sites in each protease domain of the trimer (Sohn et al. 2007; Sohn and Sauer, 2009; Mauldin and Sauer, 2013). Based on interactions observed in DegS crystal structures, numerous side chains have previously been proposed to be important for allosteric switching or were selected for analysis in this study (Table 2.1). Most of these amino acids lie between the binding sites for OMP peptide in the PDZ domains and the proteolytic active sites. In the sections below, we discuss evidence for or against these residues playing important roles in allosteric switching.

To monitor proteolytic activity *in vitro*, we purified wild-type or mutant variants of DegS without the membrane anchor and determined second-order rate constants (k_{cat}/K_M) for cleavage of sub-K_M concentrations of a ^{35}S-labeled protein fragment corresponding to the periplasmic domain of RseA in the presence of saturating Tyr-Tyr-Phe (YYF) peptide (Sohn et al., 2007). The effects of different mutations were measured in otherwise wild-type backgrounds and also in combination with the H198P mutation, which stabilizes active DegS (Sohn et al., 2009; 2010) and increased the proteolytic activity of otherwise wild-type DegS ~6-fold under the assay conditions used (Fig. 2.2). The H198P mutation increased the relative proteolytic activities of some but not all mutations that diminish DegS activity (compare top and bottom panels in Fig. 2.2), allowing the relative importance of different mutations for proteolysis and allosteric switching to be determined.

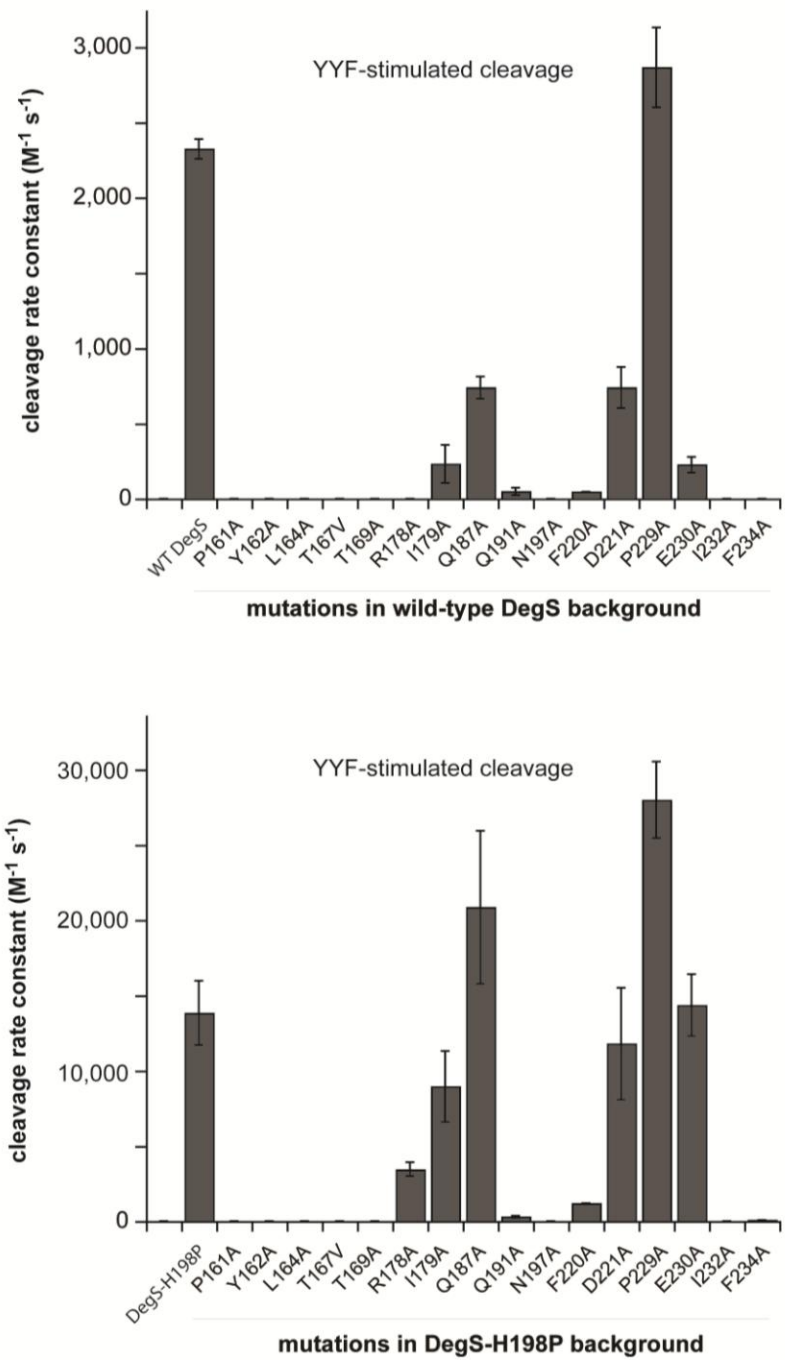

Fig. 2.2. Mutational effects on DegS cleavage of RseA. Effects of DegS mutations in an otherwise wild-type background (upper panel) or in an H198P background (lower panel) on OMP-peptide stimulated proteolytic activity, expressed as the second-order rate constant (k_{cat}/K_M) for RseA cleavage. Values are averages of two or more independent trials ± SEM. Cleavage reactions contained different sub-K_M concentrations of ^{35}S-labelled RseA, DegS or variants (1 μM trimer), and YYF OMP peptide (230 μM). Initial cleavage rates normalized by total enzyme were plotted as a function of the RseA concentration, and the second-order rate constant was determined from the slope of a linear fit.

Residues that Play Major Roles in Allosteric Switching

The side chains of Pro^{161}, Tyr^{162}, Leu^{164}, Thr^{167}, Thr^{169}, Gln^{191}, Asn^{197}, Ile^{232}, and Phe^{234} in DegS play very important roles in allosteric switching by the following criteria. The P161A, Y162A, L164A, T167V, T169A, Q191A, N197A, I232A, and F234A mutants had less than 2% of YYF-stimulated wild-type cleavage activity, and combining these mutations with the H198P mutation did not rescue cleavage activity appreciably (Fig. 2.2; Table 2.1). The Arg^{178} and Phe^{220} side chains of DegS play somewhat important roles, as the R178A and F220A mutants had almost no cleavage activity, but the R178A/H198P and F220A/H198P mutants had activities between 9-24% of the parental enzyme. All of the mutant enzymes were soluble and well-behaved during purification, suggesting that the mutations had no substantial effects on folding or trimerization, and previously determined crystal structures of ΔPDZ variants of Y162A, Y162A/H198P, T167V/H198P, and Q191A showed that these mutants form stable trimers with the protease domain in the proteolytically inactive conformation (Sohn et al., 2010).

By monitoring changes in the anisotropy of a fluorescein-labeled OMP peptide as a function of increasing concentrations of mutant DegS variants (Sohn et al., 2007), we determined binding affinities for the P161A, Y162A, L164A, T167V, T169A, R178A, Q191A, N197A, F220A, I232A, and F234A proteins in wild-type and H198P enzyme backgrounds. Each mutant bound OMP peptide with a K_D similar to or slightly stronger than wild-type DegS or $DegS^{H198P}$ (Table 2.1). Thus, the observed proteolytic defects of these mutants is not a consequence of an inability to bind OMP peptide. Rather, OMP-peptide binding to these mutants is not sufficient to shift most enzymes from the inactive to the active protease conformation.

Residues that Play Minor Roles or No Role in Allosteric Switching

Based on the crystal structures of active and inactive DegS, the side chains of Ile^{179}, Pro^{183}, Gln^{187}, Asp^{221}, and Glu^{227} were proposed to play important roles in activation (Wilken et al., 2004; Hasselblatt et al., 2007). Both the P183A and E227A DegS mutants were previously found to have OMP-stimulated activities similar to or slightly higher than wild-type DegS (Sohn *et al*., 2007), indicating that these side chains play no significant role in allosteric switching. Here, we found that I179A, Q187A, and D221A DegS displayed reduced YYF-stimulated cleavage activity compared to wild-type DegS (Fig. 2.2), but I179A/H198P, Q187A/H198P, and D221A/H198P DegS had YYF-stimulated cleavage activities that were 65% or more of the H198P parent (Fig. 2.2; Table 2.1). Thus, the Ile^{179}, Gln^{187}, and Asp^{221} side chains play minor roles in stabilizing active compared to inactive DegS but are not critical determinants of allostery.

Pro^{229} and Glu^{230} assume different conformations in active and inactive DegS structures (Sohn et al., 2010). We found that the P229A mutant was more active than wild-type DegS and H198P/P229A was more active than H198P (Fig. 2.2). Thus, the pyrrolidine ring of Pro^{229} is not important for allosteric activation. The E230A mutant had ~10% of wild-type activity, whereas H198P/E230A had activity within error of H198P (Fig. 2.2). Hence, the Glu^{230} side chain plays a minor role in DegS activation.

Structural Roles of Key Allosteric Residues

Prior to examination of the structural roles of DegS side chains that play important roles in allosteric switching, we sought to resolve apparent discrepancies among active and inactive crystal structures determined by different groups. For example, the side chains of Thr^{167}, Arg^{178},

and Gln^{191} form a hydrogen-bond network in the all of the active DegS structures determined in our lab (Sohn et al., 2007; 2009; 2010), but a badly eclipsed rotamer of Thr^{167} prevents hydrogen bonding in the 1SOZ structure determined by another group (Fig. 2.3A; Wilken et al., 2004; Hasselblatt et al., 2007). When we re-refined this structure, improving *R* factors and geometry (Table 2), the side chains of Thr^{167}, Arg^{178}, and Gln^{191} formed a hydrogen-bonding network (Fig. 2.3B) similar to those in our previous DegS structures. We also re-refined several inactive or hybrid structures of DegS to improve geometry. As determined by MolProbity analysis (Chen et al., 2010), for example, the 1TE0 structure of inactive DegS (Zeth, 2004) had extremely poor geometry (23% poor rotamers; 7% Ramachandran outliers; 13% Cβ deviations; 3% bad backbone bonds; 3% bad backbone angles), suggesting a highly strained conformation or a poorly refined structure. By contrast, the 1SOT structure of full-length inactive DegS (Wilken *et al*., 2004) had somewhat better geometry (6% poor rotamers; 3% Ramachandran outliers; 0.4% C_β deviations; 0.1% bad backbone bonds; 0.4% bad backbone angles), suggesting less strain or better refinement. The 1VCW structure of active DegS after removal of bound OMP peptide by soaking (Wilken *et al*., 2004) also had geometric issues (8% poor rotamers; 4% Ramachandran outliers; 1% Cβ deviations; 0.2% bad backbone bonds; 0.8% bad backbone angles). Our re-refined 1TE0, 1SOT, and 1VCW structures had improved *R* factors and no poor rotamers, Ramachandran outliers, Cβ deviations, or bad backbone bonds or angles (Table 2.2). Thus, inactive or hybrid DegS does not assume an obviously strained conformation.

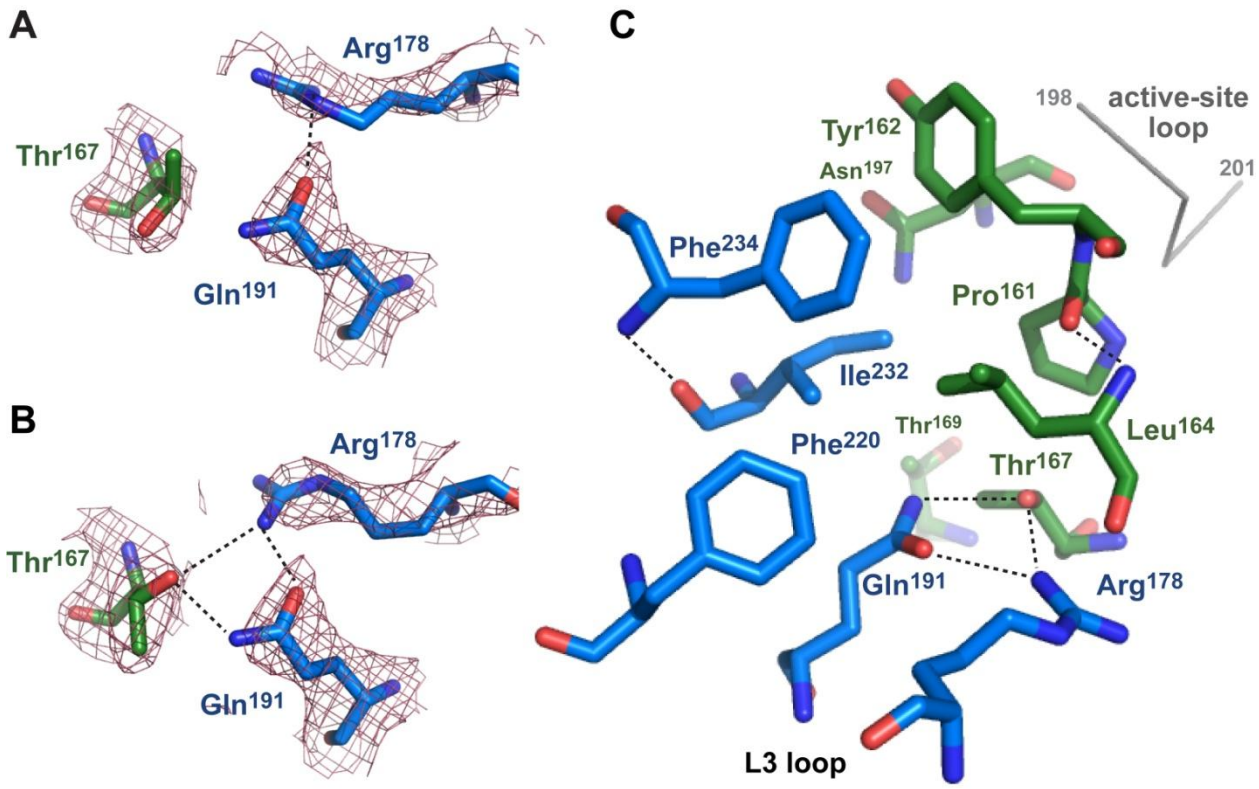

Fig. 2.3. Structural determinants of DegS activation. (A) Electron-density map ($2F_O–F_C$; contoured at 1.3 σ) for Thr[167] in chain B (dark green carbons) and Arg[178] and Gln[191] in chain C (marine carbons) in the 1SOZ DegS trimer. Thr[167] is modeled in an eclipsed conformation (χ 116°) found in only 0.1% of high-resolution structures. A hydrogen bond is shown as a dashed black line. (B) Electron-density map (same residues and parameters as panel A) but for the 4G0G re-refined structure of 1SOZ. Thr[167] is modeled as a rotamer (χ 290°) found in 18.7% of high-resolution structures and forms hydrogen bonds (dashed black lines) with Arg[178] and Gln[191]. (C) Residues identified as being very important or somewhat important for DegS allostery cluster between the active-site loop containing the catalytic Ser[201] and oxyanion hole (top right) and the L3 loop (bottom center). Residues with marine-colored carbons are from one subunit of the 4G0G trimer and those with dark-green carbons are from another subunit. The residues shown represent one of the three activation clusters in the DegS trimer. Hydrogen bonds are represented as dashed black lines.

The residues we identified as playing the most important roles in allosteric activation cluster together at the subunit-subunit interfaces of the active conformation of the DegS trimer (Fig. 2.3C). The cluster is stabilized by hydrophobic packing between the side chains of Tyr[162], Leu[164], Phe[220], Ile[232], and Phe[234], and by hydrogen bonds involving side-chain atoms of Thr[167], Arg[178], and Gln[191] or main-chain atoms of Pro[161] Leu[164], Phe[220], and Ile[232]. OMP-peptide binding causes repositioning of the L3 loop, which includes Arg[178], on the outer edge of the cluster. Main-chain and side-chain atoms from Pro[161] and Tyr[162] on the inner edge of the cluster contact and stabilize

the functional conformation of the active-site loop (residues 198-201) that forms the oxyanion hole and contains the catalytic Ser^{201}. The side chains of Thr^{169} and Asn^{197} make hydrogen bonds that indirectly connect the active-site loop to parts of the activation cluster. Importantly, these "activation clusters" are present in all crystal structures of DegS in the active conformation, including DegS with bound OMP peptides and $DegS^{\Delta PDZ}$ (Wilken *et al*., 2004; Zeth, 2004; Hasselblatt et al., 2007; Sohn et al., 2007; 2009; 2010). Moreover, activation clusters with very similar structural features are present in the functional conformations of a DegS ortholog from *Mycobacterium tuberculosis* (2Z9I; Mohamedmohaideen et al., 2008) and in *E. coli* DegP (3OU0; 3OTP; Kroger et al., 2008; Kim et al., 2011).

In the inactive conformation of full-length DegS, represented by the re-refined 1TE0 structure, many residues of the activation cluster occupy substantially different positions than in the active conformation. For example, the side chains of Arg^{178}, Phe^{220}, and Tyr^{162} move more than 10 Å, disrupting numerous packing and polar interactions. Indeed, all of the hydrogen bonds present in the functional activation cluster are missing in the inactive conformation. As a consequence of these structural rearrangements, the 198-201 active-site loop adopts an altered conformation which destroys the oxyanion hole. The R178A mutation has two effects. It destabilizes the activation cluster in active DegS by removing part of a hydrogen-bond network but also removes an autoinhibitory salt-bridge with Asp^{320} in the unliganded PDZ domain in inactive DegS (Sohn et al., 2007), which is likely to ameliorate the severity of this mutation. Interestingly, after removal of OMP peptide from active DegS by crystal soaking, the activation clusters remained intact, except for Arg^{178}, which again formed a salt-bridge with Asp^{320} in the PDZ domain, and Phe^{220}, which became disordered. Like R178A, F220A was one of the least severe of the activation-cluster mutations (Fig. 2.2).

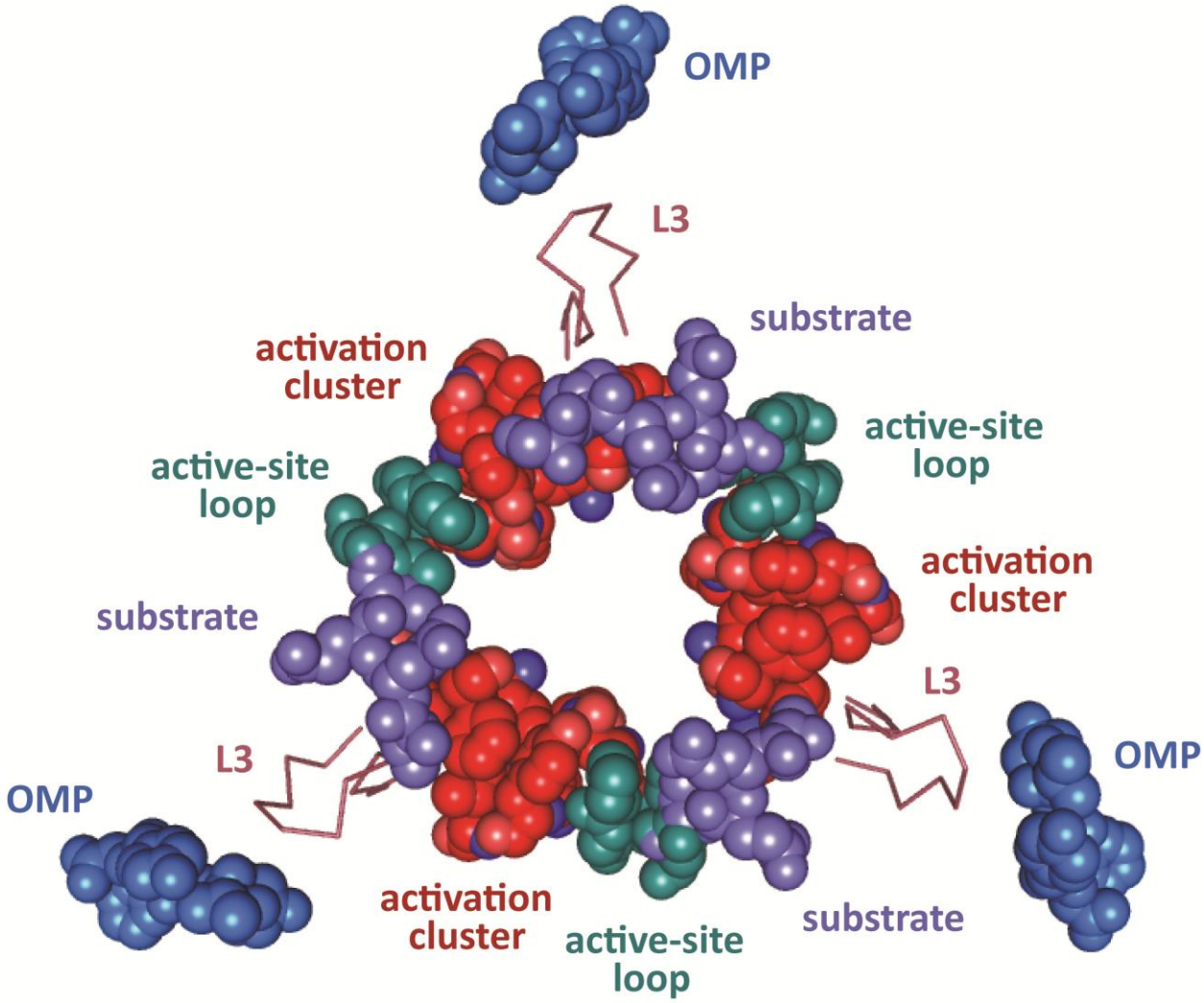

Fig. 2.4. Allosteric ligands and catalytic and regulatory elements in active DegS. Positions of OMP peptides, L3 loops, activation clusters, active-site loops, and modeled substrate in an active DegS trimer (3GDS). The position of substrate was modeled by aligning 4G0G with a DegS ortholog from *Mycobacterium tuberculosis* with a bound substrate-cleavage product (2Z9I; Mohamedmohaideen et al., 2008). Although the PDZ-bound OMP peptides are adjacent to the L3 loops, there are no critical residues between the OMP peptide and the activation clusters, suggesting that OMP-peptide binding destabilizes autoinhibitory interactions rather than directly stabilizing the active conformation. Substrate binding ties together all of the active-site loops and activation clusters in the trimer, providing a mechanism for allosteric substrate stabilization of the active conformation.

Parts of the RseA substrate are likely to interact directly with the activation cluster. For example, the carbonyl oxygen of the scissile peptide bond would bind in the oxyanion hole, which is mimicked by fluorophosphate modification of the active-site Ser^{201} side chain in many structures (Sohn et al., 2007; 2009; 2010). The S5-S1 positions of RseA are also likely to interact with parts of the DegS activation cluster, based upon structures of orthologs with peptide fragments bound

to the active site (Mohamedmohaideen et al., 2008; Kim et al., 2011). Indeed, some effects of the F220A mutation on RseA cleavage may arise from weaker substrate binding. As shown in Fig. 2.4, part of a bound substrate is predicted to contact the active-site loop and adjacent activation cluster. We assume that some of these contacts are not made in inactive DegS, explaining allosteric activation by preferential substrate binding to active DegS.

Fig. 2.4 shows that bound OMP peptides are not in close physical proximity to the activation clusters. Moreover, mutations in L3-loop residues that lie between bound OMP peptide and the activation cluster do not have substantial defects in proteolytic activity, supporting a model in which OMP binding serves only to relieve autoinhibitory interactions that stabilize the inactive state and does not play a role in directly stabilizing the active conformation of the protease domain (Sohn et al. 2007; 2010). This loss-of-inhibition model also explains why the conformations of the residues of the active site and activation cluster are almost identical in $DegS^{\Delta PDZ}$ and in OMP-peptide bound DegS.

Mutations that Block Allosteric Switching in DegP

The DegP protease differs from DegS in several ways. First, the allosteric transition from inactive to proteolytically active DegP trimers is driven by binding of one degron in a protein substrate to the active site and by binding of a second C-terminal degron in the same substrate to a tethering site in the DegP PDZ1 domain (Kim et al., 2011). Second, proteolytic activation is accompanied by assembly of DegP trimers into polyhedral cages with 12, 18, 24, or 30 subunits (Jiang et al., 2008; Kroger et al., 2008; Kim et al., 2011), although cage formation is not required for proteolytic activation (Kim et al., 2012). To test if DegP uses a pathway of allosteric activation similar to DegS, we focused on DegP residues Thr^{176}, Arg^{187}, and Gln^{200}, which form

a hydrogen-bond network in active DegP (Fig. 2.5A) but not in the inactive enzyme (Kroger et al., 2002; 2008; Kim et al., 2011). These residues correspond to Thr^{167}, Arg^{178}, and Gln^{191} in DegS, and the networks formed by each set of residues in the active structures are similar (cf. Figs. 2.3B and 2.5A). If these DegP interactions are important for allosteric switching, then mutation of these residues should prevent or greatly diminish proteolytic activity, weaken substrate binding, and reduce or eliminate the positive cooperativity of substrate binding. To test these predictions, we made individual T176V, R187A, and Q200A mutations in DegP. Each mutation severely compromised substrate degradation. For example, purified $DegP^{T176V}$, $DegP^{R187A}$, and $DegP^{Q200A}$ exhibited no detectable degradation of lysozyme denatured by carboxymethylation of cysteines after 40 min, whereas wild-type DegP degraded most of this substrate within 5 min (Fig. 2.5B). To assay degradation activity more quantitatively, we used a fluorescent 23-residue peptide (p23) derived from lysozyme at a concentration ~20-fold above the wild-type K_M. $DegP^{Q200A}$ cleaved p23 at a rate much lower than wild-type DegP, whereas the rate of cleavage of p23 by $DegP^{T176V}$ and $DegP^{R187A}$ was negligible (Fig. 2.5C).

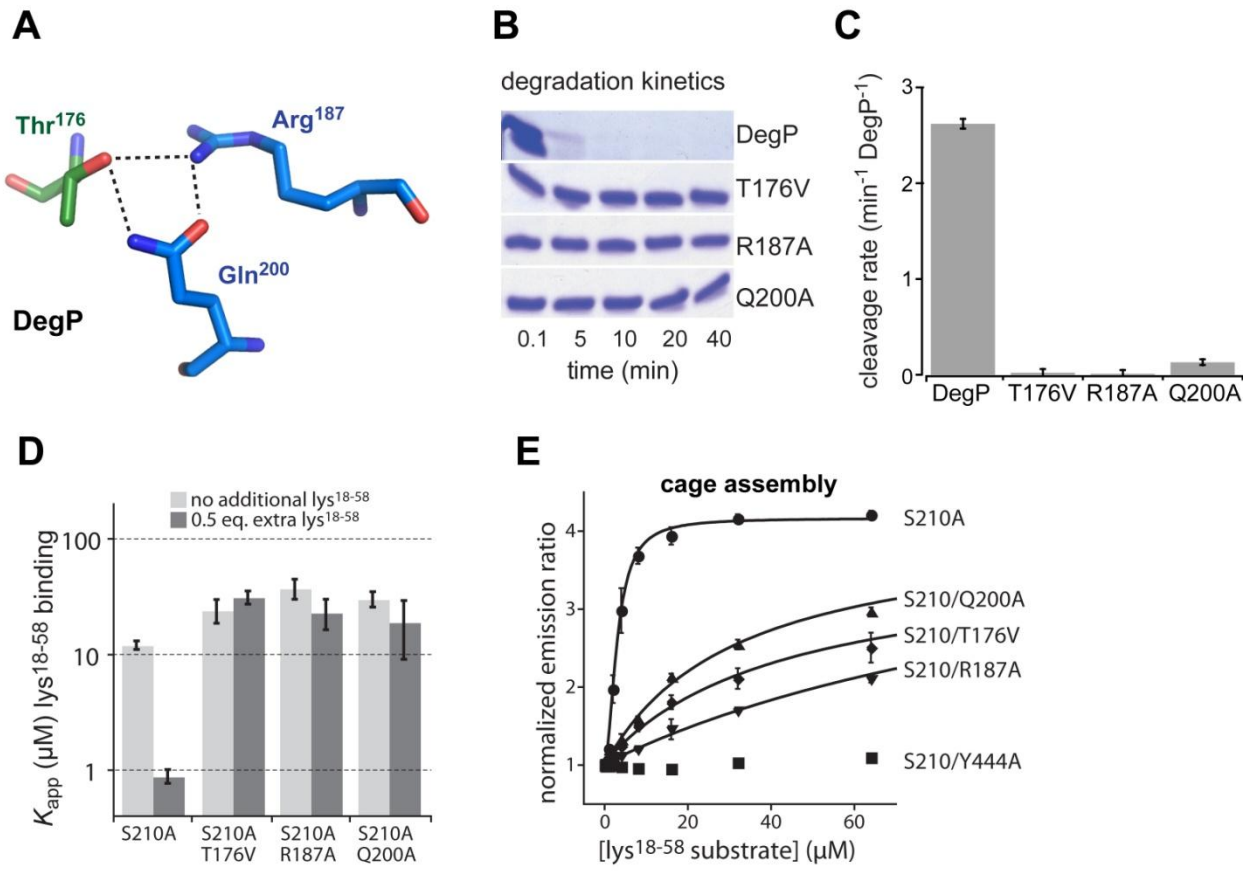

Fig. 2.5. Effects of activation-cluster mutations on DegP activity and cage assembly. (A) The side chain of Thr^{176} from one DegP subunit (dark-green carbons) forms hydrogen bonds with the side chains of Arg^{187} and Gln^{200} in an adjacent subunit (marine carbons) in the protease domain of an active DegP trimer (3OTP). (B) Kinetics of degradation of carboxymethylated lysozyme (5 μM) by wild-type DegP and the T176V, R187A, or Q200A variants (1 μM) at room temperature was assayed by SDS-PAGE and staining with Coomassie Blue. (C) Rates of cleavage of the p23 substrate (40 μM) by wild-type DegP or variants (1 μM) were determined at room temperature. Error bars are averages ±1 SD (N = 3). (D) Apparent equilibrium dissociation constants (K_{app}) for binding of different concentrations of proteolytically inactive $DegP^{S210A}$ or variants to a fluorescent substrate ($^{flC}lys^{18-58}$; 50 nM) were determined in the absence or presence of unlabeled lys^{18-58} at one-half of the DegP concentration by changes in fluorescence anisotropy (Kim et al., 2011; Kim & Sauer, 2012). Positive cooperativity makes binding stronger in the presence of unlabeled lys^{18-58} for variants, like $DegP^{S210A}$, that can switch between the inactive and active conformations. The T167V, R187A, and Q200A mutations weakened binding and eliminated positive cooperativity. Bars represent the error of fitting of individual binding curves to a hyperbolic binding equation. (E) Polyhedral-cage assembly of DegP variants as a function of added lys^{18-58} substrate was monitored by increases in FRET between trimers labeled with donor and acceptor dyes (Kim et al., 2011). Emission ratios were normalized to data in the absence of substrate and fitted to a Hill equation ($y = y_0 + max \bullet [lys^{18-58}]^h/(K_{app}{}^h + [lys^{18-58}]^h)$) for $DegP^{S210A}$ or to a hyperbolic equation ($y = y_0 + max \bullet [lys^{18-58}]/(K_{app} + [lys^{18-58}])$) for variants containing the T176V, R187A, or Q200A mutations. No assembly of the $DegP^{S210A/Y444A}$ variant was observed, as expected because the Y444A mutation removes a critical interaction that stabilizes cages (Kim et al., 2011). Error bars are averages ±1 SD (N = 3).

To assay substrate binding, we monitored the change in fluorescence anisotropy of a fluorescent peptide derived from residues 18-58 of lysozyme (lys^{18-58}) upon addition of DegP variants. In one set of experiments, equilibrium binding curves and apparent affinities were determined after incubation of a low concentration of fluorescent lys^{18-58} with different concentrations of $DegP^{S210A}$ (a proteolytically inactive variant missing the catalytic serine), $DegP^{S210A/T176V}$, $DegP^{S210A/R187A}$, or $DegP^{S210A/Q200A}$. In a second set of experiments, binding mixtures were supplemented with non-fluorescent lys^{18-58} at one-half of the enzyme concentration, which should result in stronger binding for variants that display positively cooperative substrate binding (Kim et al., 2011). Addition of unlabeled substrate strengthened the apparent affinity of $DegP^{S210A}$ for fluorescent lys^{18-58} from ~12 μM to ~1 μM (Fig. 2.5D). By contrast, $DegP^{S210A/T176V}$, $DegP^{S210A/R187A}$, and $DegP^{S210A/Q200A}$ displayed comparable affinities (~30 μM) in the presence and absence of unlabeled substrate (Fig. 2.4D). Thus, the T176V, R187A, and Q200A mutations almost completely eliminate degradation, weaken substrate binding, and abolish positive cooperativity, as expected if these variants are largely trapped in the inactive state, even when substrate is bound.

Formation of DegP cages was monitored by fluorescence resonance energy transfer (FRET) between trimers labeled with donor dyes and trimers labeled with acceptor dyes as described (Kim et al., 2011). Mixtures of acceptor and donor labeled trimers were prepared in the S210A, S210A/T176V, S210A/R187A, and S210A/Q200A backgrounds and FRET was assayed as a function of increasing quantities of lys^{18-58} substrate (Fig. 2.5E). Notably, we observed substrate-dependent increases in FRET for the T176V, R187A, and Q200A variants, although compared to the S210A experiment substantially more lys^{18-58} was required to drive an equivalent level of cage assembly by the variants. As expected, no change in FRET was observed for a variant

bearing the Y444A mutation, which removes contacts required for cage formation (Kim et al., 2011). These results support a model in which the T176V, R187A, and Q200A variants assemble into cages in which the component trimers remain in the "inactive" conformation, albeit requiring higher substrate concentrations because of weaker and non-cooperative substrate binding.

Discussion

Our results identify a set of amino acids that play critical roles in allosteric activation of the *E. coli* DegS protease. Mutation of these residues almost completely eliminates proteolytic activity in the presence of OMP peptides that activate substrate cleavage by wild-type DegS. From an energetic perspective, if a single mutation in one activation cluster destabilizes active DegS by ~1-2 kcal/mol relative to inactive DegS, then the active trimer would be destabilized by 3-6 kcal/mol and little or no activation by substrate and OMP-peptide binding would be expected. The activation cluster of DegS is highly conserved in the *E. coli* DegP protease. Indeed, we found that mutation of some of these residues in DegP eliminated or dramatically decreased proteolytic activity, as well as reducing the affinity and eliminating the positive cooperativity of substrate binding. Strikingly, the amino acids that are critical determinants of allosteric activation of DegS are also highly conserved in homologous proteases from all kingdoms of life (Fig. 2.6). Thus, we propose that a conserved mechanism of allosteric activation is a fundamental feature of this entire super-family of proteases, including human HtrA enzymes linked to a wide spectrum of diseases.

Fig. 2.6. Side chains important for DegS allostery are conserved in the HtrA family. Residues shown here to be very important (red labels) or somewhat important (orange labels) for allosteric activation of DegS are largely conserved in HtrA proteases from all kingdoms of life. Residues that play minor roles (blue labels) or no role (black label) in DegS activity are far less conserved. HtrA sequences from *E. coli* (3), *H. sapiens* (4), *Synechocystis* (3), *D. rerio*, *A. thaliana*, *C. reinhardtii*, *D. melanogaster*, *B. dendrobatidis*, *A. pseudotrichonymphae,* and *K. cryptofilum* were aligned using ClustalW2 (Larkin *et al.*, 2007) and submitted to WebLogo (Crooks *et al.*, 2004) for visualization of conservation information. A higher number of bits indicates greater conservation for a given position.

Why is allosteric activation of HtrA proteases so important? The activities of all intracellular proteases must be carefully regulated to allow them to degrade the proper target substrates but to avoid degrading proteins required for cellular function. By linking proteolytic activation to assembly of specific enzyme-substrate or enzyme-substrate-activator complexes, these potentially dangerous enzymes can be maintained in an inactive state until the appropriate substrates and/or activators are present. Moreover, because allosteric activation is reversible, these proteases switch back to inactive conformations once protein substrates are degraded or activators are removed. Cage formation provides a second level of cellular protection for many HtrA proteases, as activation leads to assembly of complexes in which the proteolytic active sites are sequestered and only accessible to unfolded proteins that can enter the degradation chamber. Indeed, recent studies show that DegP mutations that prevent cage formation and facilitate allosteric activation result in rogue proteolysis that kills cells (Kim et al., 2014).

For DegS, an unresolved question is how OMP-peptide binding to the PDZ domains transmits a signal that results in remodeling the protease domain into an active conformation. An early model suggested that contacts between residues of the OMP peptide and the L3 loop of DegS directly stabilized the active conformation (Wilken et al., 2004). This model, however, is inconsistent with numerous results, including the robust activity of $DegS^{\Delta PDZ}$ and crystal structures of OMP-bound active DegS that show no conserved contacts between the OMP peptide and the L3 loop (Sohn et al., 2007; 2010). Nevertheless, OMP-peptide binding is a key step in activation of full-length DegS and thus these binding events must either destabilize inactive DegS or stabilize active DegS by some mechanism. One possibility is that OMP-peptide binding causes conformational changes in the PDZ domain that then result in clashes with the L3 loop, initiating the conformational change in the protease domains (Sohn and Sauer, 2009). OMP-peptide binding to a single PDZ domain stimulates proteolytic activation of both the attached and neighboring protease domains in the DegS trimer (Mauldin and Sauer, 2013). The clusters of DegS residues that mediate allosteric switching are located at subunit-subunit interfaces in the protease domain, providing a simple mechanism by which binding of one OMP peptide could change the conformations of all subunits in the DegS trimer.

Methods

Protein Expression and Purification

Wild-type and mutant variants of *E. coli* DegS (residues 27-355) with an N-terminal His_6 tag replacing the wild-type membrane anchor and an ^{35}S-labeled variant of the periplasmic domain of *E. coli* RseA (residues 121-216) were expressed and purified as described (Sohn et al., 2007; Cezairliyan and Sauer, 2009). YYF peptide was synthesized by GenScript and purified by high-pressure liquid chromatography. DegP variants were purified as described (Kim et al., 2011).

Enzymatic and Biochemical Assays

DegS cleavage of RseA and OMP-peptide binding assays were performed as described (Sohn et al., 2007; Cezairliyan and Sauer, 2009). Briefly, cleavage was performed by incubating DegS or variants with YYF tripeptide and different sub-K_M concentrations of ^{35}S-RseA. Time points were quenched in 10% trichloroacetic acid and acid-soluble radioactive cleavage products were quantified by scintillation counting to calculate cleavage rates. Binding assays were performed by titrating increasing DegS or variants against a fixed concentration of the fluorescent OMP peptide fluorescein-DNRDGNVYYF and monitoring changes in fluorescence anisotropy (excitation 480 nm; emission 520 nm), after correction for protein scattering. Binding curves were fit using Prism (GraphPad). Substrate cleavage by DegP, binding of substrate to proteolytically inactive DegP, and substrate-mediated cage assembly assays were performed as described (Kim et al., 2011; Kim and Sauer, 2012).

Structural Refinement

Structure factors for 1SOT, 1SOT, 1TE0, and 1VCW were obtained from the Protein Data Bank. Re-refinement was performed using COOT (Emsley and Cowtan, 2004) for model building, MolProbity (Chen et al., 2010) for assessment of model geometry, and PHENIX (Adams et al., 2010) for refinement.

Sequence Alignment

The sequences for the following HtrA proteins (with associated accession numbers) were downloaded from UniProt: *E. coli* DegS (P0AEE3), *E. coli* DegP (P0C0V0), *E. coli* DegQ (P39099), *Synechocystis* HtrA (HTRA_SYNY3), *Synechocystis* HhoA (P72780), *Synechocystis* HhoB (P73940), *H. sapiens* HtrA1 (Q92743), *H. sapiens* HtrA2 (O43464), *H. sapiens* HtrA3

(P83110), *H. sapiens* HtrA4 (P83105), *D. rerio* HtrA1a (Q6GMI0), *A. thaliana* DegP1 (O22609), *D. melanogaster* HtrA2 (Q9VFJ3), *C. reinhardtii* DegP-type protease (A8HQB3) *B. dendrobatidis* putative uncharacterized protein (F4P0R9), *A. pseudotrichonymphae* DegQ (B6YQJ5) and *K. cryptofilum* Serine protease Do (B1L493). Sequences were aligned in ClustalW2 (Larkin *et al.*, 2007). Alignments at positions highlighted in this paper were collected and submitted to WebLogo (Crooks *et al.*, 2004) for visualization.

Accession Numbers

The re-refined 1SOT, 1SOT, 1TE0, and 1VCW structures of DegS have been deposited in the Protein Data Bank with accession codes 4G0E, 4G0G, 4G18, and 4G15, respectively.

Acknowledgements

Supported by NIH grant AI-16892 and a Charles A. King Trust Postdoctoral Fellowship to S.K. T.A.B. is an employee of the Howard Hughes Medical Institute.

References

Adams, P.D. et al. (2010). PHENIX: a comprehensive Python-based system for macromolecular structure solution. *Acta Crystallogr.* D *66*, 213–221.

Ades, S.E., Connolly, L.E., Alba, B.M., and Gross, C.A. (1999). The *Escherichia coli* sigma(E)-dependent extracytoplasmic stress response is controlled by the regulated proteolysis of an anti-sigma factor. Genes Dev. *13*, 2449–2461.

Ades, S.E. (2008). Regulation by destruction: design of the σ^E envelope stress response. Curr. Opin. Microbiol. *11*, 535–540.

Akiyama, Y., Kanehara, K., and Ito, K. (2004). RseP (YaeL), an *Escherichia coli* RIP protease, cleaves transmembrane sequences. EMBO J. *23*, 4434–4442.

Alba, B.M., and Gross, C.A. (2004). Regulation of the *Escherichia coli* sigma-dependent envelope stress response. Mol. Microbiol. *52*, 613–619.

Bowden, M.A. *et al*. (2010). High-temperature requirement factor A3 (Htra3): a novel serine protease and its potential role in ovarian function and ovarian cancers. Mol. Cell. Endocrinol. *327*, 13–18.

Chaba, R., Grigorova, I.L., Flynn, J.M., Baker, T.A., and Gross, C.A. (2007). Design principles of the proteolytic cascade governing the sigmaE-mediated envelope stress response in *Escherichia coli*: keys to graded, buffered, and rapid signal transduction. Genes Dev. *21*, 124–136.

Chen, V.B., Arendall, W.B., Headd, J.J., Keedy, D.A., Immormino, R.M., Kapral, G.J., Murray, L.W., Richardson, J.S., and Richardson, D.C. (2010). MolProbity: all-atom structure validation for macromolecular crystallography. Acta Crystallogr. D Biol. Crystallogr. *66*, 12–21.

Chien, J., Campioni, M., Shridhar, V., and Baldi, A. (2009). HtrA serine proteases as potential therapeutic targets in cancer. Curr. Cancer Drug Targets *9*, 451–468.

Coleman, H.R., Chan, C.C., Ferris, F., and Chew, E.Y. (2008). Age-related macular degeneration. Lancet *372*, 1835–1845.

Crooks, G.E., Hon, G., Chandonia, J.M., and Brenner, S.E. (2004). WebLogo: A sequence logo generator. Genome Research *14*, 1188–1190.

Flynn, J.F., Levchenko, I., Sauer, R.T. and Baker, T.A. (2004). Modulating substrate choice: the SspB adaptor delivers a regulator of the extracytoplasmic-stress response to the AAA+ protease ClpXP for degradation. Genes Dev. *18*, 2292–2301.

Emsley, P., and Cowtan, K. (2004). Coot: model-building tools for molecular graphics. Acta Crystallogr. D *60*, 2126–2132.

Grau, S. *et al*. (2005). Implications of the serine protease HtrA1 in amyloid precursor protein processing. Proc. Natl. Acad. Sci. USA *102*, 6021–6026.

Hara, K. *et al*. (2009). Association of HTRA1 mutations and familial ischemic cerebral small-vessel disease. N. Engl. J. Med. *360*, 1729–1739.

Hasselblatt, H., Kurzbauer, R., Wilken, C., Krojer, T., Sawa, J., Kurt, J., Kirk, R., Hasenbein, S., Ehrmann, M., and Clausen, T. (2007). Regulation of the sigmaE stress response by DegS: how the PDZ domain keeps the protease inactive in the resting state and allows integration of different OMP-derived stress signals upon folding stress. Genes Dev. *21*, 2659–2670.

Jiang, J., Zhang, X., Chen, Y., Wu, Y., Zhou, Z.H., Chang, Z., and Sui, S.F. (2008). Activation of DegP chaperone-protease via formation of large cage-like oligomers upon binding to substrate proteins. Proc. Natl. Acad. Sci. USA *105*, 11939–11944.

Kanehara, K., Ito, K., and Akiyama, Y. (2002). YaeL (EcfE) activates the sigma(E) pathway of stress response through a site-2 cleavage of anti-sigma(E), RseA. Genes Dev. *16*, 2147–2155.

Kim, S., and Sauer, R.T. (2012). Cage assembly of DegP protease is not required for substrate-dependent regulation of proteolytic activity or high-temperature cell survival. Proc. Natl. Acad. Sci. USA *109*, 7263–7268.

Kim, S., and Sauer, R.T. (2014). Distinct regulatory mechanisms balance DegP proteolysis to maintain cellular fitness during heat stress. Genes Dev. *28*, 902–911.

Kim, S., Grant, R.A., and Sauer, R.T. (2011). Covalent linkage of distinct substrate degrons controls assembly and disassembly of DegP proteolytic cages. Cell *145*, 67–78.

Krojer, T., Garrido-Franco, M., Huber, R., Ehrmann, M., and Clausen, T. (2002). Crystal structure of DegP (HtrA) reveals a new protease-chaperone machine. Nature *416*, 455–459.

Krojer, T., Sawa, J., Schafer, E., Saibil, H.R., Ehrmann, M., and Clausen, T. (2008). Structural basis for the regulated protease and chaperone function of DegP. Nature *453*, 885–890.

Larkin, M.A., Blackshields, G., Brown, N.P., Chenna, R., McGettigan, P.A., McWilliam, H., Valentin, F., Wallace, I.M., Wilm, A., Lopez, R., Thompson, J.D., Gibson, T.J., and Higgins, D.G. (2007). ClustalW and ClustalX version 2. Bioinformatics *23*, 2947–2948.

Li, X., Wang, B., Feng, L., Kang, H., Qi, Y., Wang, J., and Shi, Y. (2009). Cleavage of RseA by RseP requires a carboxyl-terminal hydrophobic amino acid following DegS cleavage. Proc. Natl. Acad. Sci. USA *106*, 14837–14842.

Lima, S., Guo, M.S., Chaba. R., Gross, C.A., and Sauer, R.T. (2013). Dual molecular signals mediate the bacterial response to outer-membrane stress. Science *340*, 837–841.

Mauldin, R.V., and Sauer, R.T. (2013). Allosteric regulation of DegS protease subunits though a shared energy landscape. Nat. Chem. Biol. *9*, 90–96.

Milner, J.M., Patel, A., and Rowan, A.D. (2008). Emerging roles of serine proteinases in tissue turnover in arthritis. Arthritis Rheum. *58*, 3644–3656.

Mohamedmohaideen, N.N., Palaninathan, S.K., Morin, P.M., Williams, B.J., Braunstein, M., Tichy, S.E., Locker, J., Russell, D.H., Jacobs, W.R., and Sacchettini, J.C. (2008). Structure and function of the virulence-associated high-temperature requirement A of *Mycobacterium tuberculosis*. Biochemistry *47*, 6092–6102.

Monod, J., Wyman, J., and Changeux, J.P. (1965). On the nature of allosteric transitions: A plausible model. J. Mol. Biol. *12*, 88–118.

Sohn, J., and Sauer, R.T. (2009). OMP peptides modulate the activity of DegS protease by differential binding to active and inactive conformations. Mol. Cell *33*, 64–74.

Sohn, J., Grant, R.A., and Sauer, R.T. (2007). Allosteric activation of DegS, a stress sensor PDZ protease. Cell *131*, 572–583.

Sohn, J., Grant, R.A., and Sauer, R.T. (2009). OMP peptides activate the DegS stress-sensor protease by a relief of inhibition mechanism. Structure *17*, 1411–1421.

Sohn, J., Grant, R.A., and Sauer, R.T. (2010). Allostery is an intrinsic property of the protease domain of DegS: implications for enzyme function and evolution. J. Biol. Chem. *403*, 420–429.

Vande Walle, L., Lamkanfi, M., and Vandenabeele, P. (2008). The mitochondrial serine protease HtrA2/Omi: an overview. Cell Death Differ. *15*, 453–460.

Walsh, N.P., Alba, B.M., Bose, B., Gross, C.A., and Sauer, R.T. (2003). OMP peptide signals initiate the envelope-stress response by activating DegS protease via relief of inhibition mediated by its PDZ domain. Cell *113*, 61–71.

Wilken, C., Kitzing, K., Kurzbauer, R., Ehrmann, M., and Clausen, T. (2004). Crystal structure of the DegS stress sensor: How a PDZ domain recognizes misfolded protein and activates a protease. Cell *117*, 483–494.

Zeth, K. (2004). Structural analysis of DegS, a stress sensor of the bacterial periplasm. FEBS Lett. *569*, 351–358.

Table 2.1. Biochemical characterization of DegS variants. Second-order rate constants for RseA cleavage and K_D's for OMP-peptide binding are listed for DegS and variants in otherwise wild-type (WT) backgrounds or in the H198P DegS (HP) background.

variant enzyme	activity WT background ($M^{-1} s^{-1}$)		activity HP background ($M^{-1} s^{-1}$)		K_D for OMP peptide (μM)	
	basal	with YYF	basal	with YYF	WT background	HP background
WT DegS	<4.5	2300 ± 60	540 ± 42	13900 ± 2100	4.0 ± 0.4	2.5 ± 0.3
P161A	<4.5	<4.5	<4.5	<4.5	1.5 ± 0.1	2.5 ± 0.4
Y162A	<4.5	<4.5	<4.5	<4.5	1.9 ± 0.4	n.d.
L164A	<4.5	<4.5	<4.5	<4.5	2.8 ± 0.6	2.5 ± 0.5
T167V	<4.5	<4.5	<4.5	<4.5	1.8 ± 0.1	1.9 ± 0.7
T169A	<4.5	<4.5	<4.5	<4.5	1.8 ± 0.1	2.0 ± 0.2
R178A	<4.5	<4.5	160 ± 28	3400 ± 470	3.6 ± 0.2	4.0 ± 0.1
I179A	<4.5	230 ±130	260 ± 150	9000 ± 2400	2.3 ± 0.4	1.6 ± 0.1
Q187A	<4.5	740 ± 74	800 ± 330	21000 ± 5100	2.3 ± 0.1	1.5 ± 0.1
Q191A	<4.5	<4.5	<4.5	<4.5	3.4 ± 1.3	1.4 ± 0.1
N197A	<4.5	49 ± 24	<4.5	300 ± 68	1.4 ± 0.1	0.7 ± 0.1
F220A	<4.5	46 ± 1	50 ± 11	1200 ± 11	2.1 ± 0.1	1.6 ± 0.1
D221A	<4.5	740 ± 140	1400 ± 390	12000 ± 3700	3.2 ± 0.2	1.7 ± 0.1
P229A	<4.5	2900 ± 270	640 ± 420	28000 ± 2500	1.6 ± 0.2	2.0 ± 0.1
E230A	<4.5	230 ± 50	300 ± 150	14000 ± 2000	5.7 ± 1.3	1.8 ± 0.4
I232A	<4.5	<4.5	<4.5	<4.5	2.2 ± 0.3	2.7 ± 0.3
F234A	<4.5	<4.5	<4.5	70 ± 15	5.9 ± 0.6	2.9 ± 0.1

(n.d.) not determined

Table 2.2. Re-refined structures statistics. Statistics for refinement and geometry of original structures (1SOZ, 1SOT, 1TE0, and 1VCW) and the same structures re-refined here (4G0G; 4G0E, 4G18, and 4G15).

PDB ID	ref.	ligand	resolu-tion (Å)	R_{work} / R_{free}	clash per-centile	poor rotamers %	Rama. outliers %	Rama. favored %	bad backbone bonds	bad backbone angles	Cβ deviations >0.25 Å	MolProbity score (rank percentile)
1SOZ	(1)	OMP peptide	2.4	0.231 / 0.272	40	5.3	3.5	87	3	7	30	3.05 (21)
4G0G (a)	(2)	OMP peptide	2.4	0.204 / 0.231	100	0	0	98	0	0	0	1.08 (100)
1SOT	(1)	apo	2.3	0.198 / 0.248	29	8.9	3.3	86	1	1	9	3.34 (13)
4G0E (b)	(2)	apo	2.3	0.184 / 0.217	100	0	0	100	0	0	0	0.75 (100)
1TE0	(3)	apo	2.2	0.245 / 0.295	8	23	7	85	73	140	186	3.81 (1)
4G18 (c)	(2)	apo	2.2	0.181 / 0.220	100	0	0	98	0	0	0	0.89 (100)
1VCW	(1)	OMP peptide removed	3.05	0.233 / 0.301	42	8.2	4.4	82	9	11	73	3.55 (36)
4G15 (d)	(2)	OMP peptide removed	3.05	0.230 / 0.256	100	0	0	96	0	0	0	1.53 (100)

(a) re-refinement of 1SOZ
(b) re-refinement of 1SOT
(c) re-refinement of 1SOT
(d) re-refinement of 1VCW
(1) Wilken et al. (2004)
(2) This work
(3) Zeth (2004)

Chapter 3

Allosteric activation of the DegS stress-response protease by OMP-peptide binding requires a steric clash that destabilizes autoinhibitory interactions

This work will be submitted as de Regt AK, Baker TA, Sauer RT.

A.K.D. performed all experiments and wrote the initial manuscript.

Abstract

E. coli senses envelope stress using a signaling cascade initiated when the DegS protease cleaves a transmembrane inhibitor, releasing a transcription factor to up-regulate response genes. Each subunit of the DegS trimer contains a protease domain and a PDZ domain. During outer-membrane stress, unassembled outer-membrane proteins (OMPs) accumulate in the periplasm and their C-terminal peptides activate DegS by binding to its PDZ domains. In the absence of stress, autoinhibitory interactions stabilize an inactive conformation of DegS. No satisfactory mechanism explains how OMP-peptide binding breaks these autoinhibitory interactions. Here, we present evidence that peptide binding initiates a steric clash between the side chains of a PDZ residue and an L3-loop residue that results in rearrangement of the loop and the breaking of autoinhibitory interactions. DegS variants with a very small residue at either of the clashing positions bind OMP peptide but are not activated. In contrast, L3 loops with a wide variety of medium- and large-sized residues at the clashing position support OMP-activation both *in vitro* and *in vivo*. These results provide a simple mechanism for the allosteric activation of DegS by OMP-peptide binding and explain why the L3-loop sequence is poorly conserved in homologs.

Introduction

The *Escherichia coli* DegS protease is anchored to the periplasmic face of the inner membrane, where it functions to sense outer-membrane stress (Ades, 2008; Guo and Gross, 2014). Like many intracellular enzymes, DegS is only activated under the correct conditions. In this case, outer-membrane porins (OMPs) accumulate in the periplasm when their assembly into the outer membrane is compromised. The C-terminal peptides of these unassembled OMPs bind DegS and activate cleavage of the periplasmic portion of RseA, a transmembrane anti-sigma factor (Walsh et al., 2003). This cleavage event initiates a proteolytic cascade that ultimately releases the σ^E transcription factor into the cytoplasm to stimulate transcription of stress-response genes (Chaba *et al*., 2007). Under non-stress conditions, OMPs do not accumulate in the periplasm, DegS cleavage of RseA is minimal, and σ^E remains bound to the cytoplasmic domain of RseA in an inactive state (Ades, 2008).

Each subunit of DegS consists of a membrane anchor, a trypsin-like protease domain, and a PDZ domain. The PDZ domain binds OMP peptides (Walsh et al., 2003). Crystal structures of DegS, both in active and inactive conformations, show that the protease domains pack to form a trimer with the PDZ domains on the periphery (Wilken *et al.*, 2004; Zeth 2004; Hasselblatt *et al.*, 2007; Sohn *et al.*, 2009). DegS proteolytic activity is well-described by a two-state allosteric model, in which the preferential binding of OMP peptides and the RseA substrate to the active enzyme stabilizes this species in a positively cooperative manner (Fig. 3.1; Sohn and Sauer, 2009). This positive cooperativity allows the cellular system to respond to small changes in OMP concentration. OMP peptides of different lengths and sequences activate DegS to varying extents, depending on their relative affinities for the inactive and active states (Sohn and Sauer, 2009). The most activating OMP peptide identified is Tyr-Tyr-Phe (YYF), which increases DegS

cleavage activity ~1000-fold (Sohn and Sauer, 2009). Allostery is an intrinsic property of the protease domain of DegS, and peptide binding to one PDZ domain activates both *cis* and *trans* protease domains (Mauldin and Sauer, 2013). Activation involves the rearrangement of a network of conserved residues at each subunit interface as well as the formation of a functional oxyanion hole at each catalytic site (Wilken *et al.*, 2004; Sohn *et al.*, 2010; de Regt *et al.*, 2014).

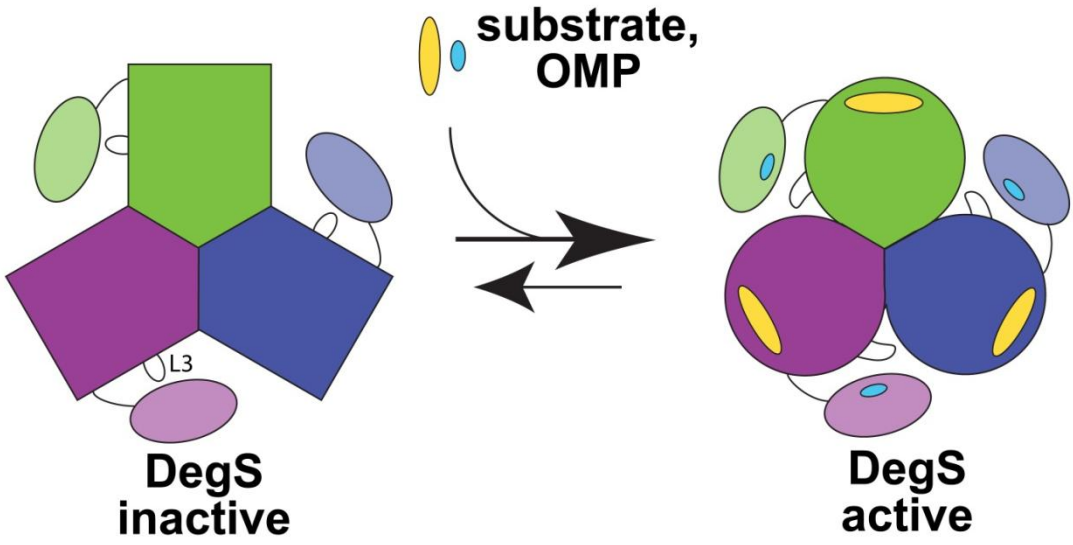

Fig. 3.1. Allosteric activation of DegS. Cartoon depiction of the inactive and active states of the DegS trimer (subunits colored green, purple, and blue). The protease domains (darker colors) pack together at the center of the trimer and the PDZ domains (lighter colors) are on the periphery. The allosteric equilibrium between inactive and active DegS is controlled by the binding of OMP peptide (cyan ovals) to the PDZ domains and RseA substrate (yellow ovals) to the protease domains. The L3 loop of the protease domain makes autoinhibitory interactions with the PDZ domains that stabilize the inactive state and are broken upon OMP-peptide binding.

In the absence of OMP peptide, virtually all DegS molecules are in the inactive conformation. Two models have been proposed for OMP-peptide activation of the protease. Both models involve the L3 loop (residues 176–189) of the protease domain, which extends towards the PDZ domain and assumes different conformations in active and inactive DegS. One model posits that PDZ-bound OMP peptides make specific contacts with the L3 loop that stabilize active DegS (Wilken et al., 2004; Hasselblatt et al., 2007). However, in multiple crystal structures of OMP-

peptide-bound DegS, there are no consistent or conserved interactions between the bound OMP peptide and the protease domain (Sohn *et al.*, 2009). A second model posits that the inactive conformation of the enzyme is stabilized by autoinhibitory contacts mediated in part by contacts between the L3 loop and the PDZ domain, with OMP-peptide binding resulting in destabilization or breaking of these inhibitory interactions (Walsh et al., 2003; Sohn et al., 2007; Sohn and Sauer, 2009). The primary evidence for this second model is that mutations that remove apparent autoinhibitory interactions activate DegS in the absence of OMP peptide (Sohn et al., 2007; Sohn *et al.*, 2009; Sohn *et al.*, 2010). Importantly, however, there is no satisfactory explanation for the mechanism by which OMP-peptide binding to the PDZ domain normally weakens or breaks autoinhibitory interactions.

Here, we present evidence that OMP-peptide binding results in a steric clash between a side chain in the PDZ domain and a side chain in the L3 loop. This clash effectively forces rearrangement of the L3 loop, thereby weakening or breaking autoinhibitory interactions. When a very small L3 residue is placed at the clashing position, OMP peptides bind but result in almost no DegS activation. However, a wide variety of larger L3 amino acids at the clashing position support OMP-peptide activation *in vitro* and *in vivo*. These results provide a simple mechanism for the allosteric activation of DegS by OMP-peptide binding and explain why the sequence of the L3 loop is poorly conserved in homologs.

Results

L3 interactions autoinhibit DegS

Crystal structures of inactive DegS reveal interactions made by side-chain or main-chain atoms of the L3 loop that are absent in the structure of active DegS stabilized by OMP-peptide binding (Wilken *et al.*, 2004; Zeth 2004; de Regt *et al*., 2014). In inactive DegS, for example, Arg^{178} in the L3 loop forms a salt bridge with Asp^{320} in the PDZ domain, Pro^{183} in the L3 loop makes a packing interaction with Tyr^{351} in the PDZ domain, the backbone carbonyl of Leu^{181} in the L3 loop hydrogen bonds to the side chain of Arg^{256} in a short linker between the protease and PDZ domains, and the side chain of Leu^{181} makes a packing interaction with hydrophobic side chains in the terminal helix of the protease domain, just before this linker (Fig. 3.2A). Our model posits that these interactions are autoinhibitory and keep most DegS molecules in the inactive conformation. Consistently, previous studies show that the P183A, D320A, and R256A mutants have basal proteolytic activity increased by ~6-fold, ~30-fold, and ~150-fold, respectively, compared to wild-type DegS but are still activated by OMP-peptide binding (Sohn et al., 2007).

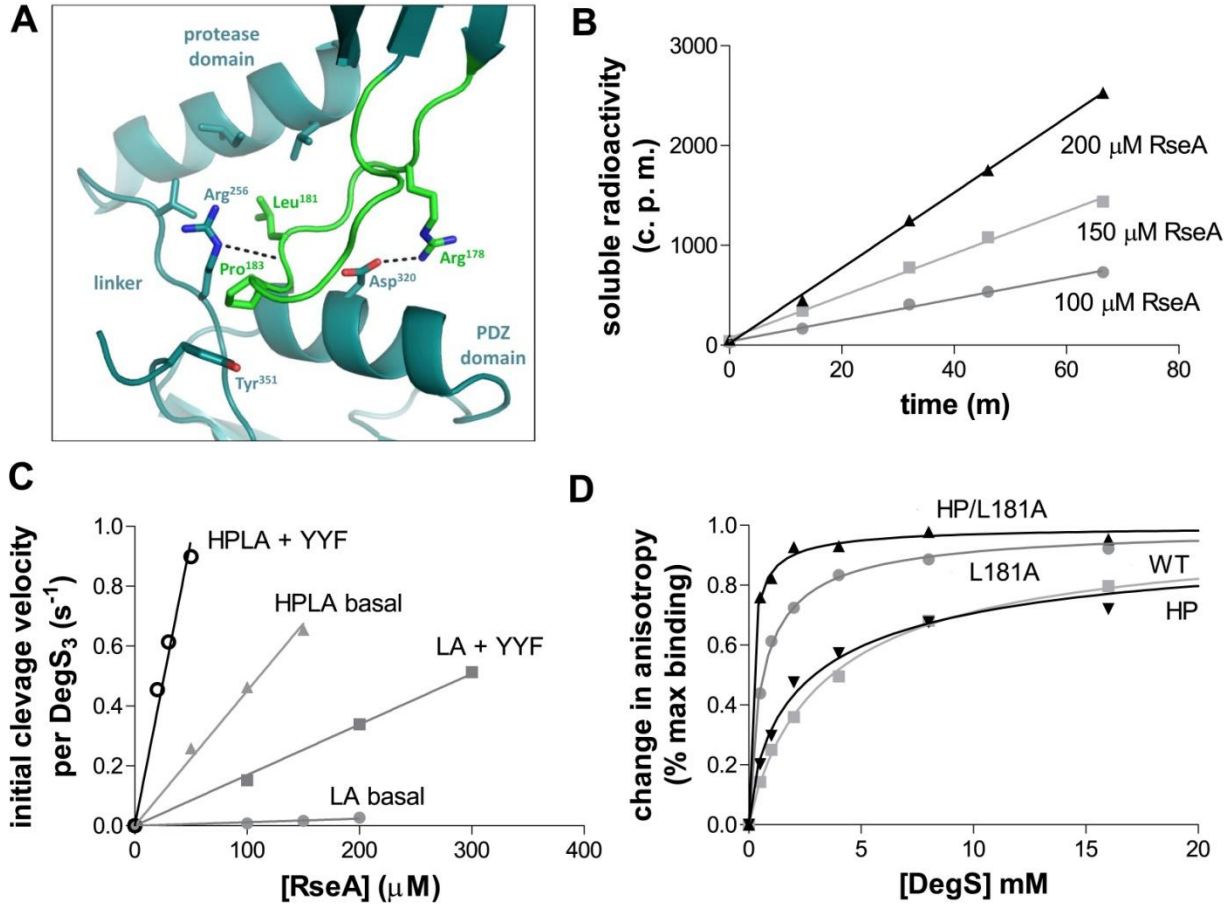

Fig. 3.2. The L3 loop makes autoinhibitory contacts. (A) Autoinhibitory interactions involving L3-loop residues (colored light green) stabilize the inactive conformation of DegS. Arg^{178} makes a salt-bridge with Asp^{320} in the PDZ domain, Pro^{183} packs against Tyr^{351} in the PDZ domain, the backbone of Leu181 makes a hydrogen bond with Arg^{256} in the linker before the PDZ domain. (PDB ID: 4G0E). (B) Basal cleavage of different concentrations of ^{35}S-labelled RseA by L181A DegS (1 μM trimer) was assayed by the time-dependent release of acid-soluble peptides. The slope of each plot was divided by the specific activity of the radioactive substrate and by the enzyme concentration to calculate a cleavage rate per enzyme (units s^{-1}). (C) Cleavage rates (determined as shown in panel B) were plotted as a function of RseA concentration for L181A or H198P/L181A DegS (1 μM trimer) with or without YYF peptide (200 μM). The slopes of these plots correspond to the second-order rate constants (k_{cat}/K_M) for basal and YYF-activated RseA cleavage. (D) Increasing concentrations of DegS variants were incubated with a fluorescent OMP decapeptide (100 nM) and binding was monitored by changes in fluorescence anisotropy. Values of the equilibrium dissociation constant (K_D) were determined by non-linear least-squares fitting of the data to Y = [DegS]/(K_D + [DegS]) and are listed for each variant in Table 3.1.

To test if the side-chain interaction of Leu^{181} contributes to autoinhibition, we assayed basal and YYF-stimulated cleavage of RseA by the L181A mutant in an otherwise wild-type background and in combination with the H198P mutation, which stabilizes active DegS (Sohn et al., 2009; Sohn and Sauer, 2010). Fig. 3.2B shows the kinetics of L181A DegS cleavage of different

concentrations of RseA, measured by accumulation of an acid-soluble radioactive product. For each concentration, the cleavage rate was calculated from a linear fit of the kinetic data. Fig. 3.2C shows cleavage rates plotted as a function of RseA concentration for this L181A experiment, for basal cleavage by L181A/H198P DegS, and for YYF-stimulated cleavage by L181A and L181A/H198P DegS. In each case, the plots are roughly linear as expected for reactions substantially below K_M, and the slopes provide a value for the second-order rate constant k_{cat}/K_M, which we use as a measure of cleavage activity. Table 3.1 lists these activities as well as the basal and YYF-induced activities of wild-type DegS and H198P DegS. Consistent with a role in autoinhibition, the basal activity of L181A DegS was ~80-fold higher than wild-type DegS and the activity of L181A/H198P DegS was ~5-fold higher than the H198P parent (Table 3.1), which had much higher basal activity than wild-type DegS. YYF peptide enhanced the cleavage activities of L181A and L181A/H198P DegS by additional factors of ~16-fold and ~3.5-fold, to rates similar to peptide-stimulated wild-type and H198P DegS. We monitored binding of a fluorescent OMP decapeptide to L181A, L181A/H198P, and to the parental enzymes by changes in fluorescence anisotropy (Fig. 3.2D; Table 3.1). The L181A mutation resulted in stronger OMP-peptide binding by a factor of ~7-fold for the wild-type background and ~40-fold for the H198P background. These results support a model in which some of the energy of OMP-peptide binding to wild-type DegS or H198P DegS drives the allosteric transition to the active state, reducing apparent affinity (Sohn et al., 2007; Sohn and Sauer, 2009). By this model, tighter OMP-peptide binding to the L181A variants occurs because the free-energy gap between the inactive and active conformations is reduced for L181A DegS and becomes even smaller for L181A/H198P DegS.

To establish if the wild-type L3 loop functions only to maintain DegS in the inactive conformation or also contributes to activation in response to OMP-peptide binding, we created variants of DegS in which residues 183-187 of the L3 loop were deleted (Δ183-187) or mutated *en bloc* to glycines (L3-Gly5) both in otherwise wild-type and H198P backgrounds. The basal activities of both mutants were increased compared to the parental enzymes (Fig. 3.3A), supporting an autoinhibitory function of the L3 loop. However, addition of YYF peptide did not increase cleavage activity over the basal level within the measurement error (Fig. 3.3A), indicating that these L3 mutations also prevent OMP activation. Compared to the OMP-activated parental enzymes, the activities of the deletion mutant and the glycine-substitution mutant were lower in the wild-type background (~90 and ~680 $M^{-1}s^{-1}$, respectively) than the in H198P background (~5,200 and ~9,300 $M^{-1}s^{-1}$, respectively)(Fig. 3.3B). The fact that the H198P mutation increases the activities of both L3 mutants suggests that the protease domains of both enzymes still equilibrate between inactive and active conformations. However, these mutants were less active than their OMP-activated parents, suggesting either residual autoinhibition and/or reduced stability of the active conformation relative to the inactive conformation. The latter possibility would not be surprising, as a residue near the beginning of the L3 loop (Arg^{178}) and a residue just after the L3 loop (Gln^{191}) also play critical roles in stabilizing the active conformation of DegS (Sohn et al., 2010; de Regt et al., in preparation), and perturbation of either contact by the L3 mutations could easily reduce the stability of active DegS relative to inactive DegS.

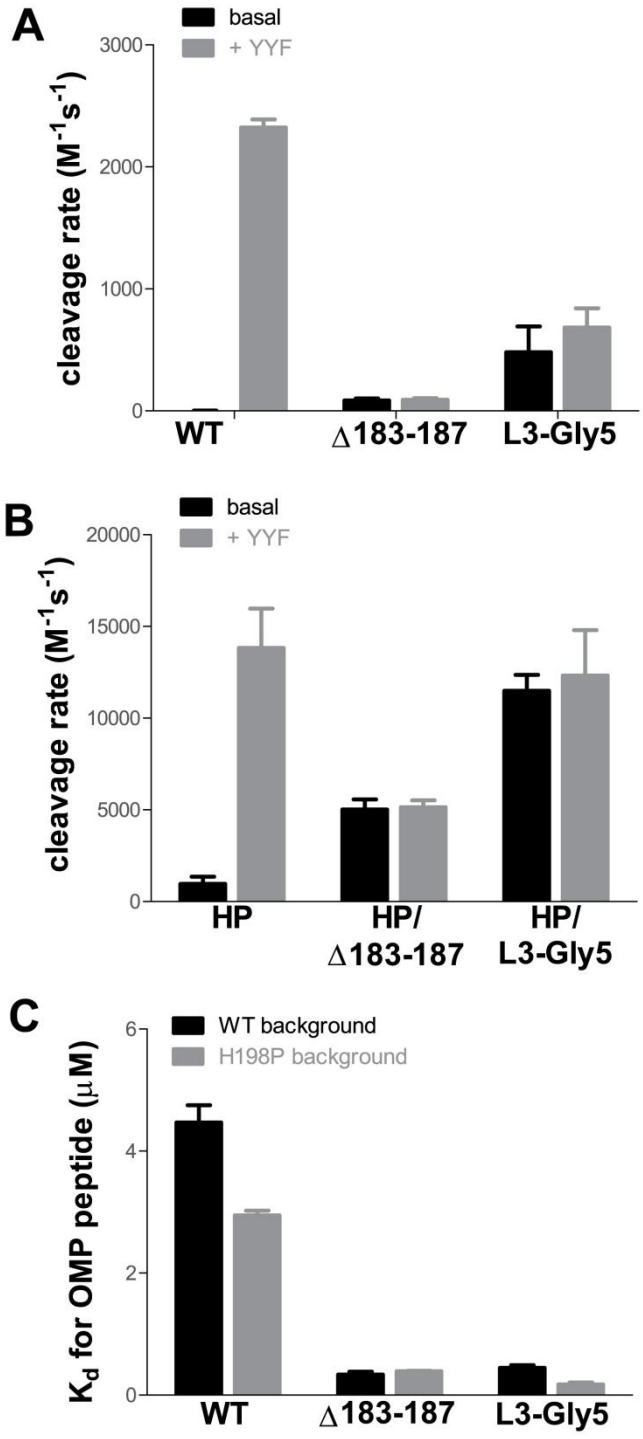

Fig. 3.3. Effects of L3 loop mutations on DegS activity and OMP-peptide binding. (A) Second-order rate constants for basal and YYF-activated cleavage of RseA by wild-type DegS (WT), $DegS^{\Delta 183\text{-}187}$, and $DegS^{L3\text{-}Gly5}$. (B) Effects of the same L3-loop mutations shown in panel A but in the H198P DegS background. (C) Equilibrium dissociation constants (K_D) of DegS variants for a fluorescent OMP decapeptide were determined from titration experiments like those in Fig. 3.2D. Values in all panels are averages ± SEM (N = 2-4).

Compared to wild-type DegS, the Δ183-187 and L3-Gly5 mutants bound to the OMP decapeptide with ~10-fold tighter affinities (Fig. 3.3C; Table 3.1). Compared to H198P DegS, the H198P/Δ183-187 and H198P/L3/Gly5 mutants had ~7-fold and 16-fold peptide tighter affinities, respectively (Fig. 3.3C; Table 3.1). Although some of these differences may arise because of direct effects of the mutations on OMP-peptide binding, the general strengthening of binding is expected if autoinhibitory interactions removed by both loop mutations keep the PDZ domain in a conformation with relatively weak OMP-peptide affinity. In combination, these results strongly suggest that the wild-type L3 loop plays important roles both in maintaining DegS in an inactive state and in mediating OMP-peptide activation of DegS.

A steric-clash model of activation

Previous studies show that Met^{319} in the PDZ domain plays an important role in activation (Sohn and Sauer, 2009). Specifically, Met^{319} assumes a different side-chain rotamer upon OMP-peptide binding to avoid a clash with the C-terminal side chain of the peptide, and the M319A mutation reduces OMP-peptide activation by ~20-fold. Asn^{182} is the L3-loop residue closest to the Met^{319} side chain in inactive DegS (Fig. 3.4A). Indeed, alignment of inactive and active DegS structures suggested that the Met^{319} rotamer in the OMP-bound active structure would clash with the side chain of Asn^{182} in inactive DegS but not in active DegS (Fig. 3.4B-D). To avoid this clash in OMP-bound inactive DegS, either or both side chains could adopt an unfavorable rotamer, or a small rearrangement of the L3 loop could occur. Any of these outcomes could destabilize the autoinhibitory conformation of the L3 loop and protease domain relative to the active conformations of the loop and protease domain, thereby altering the equilibrium constant relating the OMP-bound active and inactive conformations of DegS and leading to activation (Fig. 3.4E).

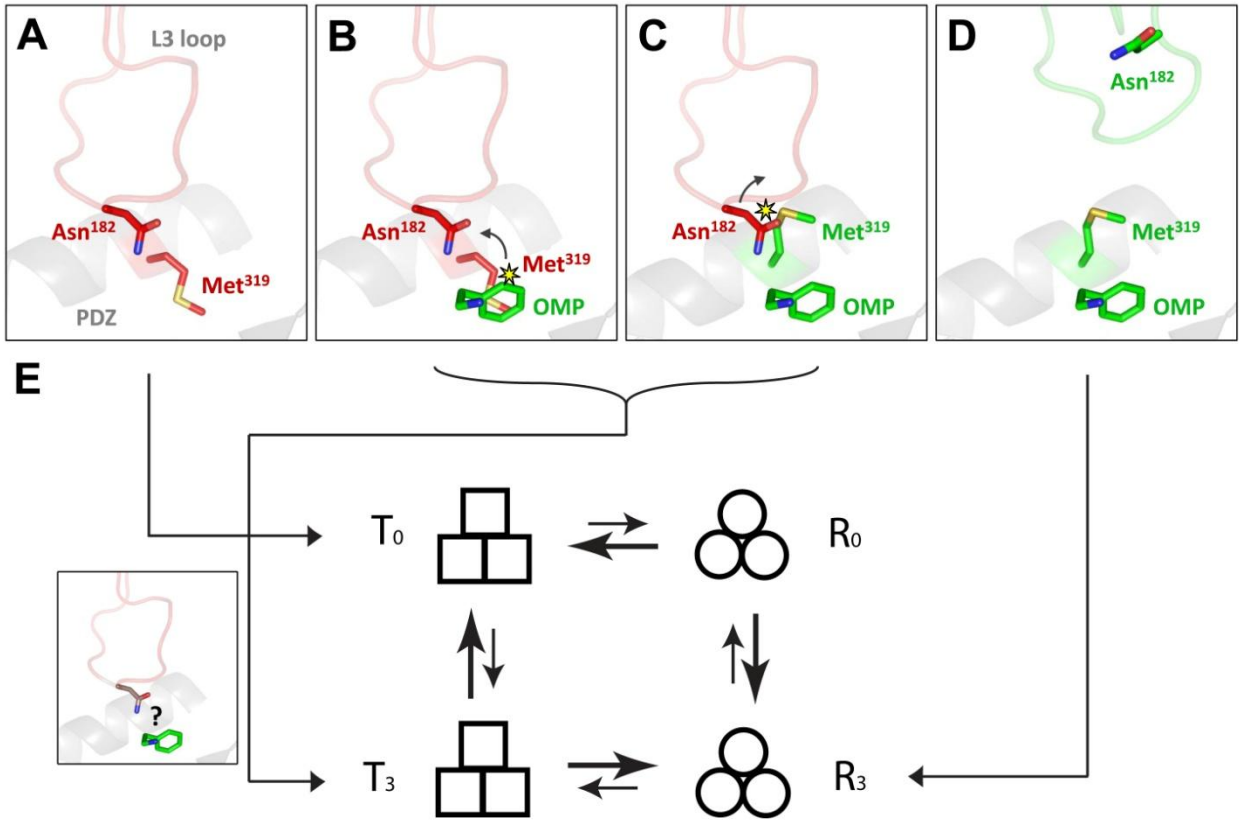

Fig. 3.4. The steric clash model of DegS activation. Alignment of inactive DegS (PDB ID: 4G0E, red) and active DegS (PDB ID: 3GDS, green) suggests a steric clash between a PDZ-domain residue and a L3-loop residue. (**A**) In inactive DegS, the Met^{319} side chain is part of the OMP-binding pocket. (**B**) If OMP peptide bound to inactive DegS as it does to active DegS, then a clash between the Met^{319} side chain and the C-terminal phenylalanine of the peptide would occur. (**C**) If the Met^{319} side chain in inactive DegS assumed the rotamer it does in active DegS, then there a clash with the Asn^{182} side chain in the L3 loop would occur. (**D**) In active DegS, the L3 loop assume a conformation in which has Asn^{182} is distant from Met^{319}. (**E**) Allosteric cycle relating peptide-free and peptide-bound species of active and inactive DegS. T_0 is the peptide-free inactive species (corresponding to panel A), R_0 is peptide-free active species, T_3 is the peptide-bound inactive species, and R_3 is the peptide-bound active species (corresponding to panel B). For wild-type DegS, ΔG is 5.6 kcal/mol for the $T_0 \rightarrow R_0$ transition and 1.2 kcal/mol for the $T_3 \rightarrow R_3$ transition in the absence of substrate (Sauer and Sohn, 2009).

This steric-clash model predicts that the size of the residue-182 side chain but not its specific chemical identity should be an important determinant of activation. In support of this model, we found that mutants with small glycine or alanine side chains (N182G and N182A) were severely defective in activation by YYF peptide, with stimulated cleavage activities of 5% or less of the wild-type level (Fig. 3.5A; Table 3.1). By contrast, YYF stimulated the activities of four variants

with larger side chains at position 182 (N182S, N182V, N182L, N182D) to substantially increased levels, in some cases higher than wild-type DegS (Fig. 3.5A; Table 3.1). These results strongly support the steric-clash model. The N182D mutant also had substantially increased basal activity (Table 3.1), which we attribute to Asp^{182} being close to Asp^{320} in the PDZ domain in the inactive conformation of DegS, with the resulting unfavorable electrostatic interactions decreasing autoinhibition and thus shifting the conformational equilibrium.

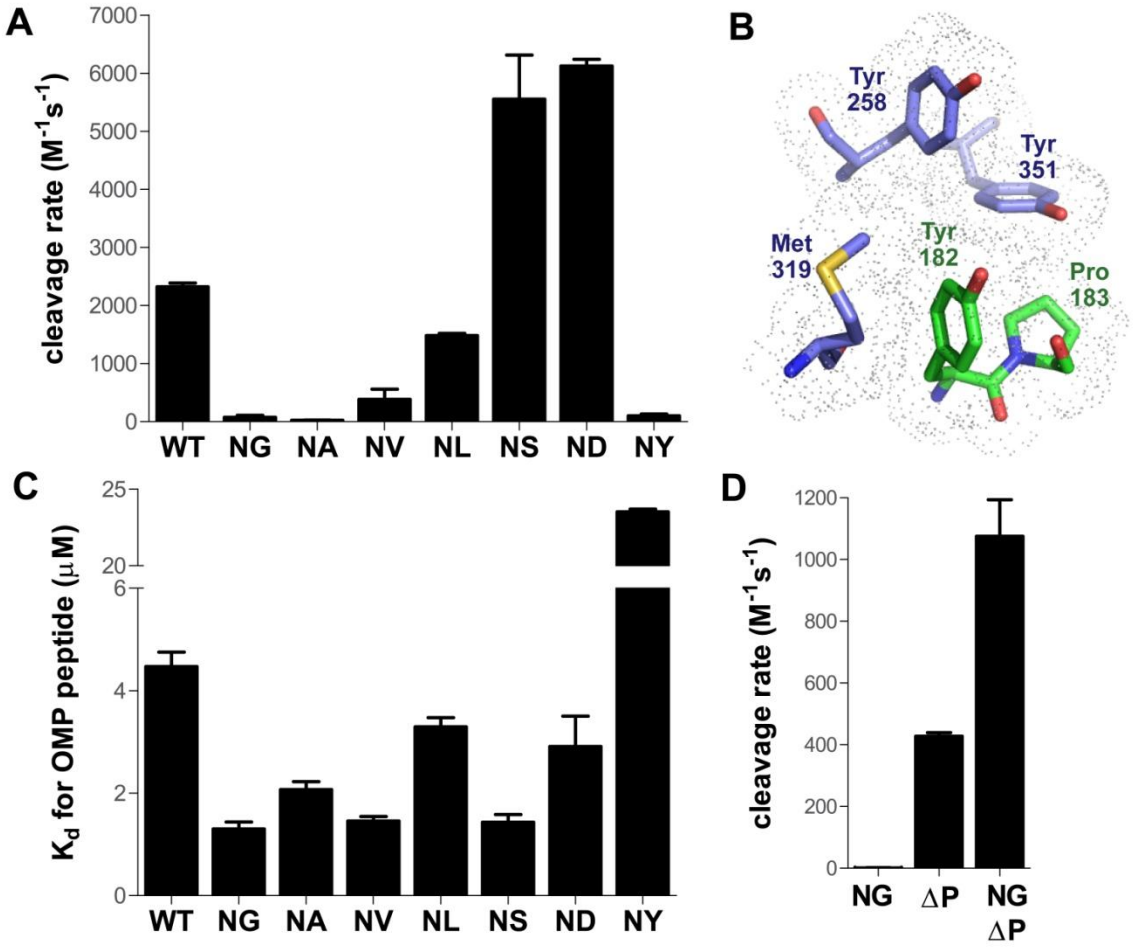

Fig 5. Large side chains at the clashing L3 position support DegS activation. (A) Second-order rate constants for RseA cleavage by residue-182 DegS variants in the presence of 200 μM YYF peptide. (B) Replacing the side chain of Asn^{182} in the inactive structure of DegS with Tyr^{182} shows autoinhibitory packing interactions with residues in the PDZ domain. Residues in the L3 loop have green carbons. Residues in the PDZ domain have blue carbons. (C) K_D's for binding of residue-182 DegS variants to the fluorescent OMP decapeptide. (D) Second-order rate constants for RseA cleavage by N182G DegS, $DegS^{\Delta PDZ}$, and N182G $DegS^{\Delta PDZ}$ in the absence of OMP peptide. Values in panels A, C, and D are averages ± SEM (N = 2-4).

Surprisingly, we found that a variant (N182Y) with an aromatic residue at position 182 was also only activated to ~5% of the wild-type level by YYF peptide (Fig. 3.5A; Table 3.1), a result seemingly in conflict with the clash model. When we modeled a Tyr^{182} side chain into the inactive conformation of DegS, however, it packed against the side chains of Tyr^{248}, Met^{319}, and Tyr^{351} in the PDZ domain (Fig. 3.5B), suggesting that the mutation adds additional autoinhibitory interactions that trap DegS largely in the inactive conformation even when OMP peptide is bound. If the Tyr^{182} side chain prevents rearrangement of the Met^{319} side chain upon OMP-peptide binding, then N182Y DegS should bind OMP peptide more weakly than wild-type DegS. Indeed, although N182G and N182A DegS and most other Asn^{182} mutants bound OMP peptide with affinities slightly better than wild-type DegS, N182Y bound with ~6-fold weaker affinity (Fig. 3.5C; Table 3.1).

To test if the N182G mutant might be not be activated because the mutation destabilizes the active conformation of the protease domain relative to the inactive conformation, we constructed N182G/ΔPDZ DegS. This variant was about twice as active as the ΔPDZ variant in an otherwise wild-type background and about half as active as YYF-stimulated DegS (Fig. 3.5D). Thus, the major defect of the N182G variant is an inability to respond to OMP-peptide activation, supporting the steric clash model.

Testing the clash model in vivo

If a steric clash between the side chains of Met^{319} and Asn^{182} is the major determinant of OMP activation, then many different L3-loop sequences should be compatible with activation. To test this possibility, we randomized the codons for residues 182-184 and tested a set of variants for

their ability to respond to OMP stimulation *in vivo*. For these studies, we expressed DegS variants from a plasmid in a Δ*degS* strain of *E. coli* carrying a σ^E-dependent chromosomal *lacZ* reporter (Ades *et al*., 1999). To assay OMP dependence, the test strain contained a second plasmid expressing a fusion of cytochrome b_{562} to a C-terminal sequence ending in YYF (*cyt*-YYF) under arabinose control (Chaba *et al*., 2011). When wild-type DegS was expressed in the test strain, addition of 0.2% arabinose resulted in strong induction of β-gal activity if the *cyt*-YYF protein was present but not if an otherwise identical protein lacking the C-terminal YYF sequence was present (Fig. 3.6A). A catalytically inactive DegS (S201A) resulted in minimal β-galactosidase activity with or without arabinose induction of *cyt*-YYF (Fig. 3.6A).

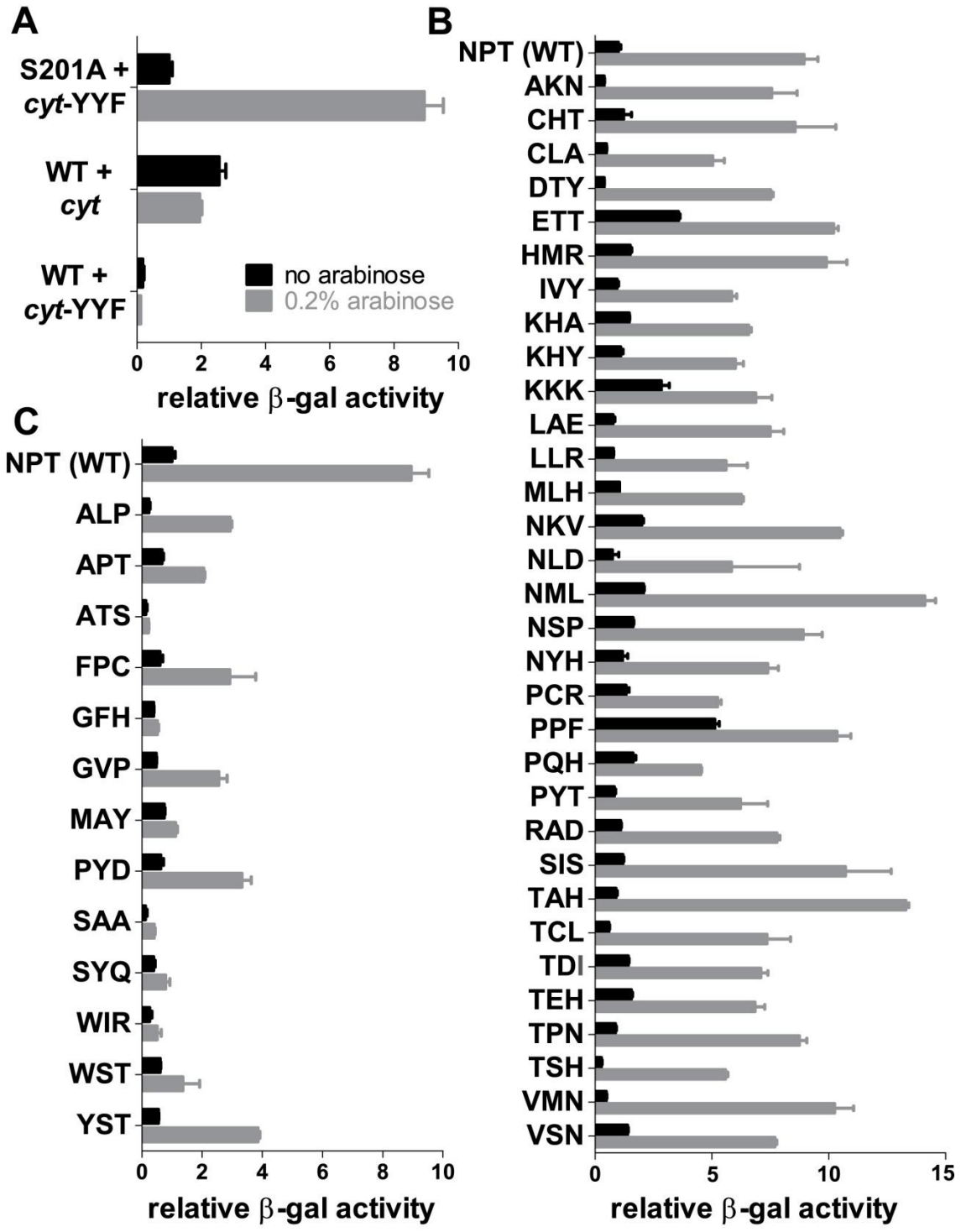

Fig. 3.6. Large side chains also support activation *in vivo.* (A) β-galactosidase levels in a Δ*degS* strain carrying a σ^E-dependent *lacZ* reporter, a plasmid expressing wild-type (WT) DegS or the catalytically inactive S201A variant, and a plasmid expressing arabinose-inducible cytochrome b_{562} with (*cyt*-YYF) or without (*cyt*) a YYF C-terminal tail. (B) β-galactosidase levels, with or without arabinose induction of *cyt*-YYF, for DegS library variants with different residues at positions 182-184 All of the variants shown have arabinose-induced activity at least 4-fold higher than the basal activity of wild-type (WT) DegS. (C) DegS variants from the L3 library with arabinose-induced activity less than 4-fold higher than the WT basal activity are shown. Values in all panels are averages ± SEM (N = 2-8).

We assayed β-gal levels in strains transformed with 45 DegS variants with L3-loop mutations with and without arabinose induction of *cyt*-YYF. Of these DegS variants, 32 supported good to strong β-gal induction in the presence of arabinose (4-fold or more over the wild-type basal activity; Fig. 3.6B). Among these variants, 16 different amino acids were represented at position 182 (ACDEGHIKLMNPRSTV), 16 at position 183 (ACDEFHIKLMPQSTVY), and 14 at position 184 (ADEFHIKLNPRTVY). Thus, the sequence determinants for DegS function and OMP activation at these L3-residue positions are extremely relaxed. Based on the failure of the N182A mutant to be strongly activated by YYF *in vitro*, we were surprised to find that a variant with an AKN^{184} sequence seemed fully active *in vivo*. By contrast and in line with results *in vitro*, the N182A or APT^{184} variant displayed weak induction in the cellular assay (Fig. 3.6C). For AKN^{184}, it seems likely that Lys^{183} or Asn^{184} compensates for Ala^{182} and restores OMP responsiveness.

For 13 DegS variants, either no or low levels of β-gal induction were observed (Fig. 3.6C). In six cases, these results were expected because residue 182 was a glycine, alanine, or tyrosine (GFH^{184}, GVP^{184}, APT^{184}, ATS^{184}, ALP^{184}, and YST^{184}). Position 182 was a tryptophan or phenylalanine in three additional variants in this category (FPC^{184}, WIR^{184}, and WST^{184}), suggesting that any aromatic ring can pack with residues in the PDZ domain to stabilize inactive DegS. Notably, no variants in the strongly inducing class had an aromatic residues at position 182. The reason for poor induction by the remaining variants in this class (PYD^{184}, MAY^{184}, SAA^{184}, and SYQ^{184}) is less clear. These mutations may allow the L3 loop to adopt an alternative autoinhibitory conformation that alleviates the clash between Met^{319} and the residue-182 side

chain, stabilize inactive DegS by other mechanisms, or reduce intracellular cellular levels of the mutant proteins because of increased proteolysis or decreased mRNA stability.

Discussion

In a previous study from this lab, we noted that the side-chain rotamer of Met^{319} in the PDZ domain changes between inactive DegS and OMP-bound active DegS, relieving a clash that would otherwise occur with the C-terminal phenylalanine side chain of the OMP peptide (Sohn and Sauer, 2009). Consistent with an important role for this rotamer rearrangement, the M319A mutation resulted in stronger binding of OMP peptide but very low levels of activation. However, those studies did not answer the question of how OMP-mediated repositioning of Met^{319} transmits an activating signal to the protease domain. Here, based on modeling, we hypothesized that the repositioned Met^{319} side chain would clash with the side chain of Asn^{182} in the L3 loop, unless one or both of these side chains and/or the loop adopted unfavorable conformations that destabilize the autoinhibitory conformation and shift the equilibrium to favor active DegS (Fig. 3.4E). In support of this model, we find that mutants with very small side chains at position 182 (N182G and N182A) show less than 5% of the level of wild-type activation by OMP peptide but have no defects in OMP-peptide binding. For these mutants, we propose that repositioning of the Met^{319} side chain in OMP-bound DegS results in very mild destabilization of the autoinhibited conformation (perhaps to avoid minor clashes with L3 backbone atoms) and thus causes little activation.

By contrast, we find that N182L, N182S, and N182D show substantial OMP activation, as expected if these larger side chains also clash with Met^{319} in OMP-bound DegS and stabilize the active conformation. Indeed, when we screened a random library in which residues 182-184 of

the L3 loop were randomly mutagenized, many different combinations of side chains at all three positions were compatible with robust OMP-mediated activation of DegS *in vivo*. Consistently, the central portion of the L3 loop shows very little sequence conservation in bacterial and metazoan DegS homologs (Fig. 3.7). These results support a simple activation model based on steric incompatibility. An alternative proposal (Wilken et al., 2004), which posits that specific interactions between the penultimate side chain of bound OMP peptide and the L3 loop stabilize active DegS and result in activation, is inconsistent with our current results and with numerous other studies (Sohn et al., 2007; 2009; Sohn and Sauer, 2009).

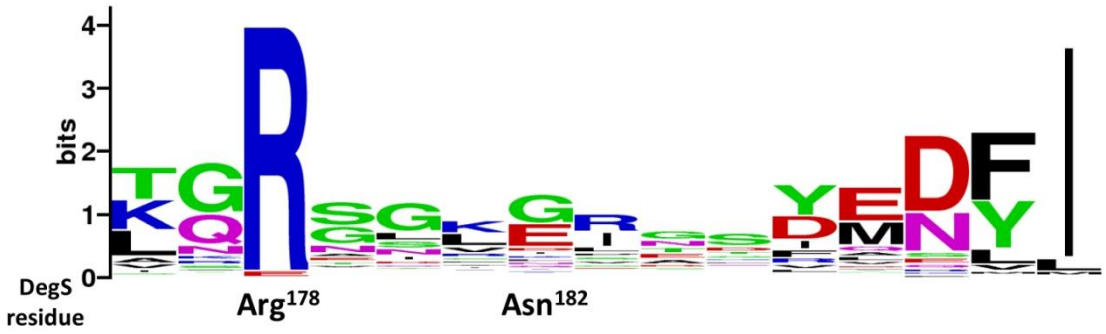

Fig. 3.7. Conservation of L3 loop residues. Residues 179-187 in the L3 loop are poorly conserved in an alignment of prokaryotic and eukaryotic proteases homologous to DegS. Figure prepared using WebLogo (Crooks et al., 2004).

OMP peptide does not activate DegS variants bearing a deletion (Δ183-187) in the L3 loop or with residues 183-187 changed to glycines (L3-Gly5), despite the presence of the wild-type Asn^{182}. The cleavage activities of these variants are still boosted substantially by the H198P mutation, which stabilizes functional DegS, indicating that they still equilibrate between inactive and active enzyme conformations. For these OMP-unresponsive mutants, we suggest that changes in the L3-loop conformation prevent a clash between Met^{319} and Asn^{182} in OMP-bound inactive DegS and thus uncouple OMP-peptide binding from activation.

The N182Y DegS mutant also displays poor OMP activation *in vitro*, as do members of our randomized library *in vivo* when position 182 is an aromatic residue. Modeling using the structure of inactive DegS suggests that autoinhibitory contacts between the side chain of Tyr^{182} (or other aromatic rings) and residues in the PDZ domain stabilize the inactive conformation of DegS. These additional autoinhibitory contacts would increase the energetic cost of converting inactive to active DegS and reduce the equilibrium population of active OMP-bound N182Y compared to inactive OMP-bound N182Y. This model predicts that N182Y variants could be activated by OMP-peptide binding if they harbored additional mutations that destabilized the inactive conformation or stabilized the active conformation. Interestingly, the N182Y mutation also decreases the affinity of DegS for OMP peptide, probably by preventing movement of Met^{319} or rearrangements of the L3 loop needed to maximize the affinity of inactive DegS for OMP peptide. Thus, the identity of the position 182 side chain plays an important role in establishing the equilibrium populations of active and inactive DegS and in allowing OMP-peptide binding to alter this equilibrium.

Our work, in combination with previous structural and biochemical studies (Wilken *et al.*, 2004; Zeth 2004; Sohn et al., 2007; Sohn and Sauer, 2009; Sohn et al., 2009), provides strong support for a model in which the L3 loop and PDZ domain play major roles in autoinhibition of proteolytic activity in OMP-free DegS and, as described above, in triggering activation in OMP-bound DegS. In inactive DegS, interactions between residues in the L3 loop and residues in the PDZ domain are clearly autoinhibitory. For example, we find that point mutations (L181A, N182D), the Δ183-187 deletion, and the L3-Gly5 mutation in the L3 loop all substantially increased the cleavage activity of DegS in the absence of OMP peptide. Previous studies show

that the P183A mutation in the L3 loop, the D320A mutation in the PDZ domain (which eliminates a salt bridge with Arg^{178} in the L3 loop), and deletion of the PDZ domain also increase the basal activity of DegS (Sohn et al., 2007). Thus, interactions between the L3 loop and the OMP-free PDZ domain stabilize inactive DegS, whereas conformational rearrangements needed to accommodate the binding of OMP peptides to the PDZ domain of inactive DegS destabilize these autoinhibitory interactions, shifting the equilibrium to favor the active DegS conformation.

Methods

Protein Expression and Purification

Variants of *E. coli* DegS (residues 27-355) with an N-terminal His_6 tag in place of the wild-type membrane anchor and a ^{35}S-labeled variant of the periplasmic domain of *E. coli* RseA (residues 121-216) were expressed and purified as described (Sohn *et al.*, 2007). Synthetic YYF peptide (GenScript) was purified by high-pressure liquid chromatography.

Enzymatic and Biochemical Assays

Cleavage and binding assays were performed at room temperature in buffer containing 150 mM sodium phosphate (pH 8.3), 380 mM NaCl, 10% glycerol and 4 mM EDTA following published protocols (Sohn *et al.*, 2007). Briefly, cleavage assays were performed by incubating 1 μM trimeric DegS or variants with or without 200 μM YYF tripeptide and three sub-K_M concentrations of ^{35}S-RseA. At different times, samples were quenched trichloroacetic acid to a final concentration of 8.6% and incubated on ice for 20 min. After centrifugation, acid-soluble radioactive cleavage products were quantified by scintillation counting. Second-order rate

constants were calculated by taking the slope of the plot of initial velocity versus substrate concentration.

OMP-peptide binding assays were performed by titrating increasing concentrations of DegS or variants against 100 nM fluorescein-DNRDGNVYYF and monitoring changes in fluorescence anisotropy (excitation 480 nm; emission 520 nm) after correction for protein scattering. Binding curves were fit using non-linear least-square algorithms implemented by Prism (GraphPad).

Construction of L3 mutant library

A *degS* plasmid with an engineered silent SalI site mid-gene was amplified and digested with SalI and BamHI restriction enzymes. Primers were constructed to amplify a portion of *degS* containing this SalI site at the 5' end and a native BamHI site at the 3' end. The latter plasmid contained an NNS NNS NNS sequence (N = A,C,G,T; S = C,G) in place of the wild-type sequence for codons 182-184. This amplified DNA was cut with SalI and BamHI and ligated into the cut vector described above. The ligation reaction was transformed into *E. coli* DH5α and colonies were selected for plasmid isolation and sequencing.

β-galactosidase assay

σ^E activity was measured by monitoring β-galactosidase (β-gal) expression from a chromosomal σ^E -dependent lacZ reporter gene in Φλ(*rpo*HP3::*lacZ*), as described (Miller *et al.*, 1972; Mecsas *et al.*, 1993; Ades *et al.*, 1999; Chaba *et al.*, 2011). Strain CAG33315 (Ades *et al.*, 1999) was transformed with plasmid BA182 (Walsh *et al.*, 2003) containing *cyt*-YYF in pBAD33. That strain was further transformed with plasmids containing DegS variants in a pEXT20 vector.

Strains were grown at 30°C in ampicillin (100 μg/mL) and chloramphenicol (34 μg/mL) overnight, diluted 1:150 into the wells of a 96-well assay plate (Corning), and allowed to grow to mid-log phase with or without 0.2% arabinose in the presence of the same concentrations of ampicillin/chloramphenicol. The plate was then incubated on ice to arrest growth, a final OD_{600} was measured, and cells were lysed with PopCulture + rlysozyme (EMD Millipore, Novagen). Lysate was added to an *ortho*-nitrophenyl-β-galactoside (ONPG) solution and OD_{420} was monitored for one hour. The slope of this line, minus a blank, was taken as the β-galactosidase activity, which was normalized to the activity of the strain containing the wild-type DegS plasmid grown in the absence of arabinose. For the no-stress-signal control, plasmid pBA175, which contains *cyt* instead of *cyt*-YYF, was transformed into CAG33315 and this strain was transformed with a wild-type DegS plasmid.

Sequence alignment

The five closest DegS homologues from each phylum of bacteria as well as the 43 closest homologues in metazoans and four *H. sapiens* HtrA proteases were aligned in ClustalW2 (Larkin *et al.*, 2007). Alignments at positions 176–189 were collected and submitted to WebLogo (Crooks *et al.*, 2004) for visualization.

Modeling

Modeling and preparation of structural figures were performed using the PyMOL Molecular Graphics System (Schrödinger, LLC).

Acknowledgements. We thank Monica Guo for advice, strains, and plasmids. Supported by NIH grant AI-16892. T.A.B. is an employee of the Howard Hughes Medical Insitute.

References

Ades SE, Connolly LE, Alba BM, Gross CA. (1999). The *Escherichia coli* σ^E-dependent extracytoplasmic stress response is controlled by the regulated proteolysis of an anti-σ factor. Genes Dev. *13*, 2449–2461.

Ades SE. (2008). Regulation by destruction: design of the sigmaE envelope stress response. Curr. Opin. Microbiol. *11*, 535–540.

Chaba R, Alba BM, Guo MS, Sohn J, Ahuja N, Sauer RT, Gross CA. (2011). Signal integration by DegS and RseB governs the σ^E-mediated envelope stress response in *Escherichia coli*. Proc. Natl. Acad. Sci. USA *108*, 2106–2111.

Crooks GE, Hon G, Chandonia JM, Brenner SE. (2004). WebLogo: A sequence logo generator. Genome Res. *14*, 1188–1190.

de Regt AK, Kim S, Sohn J, Grant RA, Baker TA, Sauer RT. (2014). Conserved pathways of allosteric communication in HtrA-family proteases. (Chapter 2 of thesis).

Guo MS, Gross CA. (2014) Stress-induced remodeling of the bacterial proteome. Curr. Biol. *24*, R424–434.

Hasselblatt, H., Kurzbauer, R., Wilken, C., Krojer, T., Sawa, J., Kurt, J., Kirk, R., Hasenbein, S., Ehrmann, M., and Clausen, T. (2007). Regulation of the sigmaE stress response by DegS: how the PDZ domain keeps the protease inactive in the resting state and allows integration of different OMP-derived stress signals upon folding stress. Genes Dev. *21*, 2659–2670.

Larkin MA, Blackshields G, Brown NP, Chenna R, McGettigan PA, McWilliam H, Valentin F, Wallace IM, Wilm A, Lopez R, Thompson JD, Gibson TJ, Higgins DG. (2007). ClustalW and ClustalX version 2. Bioinformatics *23*, 2947–2948.

Mauldin RV and Sauer RT. (2013). Allosteric regulation of DegS protease subunits though a shared energy landscape. Nat. Chem. Biol. *9*, 90–96.

Mecsas J, Rouviere PE, Erickson JW, Donohue TJ, Gross CA. (1993). The activity of σ^E, an *Escherichia* coli heat-inducible σ-factor, is modulated by expression of outer membrane proteins. Genes Dev. *7*, 2618–2628.

Miller JH. (1972). Experiments in Molecular Genetics (Cold Spring Harbor Laboratory Press, Plainview, NY).

Ponting CP. (1997). Evidence for PDZ domains in bacteria, yeast, and plants. Protein Sci. *6*, 464–468.

Sohn, J., and Sauer, R.T. (2009). OMP peptides modulate the activity of DegS protease by differential binding to active and inactive conformations. Mol. Cell *33*, 64–74.

Sohn, J., Grant, R.A., and Sauer, R.T. (2007). Allosteric activation of DegS, a stress sensor PDZ protease. Cell *131*, 572–583.

Sohn, J., Grant, R.A., and Sauer, R.T. (2009). OMP peptides activate the DegS stress-sensor protease by a relief of inhibition mechanism. Structure *17*, 1411–1421.

Sohn, J., Grant, R.A., and Sauer, R.T. (2010). Allostery is an intrinsic property of the protease domain of DegS: implications for enzyme function and evolution. J. Biol. Chem. *403*, 420–429.

Walsh NP, Alba BM, Bose B, Gross CA, Sauer RT. (2003). OMP peptide signals initiate the envelope-stress response by activating DegS protease via relief of inhibition mediated by its PDZ domain. Cell *113*, 61–71.

Wilken C, Kitzing K, Kurzbauer R, Ehrmann M, Clausen T. (2004). Crystal structure of the DegS stress sensor: How a PDZ domain recognizes misfolded protein and activates a protease. Cell *117*, 483–494.

Zeth K. (2004). Structural analysis of DegS, a stress sensor of the bacterial periplasm. FEBS Lett. *569*, 351–358.

Table 3.1. Properties of DegS variants. Activities lower than 0.5% of the OMP-activated wild type activity are reported as "<10". n.d, not determined. Values reported are averages ± SEM or 10% of average, whichever is larger (N = 2-7).

	WT activity ($M^{-1}s^{-1}$)		HP activity ($M^{-1}s^{-1}$)		K_D with OMP (μM)	
	Basal	With YYF	Basal	With YYF	WT	HP
WT	<10	2300 ± 66	960 ± 390	14000 ± 2100	4.5 ± 0.5	2.9 ± 0.4
L181A	<10	1500 ± 100	4700 ± 160	17000 ± 1300	0.6 ± 0.06	0.1 ± 0.05
Δ183-187	85 ± 17	91 ± 14	4700 ± 550	5100 ± 390	0.3 ± 0.05	0.4 ± 0.04
L3-Gly5	480 ± 210	680 ± 160	11000 ± 870	12000 ± 2500	0.4 ± 0.05	0.2 ± 0.03
N182G	<10	74 ± 35	n.d.	n.d.	1.3 ± 0.1	n.d.
N182A	<10	24 ± 5	n.d.	n.d.	2.1 ± 0.2	n.d.
N182V	<10	390 ± 170	n.d.	n.d.	1.5 ± 0.2	n.d.
N182L	<10	1500 ± 39	n.d.	n.d.	3.3 ± 0.3	n.d.
N182S	<10	5600 ± 760	n.d.	n.d.	1.4 ± 0.1	n.d.
N182D	<10	6100 ± 120	n.d.	n.d.	2.9 ± 0.6	n.d.
N182Y	<10	100 ± 30	n.d.	n.d.	24 ± 0.2	n.d.
ΔPDZ	430 ± 12	n.d.	n.d.	n.d.	n.d.	n.d.
N182G/ΔPDZ	1100 ± 120	n.d.	n.d.	n.d.	n.d.	n.d.

Chapter 4

Overexpression of CupB5 activates alginate overproduction in *Pseudomonas aeruginosa* by a novel AlgW-dependent mechanism

This work was originally published as de Regt AK*, Yin Y*, Withers TR, Wang X, Baker TA, Sauer RT, Yu HD. 2014 Mol Microbiol *93*, 415-25. *co-first authors

A.K.D. performed all biochemical experiments and wrote the first version of the manuscript that included biochemical results. Y.Y., T.R.W., W.X. performed genetics experiments. H.Y. wrote the genetics-only original manuscript.

Abstract

In *Pseudomonas aeruginosa*, alginate overproduction, also referred to as mucoidy, is negatively regulated by the transmembrane protein MucA, which sequesters the alternative sigma factor AlgU. MucA is degraded via a proteolysis pathway that frees AlgU from sequestration, activating alginate biosynthesis. Initiation of this pathway normally requires two signals: peptide sequences in unassembled outer-membrane proteins (OMPs) activate the AlgW protease, and unassembled lipopolysaccharides bind periplasmic MucB, releasing MucA and facilitating its proteolysis by activated AlgW. To search for novel alginate regulators, we screened a transposon library in the non-mucoid reference strain PAO1, and identified a mutant that confers mucoidy through overexpression of a protein encoded by the chaperone-usher pathway gene cupB5. CupB5-dependent mucoidy occurs through the AlgU pathway and can be reversed by overexpression of MucA or MucB. In the presence of activating OMP peptides, peptides corresponding to a region of CupB5 needed for mucoidy further stimulated AlgW cleavage of MucA in vitro. Moreover, the CupB5 peptide allowed OMP-activated AlgW cleavage of MucA in the presence of the MucB inhibitor. These results support a novel mechanism for conversion to mucoidy in which the proteolytic activity of AlgW and its ability to compete with MucB for MucA is mediated by independent peptide signals.

Introduction

Pseudomonas aeruginosa is an important opportunistic human pathogen, capable of thriving in different environmental niches. Activation of the AlgU-regulated extracytoplasmic stress response results in the production of copious amounts of an exopolysaccharide called alginate, forming a capsule that protects the bacterium from the host-immune system. Alginate production by *P. aeruginosa* is a particular problem for patients with cystic fibrosis, whose dehydrated mucus-filled lungs provide an environment especially suited for bacterial infection (Folkesson *et al.*, 2012). Nonmucoid strains initially colonize the lungs, and alginate overproduction caused by mutations in mucA results in a mucoid phenotype and a chronic lung infection (Ciofu *et al.*, 2005; Hogardt *et al.*, 2007; Mena *et al.*, 2008). Among many roles in pathogenesis, alginate can promote adherence to lung epithelial cells, reduce the efficiency of phagocytosis, and protect bacteria from antibiotics (Govan and Deretic, 1996; Pier *et al.*, 2001; Leid *et al.*, 2005).

The extracytoplasmic stress-response pathways in *P. aeruginosa*, *Escherichia* coli, and other Gram-negative bacteria involve regulated intramembrane proteolysis and share common features. For example, outer-membrane and periplasmic stress initiates a proteolytic cascade that ultimately degrades a transmembrane anti-sigma factor and releases the sigma factor to up-regulate stress-response genes (Alba *et al.*, 2002; Kanehara *et al.*, 2002; Walsh *et al.*, 2003; Akiyama *et al.*, 2004; Flynn *et al.*, 2004; Chaba *et al.*, 2007). In *P. aeruginosa*, proteolysis of wild type MucA, the anti-sigma factor, releases the AlgU sigma factor, which enhances transcription of the genes responsible for alginate biosynthesis from the algD promoter (Martin *et al.*, 1993; Wood *et al.*, 2006).

In *P. aeruginosa*, degradation of MucA is normally initiated by cleavage by the AlgW protease at site 1 near the periplasmic face of the inner membrane, continues with cleavage by the MucP protease at site 2 near the cytoplasmic face of the membrane, and is completed in the cytoplasm by AAA+ proteases such as ClpXP (Akiyama *et al.*, 2004; Alba *et al.*, 2002; Chaba *et al.*, 2007; Flynn *et al.*, 2004; Kanehara *et al.*, 2002; Qiu *et al.*, 2007; Qiu *et al.*, 2008b; Walsh *et al.*, 2003). Two signals are required to initiate this proteolytic cascade. The C-terminal peptides of proteins that accumulate in the periplasm during stress, including outer-membrane proteins (OMPs), bind to the PDZ domains of the trimeric AlgW protease and allosterically activate site-1 cleavage of MucA, but MucB competes for MucA binding and can inhibit this cleavage (Cezairliyan and Sauer, 2009). Recent studies show that lipopolysaccharides (LPS), a key component of the outer membrane, can bind MucB and cause release of MucA (Lima *et al.*, 2013).

Here, we identify CupB5 as a novel activator of the alginate-production pathway. CupB5, an adhesive protein, is a member of one of the chaperone/usher pathways (CupA-E) that mediate assembly of pili and play roles in bacterial pathogenesis, adhesion, and biofilm formation (Hull *et al.*, 1981; Marklund *et al.*, 1992; Soto and Hultgren, 1999; Vallet *et al.*, 2001; Giraud *et al.*, 2011; Mikkelsen *et al.*, 2009). These secretion systems, which are best characterized in Gram-negative bacteria (Sauer *et al.*, 2000; Waksman and Hultgren, 2009), contain a periplasmic chaperone that maintains proteins to be secreted in an unassembled state and an usher that transports these proteins through the outer membrane. We find that overexpression of CupB5 in the absence of its chaperone induces a mucoid phenotype in *P. aeruginosa* and provide evidence that a peptide signal in CupB5 enhances OMP-activated cleavage of MucA by AlgW, even in the presence of MucB, allowing initiation of AlgU signaling.

Results

Overexpression of CupB5 induces mucoidy

To identify new alginate regulatory genes, we performed mariner-transposon mutagenesis (Wong and Mekalanos, 2000) in the nonmucoid *P. aeruginosa* reference strain PAO1. We isolated a mucoid variant (PAO1-VE22) and identified the site of a single-copy insertion by inverse PCR and Southern-blot analysis (data not shown). The transposon insertion was six base pairs before the TAG stop codon at the 3´ end of cupB4 (Fig. 4.1A) and introduced a σ70-dependent PGm promoter that drove expression of the gentamicin resistance cassette and downstream genes (Rubin *et al.*, 1999). Alginate production by PAO1-VE22 (31 ± 1.5 μg/ml/OD_{600}) was substantially higher than that of PAO1 (8.5 ± 0.02 μg/ml/OD_{600}) after 24 h growth at 37°C. To test if altered expression of cupB4, cupB5, or cupB6 was responsible for the mucoidy of PAO1-VE22, we cloned each individual coding sequence with an N-terminal HA epitope and C-terminal H_6 tag in pHERD20T under control of an arabinose-inducible promoter (Qiu *et al.*, 2008a). Plasmids expressing the tagged variant of CupB5, but not of CupB4 or CupB6, induced mucoid conversion and high-level alginate production in PAO1 (Fig. 4.1B). Western-blot analysis indicated that the plasmid-expressed CupB4, CupB5, and CupB6 variants were detectable when overexpressed in PAO1, albeit with fragmentation of CupB5 (Fig. 4.1C). We conclude that enhanced expression of CupB5 or a CupB5 fragment induces mucoidy and increased alginate in PAO1-VE22.

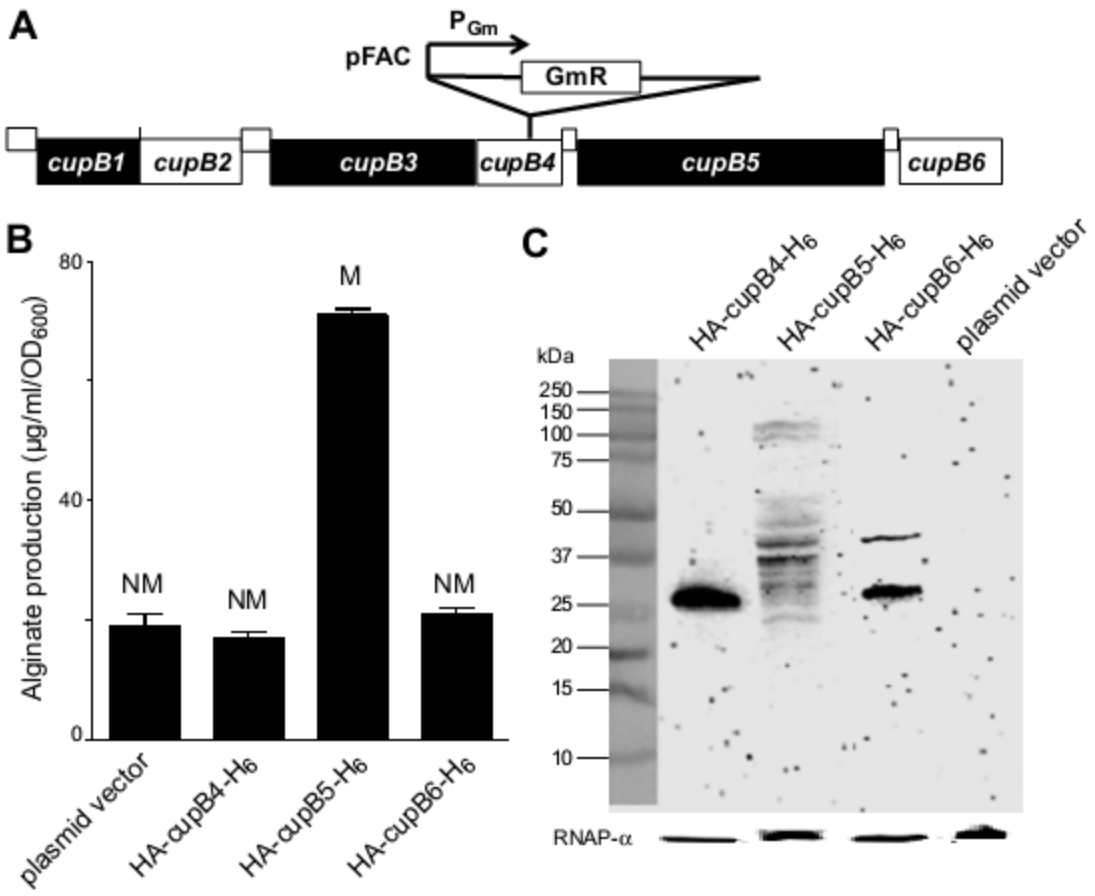

Fig. 4.1. Overproduction of CupB5 causes mucoid conversion in PAO1. (A) Organization of the cupB1-cupB6 gene cluster (www.*Pseudomonas*.com), and location of the transposon insertion site in PAO1-VE22. (B) Alginate production, measured using the carbazole assay, and colony phenotypes (M, mucoid; NM, nonmucoid) were assayed following transformation of *P. aeruginosa* strain PAO1 with plasmid HERD20T or variants expressing HA-CupB4-H_6, HA-CupB5-H_6, or HA-CupB6-H_6, and overnight growth of colonies on PIA plates (carbenecillin 300 µg ml-1, 0.1% L-arabinose) at 37ºC. Values are averages ± SEM (n=3). (C) Cell lysates of PAO1 carrying appropriate plasmids were electrophoresed on SDS polyacrylamide gels, and Western-blots using an anti-HA monoclonal antibody were used to detect HA-CupB4-H_6, HA-CupB5-H_6, or HA-CupB6-H_6. The rightmost lane shows that HA cross-reactive proteins were absent in PAO1 transformed with the pHERD20T empty-vector.

Genetic requirements for CupB5-induced mucoidy

Deletion of five single genes required for the AlgU response (algW, mucP, clpX, clpP, or algU) in PAO1 prevented mucoidy and high-level alginate production when HA-CupB5-H_6 was overproduced from a plasmid in these strains (Fig. 4.2A). In-frame deletion of algW in PAO1-VE22 also prevented alginate overproduction and mucoidy, a phenotype that was complemented by plasmid expression of AlgW but not AlgW lacking its PDZ domain (Fig. 4.2B). Consistently,

when AlgU-dependent promoters were fused to lacZ and introduced into PAO1-VE22 or PAO1-VE2, a strain in which AlgW is activated by overproduction of MucE (Qiu *et al.*, 2007), β-galactosidase levels were increased markedly compared to the same promoter fusions in PAO1 (Fig. 4.S1). CupB5 is normally an extracellular protein (Ruer *et al.*, 2008; Vallet *et al.*, 2001). However, its overexpression in the absence of corresponding levels of the CupB4 chaperone and usher could result in periplasmic accumulation that acts directly or indirectly through AlgW to activate alginate production.

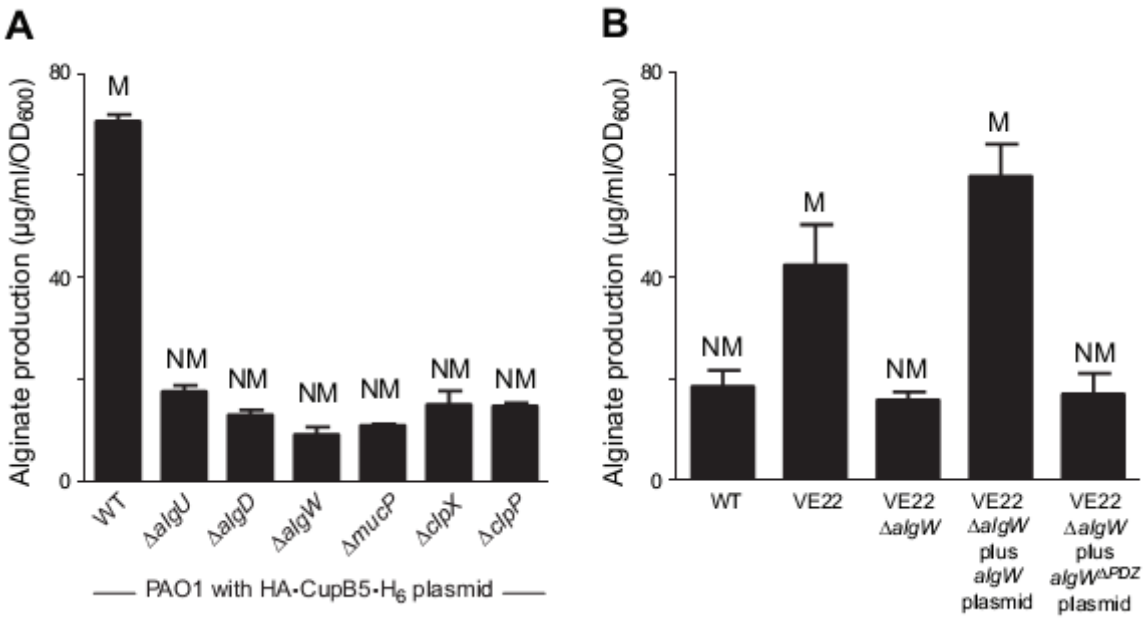

Fig. 4.2. Genetic requirements for CupB5-mediated alginate overproduction. (A) Wild-type (WT) or mutant PAO1 strains were transformed with pHERD20 encoding HA-CupB5-H6, grown on PIA plates with 0.1% L-arabinose for 24 h at 37°C to induce HA-CupB5-H_6 overexpression, and mucoid phenotypes and alginate production were determined. The algD gene encodes an enzyme required for alginate production. The algU, algW, mucP, clpX, and clpP genes are required for induction of algU-dependent alginate production. (B) Alginate production and mucoid phenotypes of different strains were measured after growth for 24 h at 37°C on PIA plates plus 300 μg ml-1 carbenecillin and 0.1% L-Ara. In both panels, values are averages ± SEM (n=3).

CupB5 contains an internal signal for alginate overproduction

Because C-terminal sequences terminating with an aromatic residue and α-carboxylate can activate AlgW, we initially tested if the C-terminal residues of CupB5 (Asn^{1016}-Ile^{1017}-Trp^{1018})

were responsible for activating AlgW and inducing mucoidy. However, overexpression of CupB5 variants with a C-terminal H_6 tag or containing a deletion of the (Asn^{1016}-Ile^{1017}-Trp^{1018} sequence and a C-terminal H_6 tag still induced mucoidy in PAO1 (Table 4.S1). Thus, the extreme C-terminal residues of CupB5 play little or no role in mediating alginate overproduction. Moreover, overproduction of variants containing just the N-terminal 491 residues of CupB5 also induced mucoidy (Table 4.S1), indicating that a major inducing signal is located in this portion of the protein.

Deletion analyses revealed that the Thr^{489}-Val^{490}-Val^{491} sequence of CupB5 appeared important for alginate overproduction. Specifically, overexpression of $CupB5^{1-491}$ produced substantially more alginate than overexpression of $CupB5^{1-489}$ or $CupB5^{1-488}$ (Fig. 4.3A), and Western blotting showed that these proteins were present at a similar intracellular levels (Fig. 4.3B). Cells expressing CupB51-490 also produced less alginate (Fig. 4.3A), but this protein appeared to be severely truncated by degradation (Fig. 4.3B). Based on these results, we hypothesized that the CupB5 activating signal included some or all of the Thr^{489}-Val^{490}-Val^{491} sequence.

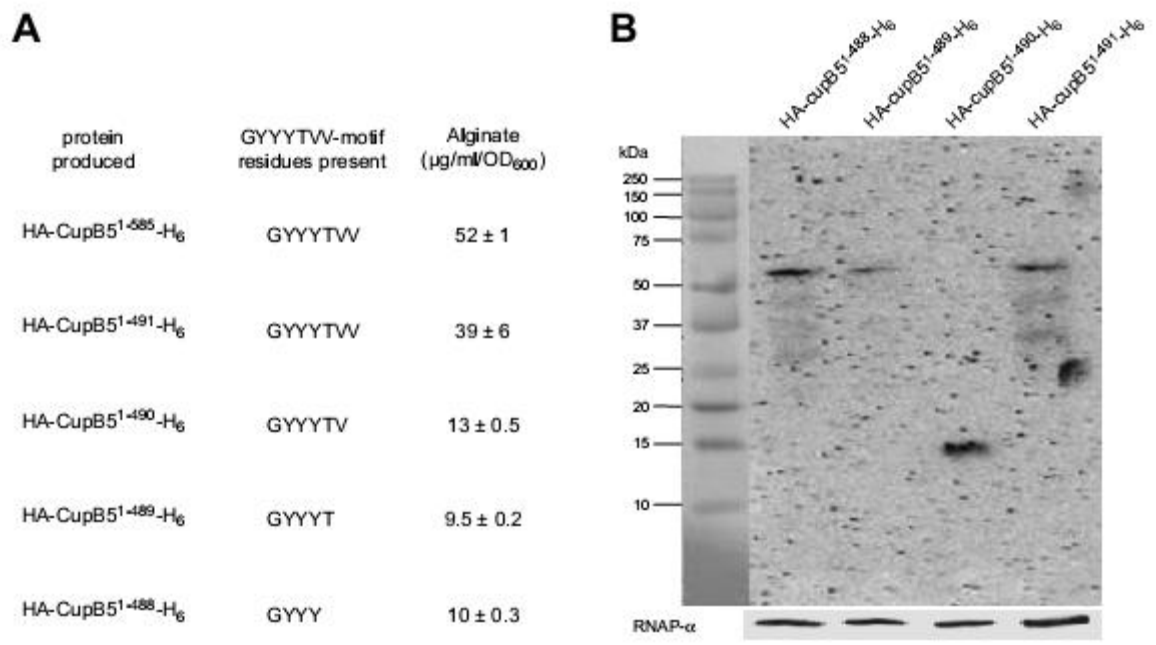

Fig. 4.3. Delineation of the CupB5 signal that activates alginate production. (A) CupB5 variants with C-terminal truncations were cloned into pHERD20T, expressed in strain PAO1, and alginate production following growth in the presence of 1% L-arabinose was assayed. Proteins containing CupB5 residues 1-585 and 1-491 contain the complete GYYYTVV491 sequence motif. The remaining proteins contain only a portion of this motif. (B) Western-blot detection using anti-HA monoclonal antibody of truncated CupB5 variants.

CupB5 peptides stimulate OMP-activated AlgW cleavage of MucA and partially relieve MucB inhibition in vitro

We initially tested if synthetic peptides including the Thr^{489}-Val^{490}-Val^{491} CupB5 sequence might stimulate alginate production in a manner analogous to OMPs by activating AlgW cleavage of ^{35}S-MucA. One peptide (GYYYTVV) corresponded to the seven C-terminal residues of $CupB5^{1-491}$, another (YVGYVTY) was a sequence-scrambled variant, and a third (GYYYT) corresponded to the C-terminus of $CupB5^{1-489}$, which did not stimulate alginate production in vivo. We assayed the kinetics of AlgW cleavage of ^{35}S-MucA in vitro by the production of acid-soluble peptide fragments in the presence of different concentrations of the CupB5 peptides. Each CupB5 peptide stimulated AlgW cleavage of ^{35}S-MucA to a small degree, but at far lower

rates than a peptide (WVF) corresponding to the C-terminal residues of MucE, a potent activator of AlgW (Fig. 4.4A & 4B). Thus, the CupB5 peptides do not substitute for OMP-like peptides in robust activation of AlgW cleavage of MucA.

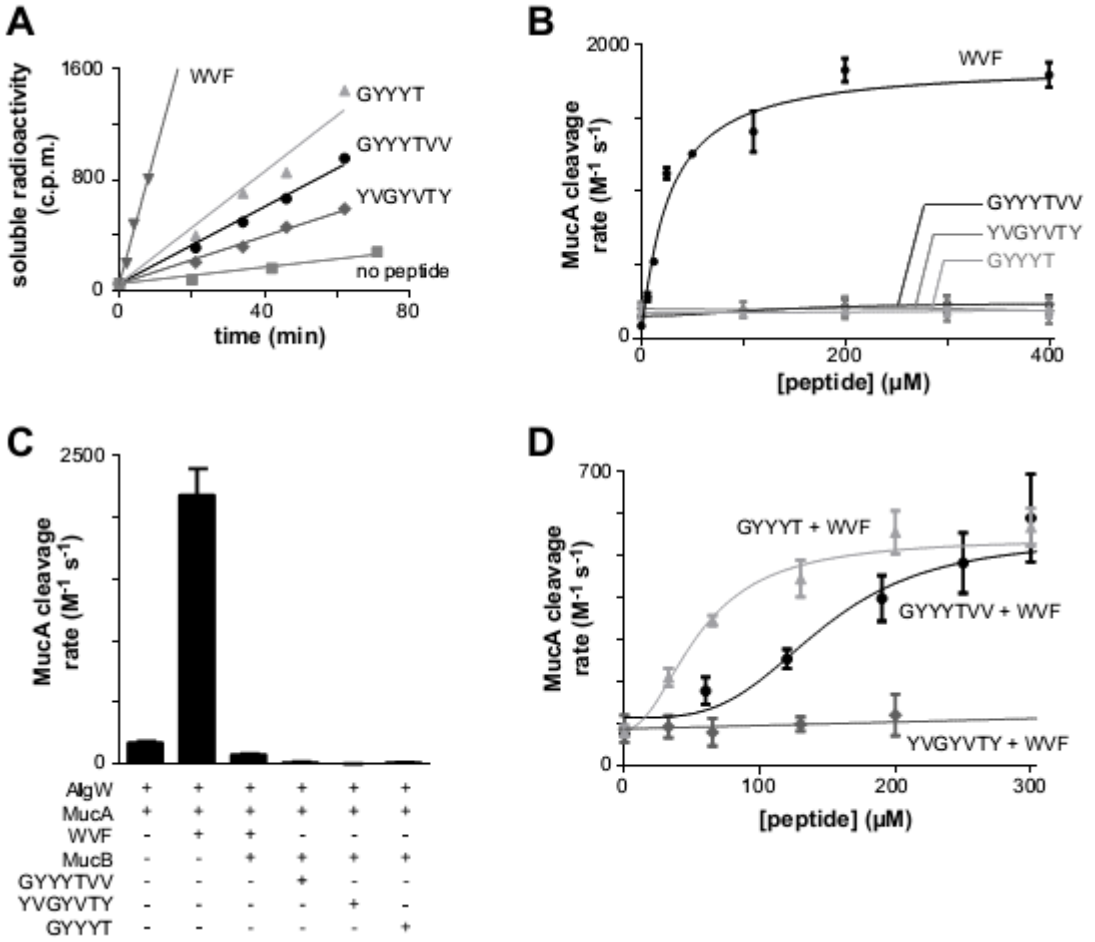

Fig. 4.4. CupB5 peptides relieve MucB inhibition of MucA cleavage by AlgW. (A) Cleavage of 35S-labelled MucA (20 μM) by AlgW (0.5 μM trimer) was assayed by the time-dependent release of acid-soluble peptides in the presence of either the OMP-like WVF peptide (400 μM), the wild-type GYYYT or GYYYTVV CupB5 peptides (400 μM), the sequence-scrambled YVGYVTY peptide (400 μM), or a buffer control. (B) Second-order rate constants for MucA cleavage were determined by incubating ^{35}S-labelled MucA (20 μM) and AlgW (0.5 μM trimer) with different concentrations of WVF or CupB5 peptides and measuring the time-dependent increase in acid-soluble products. Rates were divided by the MucA and AlgW concentrations to determine activity. Lines are fits to the equation activity = basal + stimulated/(1+(K_{act}/[peptide])h). Values are averages ± SEM (n=2). (C) Second-order rate constants for cleavage of ^{35}S-MucA (20 μM) by AlgW (0.5 μM trimer) were determined as described in panel B in the presence of different combinations of WVF peptide (110 μM), MucB (25 μM dimer), and wild-type or scrambled CupB5 peptides (405 μM). Values are averages of two or more independent trials ± SEM. (D) Second-order rate constants for cleavage of ^{35}S-MucA (20 μM) by AlgW (0.5 μM trimer) and WVF peptide (150 μM) were determined in the presence of increasing concentrations of the GYYYT, GYYYTVV, or sequence-scrambled YVGYVTY peptides. Lines are fits to the Hill equation: rate = basal + Vmax/(1 + (K_s/[peptide])h). For GYYYT, K_s was 55 ± 13 μM and h was 2.1 ± 0.9. For GYYYTVV, K_s was 143 ± 31 μM and h was 3.5 ± 2.2.

As expected from previous studies (Cezairliyan and Sauer, 2009), addition of MucB suppressed cleavage of 35S-MucA by WVF-activated AlgW (Fig. 4.4C). Moreover, addition of just the GYYYTVV, YVGYVTY, or GYYYT CupB5 peptides did not result in AlgW cleavage of MucA when MucB was present (Fig. 4.4C). Next, we tested if the wild-type or scrambled CupB5 peptides could relieve MucB inhibition of AlgW cleavage of ^{35}S-MucA in the presence of the WVF activating peptide. Importantly, titration of GYYYTVV or GYYYT into reactions containing MucA, MucB, AlgW, and WVF peptide resulted in a dose-dependent increase in the rate of MucA cleavage (Fig. 4.4D). Almost no increase in MucA cleavage was observed with the scrambled YVGYVTY peptide (Fig. 4.4D), demonstrating sequence specificity. Interestingly, activation of MucA cleavage by GYYYT occurred at lower peptide concentrations and was less cooperative as judged by the Hill constant than activation by the GYYYTVV peptide (Fig. 4.4D). Thus, the C-terminal valine residues of GYYYTVV are not necessary for activation of MucA cleavage in the presence of MucB in vitro. Although the GYYYTVV and GYYYT peptides activated AlgW cleavage of MucA to similar levels in the presence of WVF peptide and MucB, these levels were approximately one-third of the MucA cleavage rate observed with WVF and AlgW alone (compare Figs. 4B and 4D). We conclude that the CupB5 peptides can partially relieve MucB inhibition of WVF-activated AlgW cleavage of MucA.

Lipopolysaccharides bind MucB and competitively displace MucA (Lima *et al.*, 2013). Because MucB normally binds peptide sequences in MucA, it seemed plausible that CupB5 peptides might also compete for MucA binding to MucB. We tested this possibility by assaying the ability of the CupB5 peptides to elute ^{35}S-MucB from MucA that had been covalently bound to agarose resin (Fig. 4.5A). In this assay, the L-IIA lipopolysaccharide fragment and free MucA efficiently

competed with resin-bound MucA for MucB binding. However, incubation of 35S-MucB•MucA resin with the GYYYTVV, YVGYVTY, or GYYYT peptides resulted in no more 35S-MucB release than observed in the buffer control (Fig. 4.5A). This result strongly suggests that the CupB5 peptides do not relieve MucB inhibition by directly competing for its binding to MucA. Binding of the L-IIA lipopolysaccharide fragment converts MucB dimers to tetramers (Lima *et al.*, 2013). By contrast, incubation of MucB with GYYYTVV peptide resulted in no substantial change in elution during gel-filtration chromatography (Fig. 4.S2).

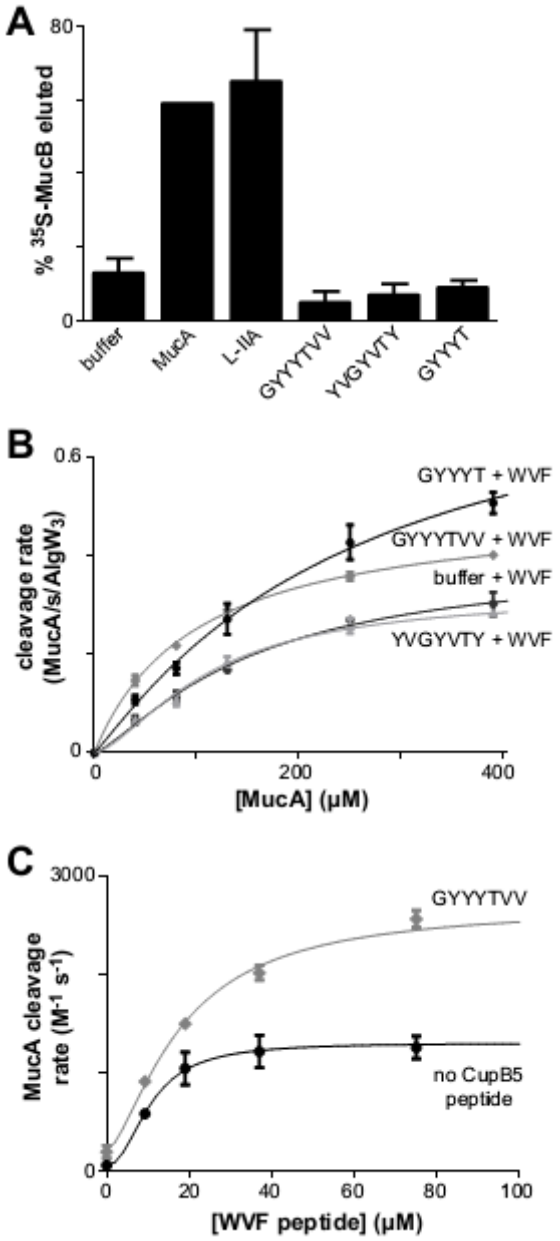

Fig. 4.5. CupB5 peptides do not compete with MucB for MucA binding but stimulate WVF-activated AlgW cleavage of MucA. (A) Release of ^{35}S-MucB from MucA-agarose following incubation with buffer, MucA (155 μM), L-IIA (20 mg/mL), or CupB5 peptides (~300 μM). For the CupB5 peptides, values are averages ± SEM (n=3). For L-IIA, the value is the average ± SEM (n=2). (B) Rates of cleavage by AlgW (0.5 μM trimer) and WVF peptide (150 μM) were measured at different concentrations of ^{35}S-MucA in the presence or absence of CupB5 peptides (300 μM). Values are averages ± SEM (n=2) and were fit to the Hill form of the Michaelis-Menten equation, rate = $V_{max}/(1 + (K_M/[substrate])h)$. (C) Rates of cleavage of ^{35}S-MucA (50 μM) by AlgW (0.5 μM trimer) were assayed at difference concentrations of WVF peptide in the presence or absence of CupB5 peptides (300 μM). Values are averages ± SEM (n=2) and were fit to the equation rate = basal + $V_{max}/(1 + (K_{act}/[peptide])h)$. Without CupB5 peptide, h was 2.2 ± 1, K_{act} was 11 ± 2 μM, and V_{max} was 1250 ± 150 $M^{-1}s^{-1}$. With GYYYTVV peptide, h was 1.5 ± 0.8, K_{act} was 18 ± 7 μM, and V_{max} was 2490 ± 490 $M^{-1}s^{-1}$.

Because CupB5 peptides did not strongly activate AlgW cleavage of MucA in the absence of the WVF peptide or release MucA from MucB, we speculated that they might act in concert with the WVF peptide to allow AlgW to bind and degrade MucA more efficiently and thus to compete better with MucB for the MucA substrate. This model predicts that MucA should be degraded at a faster rate in the presence of both the WVF and CupB5 peptides. Indeed, when we assayed the rate of cleavage of different concentrations of ^{35}S-MucA by AlgW, faster cleavage was observed when both the WVF and wild-type CupB5 peptides were present compared to only the WVF peptide or the WVF peptide and scrambled CupB5 control peptide (Fig. 4.5B). We also measured the rate of AlgW cleavage of a fixed concentration of MucA in the presence of increasing concentrations of WVF peptide with or without additional GYYYTVV peptide (Fig. 4.5C). When GYYYTVV peptide was present, the maximum rate of MucA cleavage increased almost two-fold. We conclude that the CupB5 peptides and WVF peptide act synergistically to enhance AlgW cleavage of MucA, allowing better competition with MucB.

In *E. coli*, RseA, RseB, and DegS are homologs of MucA, MucB, and AlgW. A YYF peptide efficiently activates DegS cleavage of RseA in the absence of RseB or in the presence of both RseB and lipopolysaccharides (Walsh *et al.*, 2003; Cezairliyan and Sauer, 2007; Lima *et al.*, 2013). The CupB5 peptides did not substantially stimulate cleavage of ^{35}S-RseA by YYF-activated DegS in the presence of RseB (Fig. 4.S3), suggesting that they do not interact with DegS. This result is not surprising, as DegS and AlgW share only 44% sequence homology.

Suppressing and enhancing alginate production

If CupB5 allows AlgW to compete more efficiently with MucB for MucA binding and cleavage, then overproduction of MucB in strain PAO1-VE22 would be expected to decrease alginate production. Indeed, plasmid-mediated MucB overproduction had this effect, as did plasmid-mediated overproduction of MucA (Fig. 4.6A). The latter result suggests that with enough additional uncleaved MucA, AlgU is efficiently inhibited even when more MucA is degraded than usual. Even the CupB5-induced elevated rate of AlgW cleavage of MucA in this strain must be too slow to free enough AlgU to fully enhance transcription of alginate biosynthesis genes.

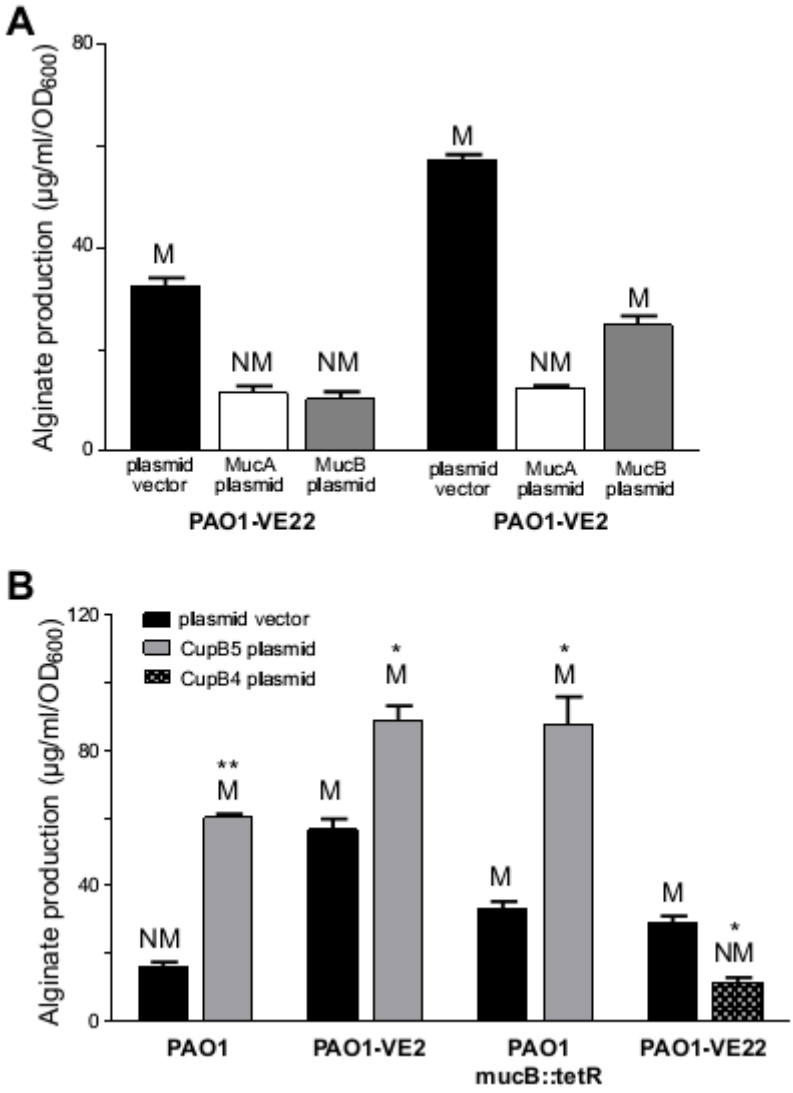

Fig. 4.6. Inducing and suppressing alginate production in *P. aeruginosa* strains. (A) Strains overproducing CupB5 (PAO1-VE22) or MucE (PAO1-VE2) were transformed with plasmid HERD20T or variants overexpressing MucA or MucB, grown at 37ºC for 24 h on PIA plates supplemented with 0.1% L-arabinose, and alginate production and colony phenotypes (M, mucoid; NM, nonmucoid) were assayed. (B) Alginate production and mucoid phenotypes were assayed in strains PAO1, PAO1-VE2 (mucE overexpressed), PAO1 *mucB::tetR* (mucB inactivated), and PAO1-VE22 (cupB5 overexpressed) transformed with the HERD20T plasmid vector or variants expressing HA-CupB4-H_6 or HA-CupB5-H_6. Values are averages ± SEM (n=3). Statistical significance was determine using the Student's t-test (*P<0.05; **<0.005).

Plasmid-expressed MucB or MucA also decreased alginate production in PAO1-VE2, a strain expressing higher MucE levels (Fig. 4.6A). The rate of AlgW cleavage of MucA in PAO1-VE2

is apparently too low to fully degrade the excess MucA, resulting in greater inhibition of AlgU and reduced alginate production. Excess MucB presumably outstrips the endogenous anti-MucB signals in PAO1-VE2 and mass action results in enhanced binding to MucA, reducing the rate of MucA cleavage by activated AlgW.

To determine how simultaneous overexpression of MucE and CupB5 affected alginate levels,, we transformed PAO1-VE2 with a plasmid expressing HA-CupB5-H_6. Notably, alginate levels in this strain were higher than in the empty-vector control (Fig. 4.6B), suggesting that activation of AlgW through MucE and through CupB5 occur synergistically. Our biochemical results predict that MucB should not be genetically required for CupB5-mediated pathway activation. To test this prediction, we used a transposon-insertion strain, PAO1-*mucB::tet*^{R}, which displayed an elevated level of basal alginate production and mucoid phenotype (Fig. 4.6B). When we transformed PAO1-mucB::tetR with a plasmid expressing HA-CupB5-H_6, alginate production increased compared to the empty-vector control (Fig. 4.6B), indicating that CupB5 overexpression induces pathway activation by a MucB-independent mechanism. Finally, we tested if expression of the CupB4 chaperone, which should facilitate export of CupB5 rather than its periplasmic accumulation, would decrease alginate production. Indeed, when we transformed PAO1-VE22 with a plasmid expressing HA-CupB4-H_6, alginate production was suppressed and the mucoid phenotype of the parent strain was reversed (Fig. 4.6B). This result supports a model in which interactions between accumulated periplasmic CupB5 and periplasmic AlgW leads to induction of alginate production and mucoidy.

Discussion

Based on results from a transposon screen in *P. aeruginosa*, we discovered that overexpression of CupB5, a protein normally secreted through the outer membrane by a chaperone-usher system, activates alginate production and results in mucoid colonies. CupB5-mediated mucoidy depends on known components of the AlgU stress-response pathway, including the AlgU transcription factor and the AlgW, MucP, and ClpXP proteases. Peptides from a region of CupB5 important for elevated alginate production in vivo stimulate cleavage of MucA by OMP-activated AlgW in vitro and partially relieve MucB inhibition of AlgW cleavage of MucA. Overexpression of either MucB or MucA in strains that overexpress CupB5 also reduces alginate production, supporting a model in which excess periplasmic CupB5 stimulates proteolytic cleavage of MucA by AlgW.

We found that expression of HA-CupB5$^{1\text{-}491}$-H_6 in PAO1 increased alginate production in vivo and demonstrated that a GYYYTVV peptide (corresponding to CupB5 residues 485-491) antagonized MucB inhibition in vitro. A peptide with the same composition as GYYYTVV but a scrambled sequence did not inhibit MucB. However, we also found that expression of HA-CupB51-489-H_6 failed to increase alginate production in vivo, whereas a GYYYT peptide (corresponding to CupB5 residues 485-489) did antagonize MucB inhibition in vitro. This discrepancy between results in vivo and in vitro could arise because the GYYYT peptide in HA-CupB5$^{1\text{-}489}$-H_6 is altered by proteolysis or is masked by tertiary structure, aggregation, or binding to another cellular component. We also note that expression of full-length HA-CupB5-H_6 and truncated HA-CupB5$^{1\text{-}585}$-H_6 resulted in somewhat higher alginate levels than expression of HA-CupB5$^{1\text{-}491}$-H_6. This variation could arise from differences in expression levels, cellular

interactions, or possibly as a consequence of additional peptide sequences in the longer proteins that facilitate pathway activation.

We initially thought that CupB5 peptides might bind MucB and compete for binding to MucA in a manner analogous to LPS. However, neither GYYYTVV nor GYYYT peptides compete with MucA-agarose for MucB binding and saturating concentrations of these peptides only partially relieve MucB inhibition in vitro. Moreover, unlike LPS, GYYYTVV did not convert MucB dimers into tetramers. By themselves, CupB5 peptides activate AlgW cleavage in vitro far less well than the OMP-like WVF peptide. However, CupB5 peptides stimulate MucA cleavage by WVF-activated AlgW, suggesting that OMP-like and CupB5 peptides bind to distinct sites in AlgW but have a common effect of stabilizing the proteolytically active enzyme.

The GYYYTVV sequence is conserved in CupB5 proteins from different strains of *P. aeruginosa* but not in CupB5 proteins from other *Pseudomonas* species (Fig. 4.S3), and some *Pseudomonas* species have no CupB5 ortholog. Thus, CupB5 activation of AlgW is specific to *P. aeruginosa*. It remains to be determined if *P. aeruginosa* utilizes other proteins in this manner or if AlgW homologs in other bacteria are activated by more than one kind of peptide signal.

Activation of the AlgU pathway requires one molecular signal (C-terminal OMP peptides) to activate site-1 cleavage of MucA by the AlgW protease and a second molecular signal (LPS) to relieve MucB inhibition of this cleavage. Overproduction of CupB5 can partially bypass this second requirement by helping OMP-bound AlgW compete with MucB for MucA binding and proteolysis. Expression of CupB5 under non-stress conditions increases alginate production

similarly to non-stress expression of MucE (Qiu *et al.*, 2007). In these experiments, a signal that directly antagonizes MucB inhibition could arise indirectly as a consequence of other molecules whose concentrations increase as a consequence of CupB5 or MucE expression or might always be present at some level in the periplasm. For example, some level of unassembled OMPs and LPS is probably always present in the periplasm. Notably, however, simultaneous expression of CupB5 and MucE results in higher levels of alginate, indicating that these signals activate the alginate pathway through synergistic mechanisms

Although CupB5 peptides, OMP peptides, and LPS molecules function by different mechanisms to activate AlgW or relieve MucB inhibition, the molecular logic that gives rise to all three signals is similar. For example, stresses that compromise the transport to and outer-membrane assembly of OMPs and LPS, or that slow usher-mediated CupB5 secretion, would all lead to the periplasmic accumulation of these molecules and activation of the AlgU pathway. Indeed, we found that alginate production was suppressed in strains that overproduced the CupB4 chaperone, allowing export of CupB5. Certain stresses might only activate AlgW through OMP signals, whereas others require an enhanced response via CupB5 or possibly other proteins secreted through the outer membrane. Clearly, however, the AlgU system integrates multiple signals, each reporting on potential dysfunction in outer-membrane assembly, structure, and/or secretion. Dysfunction in just one pathway should give rise to a buffered AlgU response, whereas dysfunction affecting multiple pathways would elicit a robust AlgU response.

Methods

Bacteria strains, plasmids, and growth conditions

Bacteria strains and plasmids used in this study are shown in Table 4.S2. *Escherichia* coli strains were grown at 37ºC in Lennox broth (LB) or LB agar. *P. aeruginosa* strains were grown at 37ºC in LB, *Pseudomonas* isolation broth (PIB, Alpha Bioscience) or on *Pseudomonas* isolation agar (PIA) plates (Difco). When required, the concentration of carbenicillin, tetracycline or gentamicin added to LB broth or plates was 100 μg ml^{-1}, 20 μg ml^{-1}, or 15 μg ml^{-1}, respectively, and 300 μg ml^{-1}, 150 μg ml^{-1}, or 200 μg ml^{-1} when added to PIB or PIA plates, respectively.

Transposon mutagenesis

Transposon mutagenesis was carried out via biparental conjugations using *E. coli* SM10 λpir carrying plasmid pFAC as the donor strain (Wong and Mekalanos, 2000) and PAO1 as the recipient strain. After incubating PAO1 and *E. coli* cells on LB agar plates at 37ºC for 6 h, bacteria were collected, re-suspended in PBS and then plated onto PIA supplemented with gentamicin (200 μg ml^{-1}). Mucoid colonies were identified. The chromosomal DNA of mucoid mutants was isolated using the QIAamp genomic DNA Extraction kit (Qiagen, USA). Approximately, 2 μg of DNA was digested with SalI overnight at 37ºC, followed by purification and self-ligation using Fast-Link DNA ligase (Epicentre, USA). The circular closed DNA was used as a template for inverse PCR using GM3OUT and GM5OUT primers (Qiu *et al.*, 2008b). The PCR products were purified and sequenced. Finally, Southern-blot hybridization was also conducted to monitor the copy number of transposon insertions using the Gmr gene as the probe (Head and Yu, 2004).

Genetic construction, transformation and conjugation

All DNA cloning was performed using PCR products digested with appropriate restriction enzymes and ligated into the *E. coli* to *Pseudomonas* shuttle vector pHERD20T (Qiu *et al.*, 2008a). All constructs of pHERD20T were sequenced to verify the correct DNA sequences. DNA sequencing was carried out by the Marshall University Genomics Core Facility. The primer sequences used for PCR cloning will be provided upon request. The transformation of One Shot TOP10 (Invitrogen, USA) was performed according to the supplier's instruction. The transfer of pHERD20T and its derivatives was performed via triparental conjugation using the helper plasmid pRK2013 (Figurski and Helinski, 1979) .

Protein preparation and Western blotting

For extraction of total cellular protein, PeriPreps™ Periplasting Kit (Epicentre, USA) was used. Bacteria were inoculated in PIB medium and incubated in shake culture for several hours, until the OD600 was ~0.6. At this point 0.1% L-arabinose was added to induce protein expression. Two hours after induction, bacteria were collected for cell lysis. The protein concentration was measured using Bio-Rad Dc protein assay reagents (Bio-Rad). Equivalent proteins were mixed with 2×sample loading buffer and analyzed on 10-20% pre-cast SDS-PAGE gels (Bio-Rad). Proteins were then transferred to a PVDF membrane (GE) by electro-blotting for immunodetection. A primary antibody, rat Anti-HA (Roche, USA), was used at a dilution of 1:5000. Goat anti-rat immunoglobulin G (heavy and light chains) conjugated with horseradish peroxidase (Pierce, USA) diluted 1: 5000 was used as the secondary antibody. Finally, the proteins on the membrane were visualized using the Amersham ECL kit (GE, USA).

Alginate assay

P. aeruginosa strains were grown at 37°C on triplicate PIA plates for 24 h. Bacteria were collected, suspended in PBS, and the OD600 was measured and adjusted to ~0.5 by addition of PBS. The suspensions were analyzed for the amount of uronic acid in comparison with a standard curve made with D-mannuronic acid lactone (Sigma-Aldrich, USA) as described (Damron *et al.*, 2009).

β-galactosidase assay

Pseudomonas strains carrying the lacZ vector pLP170 containing PalgU, and PalgDwere cultured on PIA plates. After 24 h, bacteria were harvested, resuspended in PBS, and OD600 was measured and adjusted to ~0.3. Cells were then permeabilized using toluene, and β-galactosidase activity was measured at OD420 and OD550. The results in Miller Units were calculated according to the follow formula: Miller Units=1000×[OD 420-(1.75 × OD 550)]/[Reaction time (m) × Volume (ml) × OD 600] (Miller, 1972). The reported values represent an average of three independent experiments ± SEM.

Proteins and peptides

Purifications of *P. aeruginosa* MucA, MucB and AlgW and *E. coli* RseA, RseB and DegS were performed as described after plasmid-mediated overexpression in *E. coli* strain X90(DE3) (Sohn *et al.*, 2007; Cezairliyan and Sauer, 2009). Cultures containing 100 μg/mL ampicillin were grown to an OD600 of ~0.6, and protein expression was induced with 100 mM IPTG for two h before harvesting. Cells overexpressing MucB, AlgW, RseB or DegS were resuspended in native lysis buffer [*P. aeruginosa* proteins: 50 mM sodium phosphate (pH 8), 500 mM KCl, 20 mM

imidazole; *E. coli* proteins: 50 mM sodium phosphate (pH 8), 300 mM NaCl, 10 mM imidazole] and lysed by sonication. Cells overexpressing MucA or RseA were resuspended in denaturing lysis buffer [50 mM sodium phosphate (pH 8), 8 M guanidine hydrochloride (pH 8)] and allowed to lyse at room temperature for 30 min. For all preparations, lysates were cleared by centrifugation and applied to Ni-NTA columns pre-equilibrated in native lysis buffer or denaturing lysis buffer. Columns were washed with lysis buffer and proteins eluted with elution buffer [*P. aeruginosa* proteins: 50 mM sodium phosphate (pH 8), 500 mM KCl, 500 mM imidazole; *E. coli* proteins: 50 mM sodium phosphate (pH 8), 300 mM NaCl, 300 mM imidazole]. Proteins were then dialyzed overnight against storage buffer [*P. aeruginosa* proteins: 50 mM sodium phosphate (pH 7.4), 200 mM KCl, 10% glycerol; *E. coli* proteins: 50 mM sodium phosphate (pH 8), 200 mM NaCl, 1 mM EDTA] and then again against fresh buffer before being stored frozen at –80°C. Prior to dialysis and storage, MucB and RseB were chromatographed on a size-exclusion column and only fractions corresponding to the dimer were collected. To obtain radiolabeled ^{35}S-MucA, ^{35}S-RseA, or ^{35}S-MucB, cells were grown in a defined rich medium (TekNova) lacking methionine and ^{35}S-methionine was added upon induction. Purification of 35S-MucA and 35S-RseA then proceeded as described above for unlabeled MucA and RseA. Cells expressing 35S-MucB were lysed by the addition of lysozyme and three freeze-thaw cycles, and purification then proceeded as described above. All peptides were synthesized by GenScript and purified by reverse-phase HPLC using a C18 column. Purified products were lyophilized, stored at –20°C, then resuspended in storage buffer and used immediately. The L-IIA LPS fragment was a gift from Santiago Lima (MIT) (Lima *et al.*, 2013).

Cleavage assays

Assays were performed as described (Sohn *et al.*, 2007; Cezairliyan and Sauer, 2009). Briefly, cleavage reactions were performed at 25°C in reaction buffer [*P. aeruginosa* proteins: 50 mM sodium phosphate (pH 7.4), 200 mM KCl, 10% glycerol; *E. coli* proteins: 150 mM sodium phosphate (pH 8.3), 380 mM NaCl, 10% glycerol, 4 mM EDTA]. Reactions were initiated by the addition of protease and quenched after different times by addition of cold 10% trichloroacetic acid. Following centrifugation, acid-soluble reaction products were quantified by scintillation counting and compared to total radioactivity from control samples. Cleavage activity for peptide-activation assays and experiments involving MucB are reported as a second-order rate constant calculated by dividing the rate of substrate cleavage by the substrate and enzyme concentrations. Activity at different substrate concentrations for the Michaelis-Menten curve was calculated by dividing the rate of substrate cleavage by the enzyme concentration.

MucA-resin assay

Dry cyanogen-bromide activated Sepharose B4 resin (66 mg) was washed with 1 M HCl, equilibrated with coupling buffer [25 mM sodium phosphate (pH 8.3), 50 mM NaCl], and incubated with purified MucA (900 µg) for 1.5 hours. After removal of free protein, reactive groups on the resin were blocked by incubation in 0.5 M ethanolamine (pH 8.3) for 1 h. The MucA resin was washed, resuspended in coupling buffer, and stored at 4 °C. For assays, MucA resin was drained, incubated with a four-fold molar excess of 35S-MucB, washed again, incubated with ligand for 30 min, added to a pre-wetted 96-well Multiscreen HTS-HV Filter Plate (Millipore) over a 96-well polypropylene receiving plate (Greiner), and centrifuged at 1500

x g for 1 min. Elution of 35S-MucB was measured by scintillation counting and normalized by dividing by the total initial 35S-MucB radioactivity.

Acknowledgements

This work was supported by the National Aeronautics and Space Administration West Virginia Space Grant Consortium (NASA WVSGC), the Cystic Fibrosis Foundation (CFF-YU11G0), and NIH grant AI-16892. HDY was supported by NIH P20RR016477 and P20GM103434 to the West Virginia IDeA Network for Biomedical Research Excellence, and is also the co-founder of Progenesis Technologies, LLC. T.R.W. was supported through the NASA WVSGC Graduate Research Fellowship. We thank Dongru Qiu for construction of PAO1□algD.

References

Akiyama Y., Kanehara K., Ito K. (2004). RseP (YaeL), an *Escherichia* coli RIP protease, cleaves transmembrane sequences. EMBO J 23: 4434-4442.

Alba B.M., Leeds J.A., Onufryk C., Lu C.Z., Gross C.A. (2002). DegS and YaeL participate sequentially in the cleavage of RseA to activate the sigma(E)-dependent extracytoplasmic stress response. Genes Dev 16: 2156-2168.

Boucher J.C., Yu H., Mudd M.H., Deretic V. (1997). Mucoid *Pseudomonas* aeruginosa in cystic fibrosis: characterization of muc mutations in clinical isolates and analysis of clearance in a mouse model of respiratory infection. Infect Immun 65: 3838-3846.

Cezairliyan, B.O., and Sauer, R.T. (2007). Inhibition of regulated proteolysis by RseB. Proc Natl Acad Sci USA 104: 3771-3776.

Cezairliyan B.O., Sauer R.T. (2009). Control of *Pseudomonas* aeruginosa AlgW protease cleavage of MucA by peptide signals and MucB. Mol Microbiol 72: 368-379.

Chaba R., Grigorova I.L., Flynn J.M., Baker T.A., Gross C.A. (2007). Design principles of the proteolytic cascade governing the sigmaE-mediated envelope stress response in *Escherichia* coli: keys to graded, buffered, and rapid signal transduction. Genes Dev 21: 124-136.

Ciofu O., Riis B., Pressler T., Poulsen H.E., Hoiby N. (2005). Occurrence of hypermutable *Pseudomonas* aeruginosa in cystic fibrosis patients is associated with the oxidative stress caused by chronic lung inflammation. Antimicrob Agents Chemother 49: 2276-2282.

Damron F.H., Qiu D., Yu H.D. (2009). The *Pseudomonas* aeruginosa sensor kinase KinB negatively controls alginate production through AlgW-dependent MucA proteolysis. J Bacteriol 191: 2285-2295.

Figurski D.H., Helinski D.R. (1979). Replication of an origin-containing derivative of plasmid RK2 dependent on a plasmid function provided in trans. Proc Natl Acad Sci U S A 76: 1648-1652.

Flynn J.M., Levchenko I., Sauer R.T., Baker T.A. (2004). Modulating substrate choice: the SspB adaptor delivers a regulator of the extracytoplasmic-stress response to the AAA+ protease ClpXP for degradation. Genes Dev 18: 2292-2301.

Folkesson A., Jelsbak L., Yang L., Johansen H.K., Ciofu O., Hoiby N., et al. (2012). Adaptation of *Pseudomonas* aeruginosa to the cystic fibrosis airway: an evolutionary perspective. Nat Rev Microbiol 10: 841-851.

Giraud C., Bernard C.S., Calderon V., Yang L., Filloux A., Molin S., et al. (2011). The PprA-PprB two-component system activates CupE, the first non-archetypal *Pseudomonas* aeruginosa chaperone-usher pathway system assembling fimbriae. Environ Microbiol 13: 666-683.

Govan J.R., Deretic V. (1996). Microbial pathogenesis in cystic fibrosis: mucoid *Pseudomonas* aeruginosa and Burkholderia cepacia. Microbiol Rev 60: 539-574.

Head N.E., Yu H. (2004). Cross-sectional analysis of clinical and environmental isolates of *Pseudomonas* aeruginosa: biofilm formation, virulence, and genome diversity. Infect Immun 72: 133-144.

Hogardt M., Hoboth C., Schmoldt S., Henke C., Bader L., Heesemann J. (2007). Stage-specific adaptation of hypermutable *Pseudomonas* aeruginosa isolates during chronic pulmonary infection in patients with cystic fibrosis. J Infect Dis 195: 70-80.

Hull R.A., Gill R.E., Hsu P., Minshew B.H., Falkow S. (1981). Construction and expression of recombinant plasmids encoding type 1 or D-mannose-resistant pili from a urinary tract infection *Escherichia* coli isolate. Infect Immun 33: 933-938.

Kanehara K., Ito K., Akiyama Y. (2002). YaeL (EcfE) activates the sigma(E) pathway of stress response through a site-2 cleavage of anti-sigma(E), RseA. Genes Dev 16: 2147-2155.

Leid J.G., Willson C.J., Shirtliff M.E., Hassett D.J., Parsek M.R., Jeffers A.K. (2005). The exopolysaccharide alginate protects *Pseudomonas* aeruginosa biofilm bacteria from IFN-gamma-mediated macrophage killing. J Immunol 175: 7512-7518.

Lima S., Guo M.S., Chaba R., Gross C.A., Sauer R.T. (2013). Dual molecular signals mediate the bacterial response to outer-membrane stress. Science 340: 837-841.

Marklund B.I., Tennent J.M., Garcia E., Hamers A., Baga M., Lindberg F., et al. (1992). Horizontal gene transfer of the *Escherichia* coli pap and prs pili operons as a mechanism for the development of tissue-specific adhesive properties. Mol Microbiol 6: 2225-2242.

Martin, D.W., Holloway, B.W., and Deretic, V. (1993) Characterization of a locus determining the mucoid status of *Pseudomonas* aeruginosa: AlgU shows sequence similarities with a Bacillus sigma factor. J Bacteriol 175:1153-1164.

Mathee K., McPherson C.J., Ohman D.E. (1997). Posttranslational control of the algT (algU)-encoded sigma22 for expression of the alginate regulon in *Pseudomonas* aeruginosa and localization of its antagonist proteins MucA and MucB (AlgN). J Bacteriol 179: 3711-3720.

Mena A., Smith E.E., Burns J.L., Speert D.P., Moskowitz S.M., Perez J.L., et al. (2008). Genetic adaptation of *Pseudomonas* aeruginosa to the airways of cystic fibrosis patients is catalyzed by hypermutation. J Bacteriol 190: 7910-7917.

Mikkelsen H., Ball G., Giraud C., Filloux A. (2009). Expression of *Pseudomonas* aeruginosa CupD fimbrial genes is antagonistically controlled by RcsB and the EAL-containing PvrR response regulators. PLoS One 4: e6018.

Miller J.H. (1972) beta-galactosidase assay. In: Experiments in molecular genetics. Edited by Miller JH. Cold Spring Harbor, New York: Cold Spring Harbor Laboratory, pp. 352-355.

Pier G.B., Coleman F., Grout M., Franklin M., Ohman D.E. (2001). Role of alginate O acetylation in resistance of mucoid *Pseudomonas* aeruginosa to opsonic phagocytosis. Infect Immun 69: 1895-1901.

Qiu D., Damron F.H., Mima T., Schweizer H.P., Yu H.D. (2008a). PBAD-based shuttle vectors for functional analysis of toxic and highly regulated genes in *Pseudomonas* and Burkholderia spp. and other bacteria. Appl Environ Microbiol 74: 7422-7426.

Qiu D., Eisinger V.M., Head N.E., Pier G.B., Yu H.D. (2008b). ClpXP proteases positively regulate alginate overexpression and mucoid conversion in *Pseudomonas* aeruginosa. Microbiology 154: 2119-2130.

Qiu D., Eisinger V.M., Rowen D.W., Yu H.D. (2007). Regulated proteolysis controls mucoid conversion in *Pseudomonas* aeruginosa. Proc Natl Acad Sci U S A 104: 8107-8112.
Rubin E.J., Akerley B.J., Novik V.N., Lampe D.J., Husson R.N., Mekalanos J.J. (1999). In vivo transposition of mariner-based elements in enteric bacteria and mycobacteria. Proc Natl Acad Sci U S A 96: 1645-1650.

Ruer S., Ball G., Filloux A., de Bentzmann S. (2008). The 'P-usher', a novel protein transporter involved in fimbrial assembly and TpsA secretion. EMBO J 27: 2669-2680.

Ruer S., Stender S., Filloux A., de Bentzmann S. (2007). Assembly of fimbrial structures in *Pseudomonas* aeruginosa: functionality and specificity of chaperone-usher machineries. J Bacteriol 189: 3547-3555.

Sauer F.G., Barnhart M., Choudhury D., Knight S.D., Waksman G., Hultgren S.J. (2000). Chaperone-assisted pilus assembly and bacterial attachment. Curr Opin Struct Biol 10: 548-556.
Schurr M.J., Yu H., Martinez-Salazar J.M., Boucher J.C., Deretic V. (1996). Control of AlgU, a member of the sigma E-like family of stress sigma factors, by the negative regulators MucA and MucB and *Pseudomonas* aeruginosa conversion to mucoidy in cystic fibrosis. J Bacteriol 178: 4997-5004.

Sohn J., Grant R.A., Sauer R.T. (2007). Allosteric activation of DegS, a stress sensor PDZ protease. Cell 131: 572-583.

Soto G.E., Hultgren S.J. (1999). Bacterial adhesins: common themes and variations in architecture and assembly. J Bacteriol 181: 1059-1071.

Vallet I., Olson J.W., Lory S., Lazdunski A., Filloux A. (2001). The chaperone/usher pathways of *Pseudomonas* aeruginosa: identification of fimbrial gene clusters (cup) and their involvement in biofilm formation. Proc Natl Acad Sci USA 98: 6911-6916.

Waksman G., Hultgren S.J. (2009). Structural biology of the chaperone-usher pathway of pilus biogenesis. Nat Rev Microbiol 7: 765-774.

Walsh N.P., Alba B.M., Bose B., Gross C.A., Sauer R.T. (2003). OMP peptide signals initiate the envelope-stress response by activating DegS protease via relief of inhibition mediated by its PDZ domain. Cell 113: 61-71.

Wong S.M., Mekalanos J.J. (2000). Genetic footprinting with mariner-based transposition in *Pseudomonas* aeruginosa. Proc Natl Acad Sci USA 97: 10191-10196.

Wood, L.F., Leech, A.J., and Ohman, D.E. (2006). Cell wall-inhibitory antibiotics activate the alginate biosynthesis operon in *Pseudomonas* aeruginosa: roles of σ22 (AlgT) and the AlgW and Prc proteases. Mol Microbiol 62:412-426.

Supplemental Figures and Tables

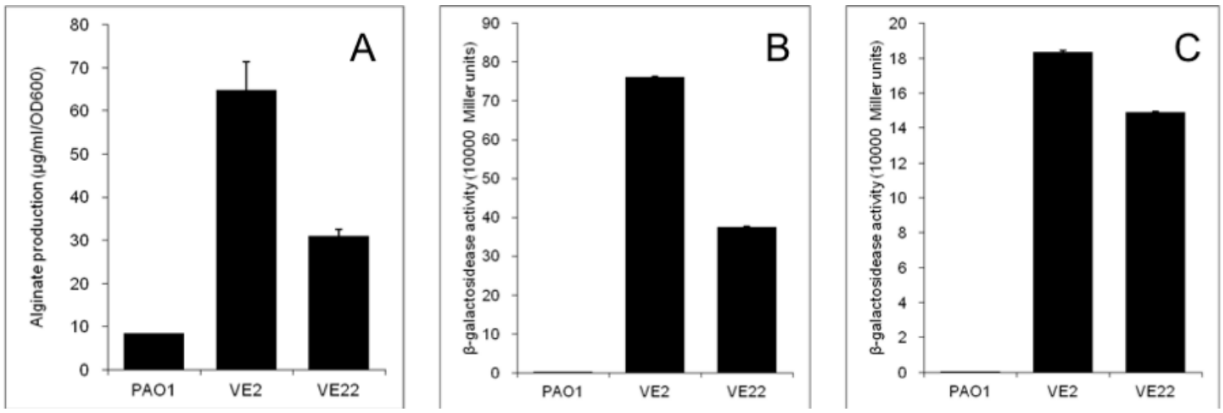

Fig. 4.S1. Alginate production and promoter activity of P_{algU} and P_{algD} in PAO1, PAO1-VE2 (*mucE* overexpressed) and PAO1-VE22 (*cupB5* overexpressed). Strains were streaked on PIA plates and cultured overnight at 37°C. For alginate assay, cells were grown on PIA plates without antibiotics. For β-galactosidase assay, carbencillin (300 µg ml^{-1}) was added to the medium to retain the plasmid. (A) Alginate production was measured after overnight culture. (B) Measurement of the activity of the *algU* promoter using pLP170-P_{algU} in different strains. The P_{algU} promoter was inserted into a pLP170 vector containing the promoterless *lacZ* gene. The P_{algU}-*lacZ* fusion in pLP170 was transferred into the respective strains via triparental conjugation. β-galactosidase activity was measured using the Miller assay as described in Experimental Procedures. (C) Measurement of activity of the *algD* promoter in different strains containing pLP170-P_{algD}.

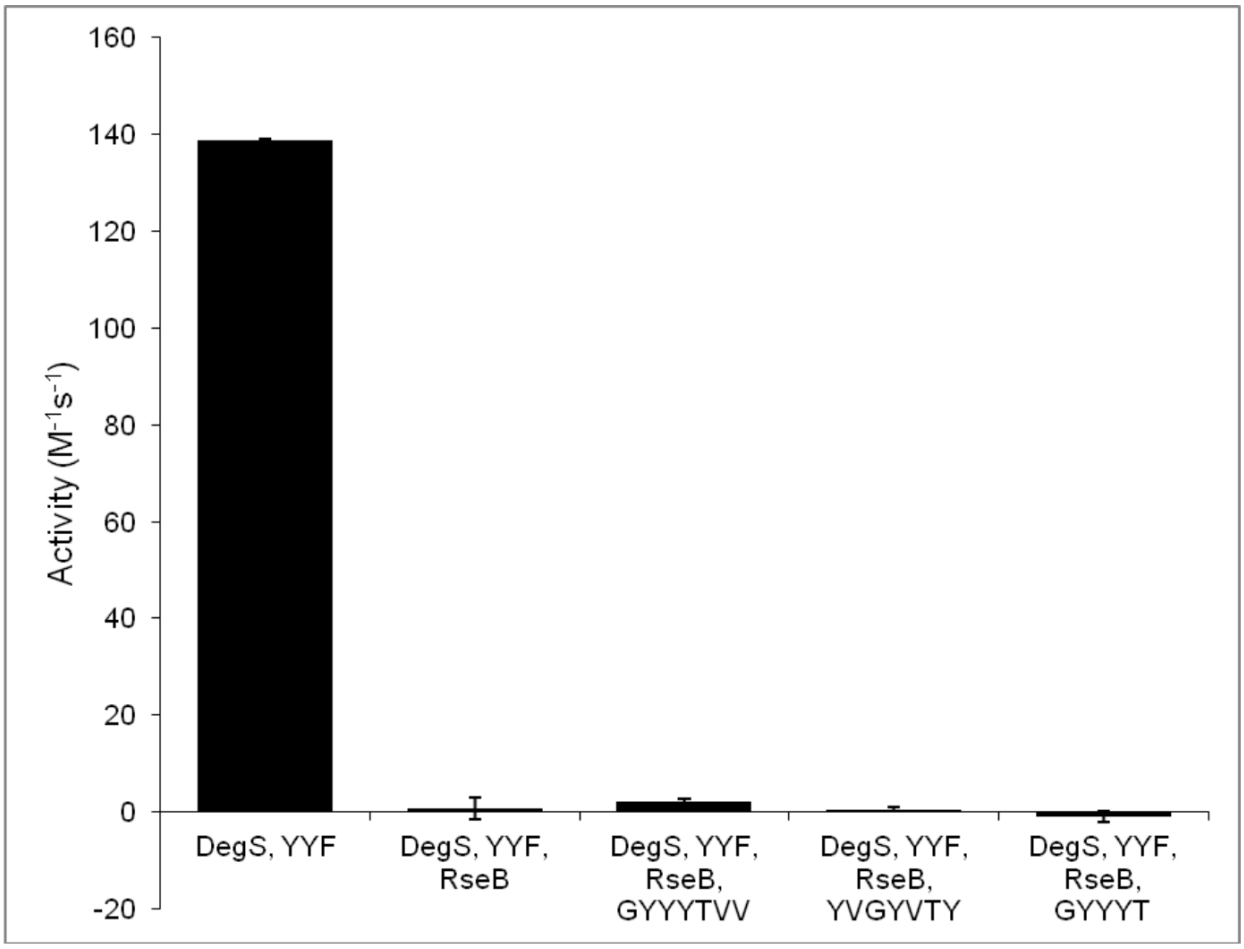

Fig. 4.S2. CupB5 peptides do not relieve RseB inhibition of RseA cleavage by DegS. Rates of cleavage of *E. coli* $RseA^{peri}$ (20 μM) by DegS (0.5 μM trimer) and YYF peptide (20 μM). When present, the concentration of RseB dimer was 25 μM and the concentrations of CupB5 peptides were 480 μM.

Fig. 4.S3. The CupB5 GYYYTVV motif is found in many orthologs in sequenced strains of *P. aeruginosa*. A total of 22 putative *Pseudomonas* orthologs of CupB5 was obtained from www.pseudomonas.com. Homology was compared using the ClustalW algorithm of MacVector software. Shown is a small portion of the CupB5 amino-acid sequence containing the GYYYTVV motif when present. PA: *P. aeruginosa*; Protegens: *P. protegens*; Pdentrifi: *P. dentrificans*; and Psyringae: *P. syringae pv. Phaseolicola*. *P. aeruginosa* PA7 has two copies of *cupB5* in its genome, *P. protegens* CHA0 has four copies, and strain *P. protegens* Pf-5 has two copies.

Table 4.S1. Truncations of CupB5 to identify the signal that activates alginate production.

Strains	C-terminal	Phenotype
HA-*cupB5*(1018)-His -PAO1	-NIWH_6	Mucoid
HA-*cupB5*(1015)-His -PAO1	-DYGH_6	Mucoid
HA-*cupB5*(585aa)-His -PAO1	-GSGH_6	Mucoid
HA-*cupB5*(531aa)-His-PAO1	-GPAH_6	Mucoid
HA-*cupB5*(520aa)-His-PAO1	-SYYH_6	Mucoid
HA-*cupB5*(510aa)-His-PAO1	-YVLH_6	Mucoid
HA-*cupB5*(507aa)-His-PAO1	-DGLH_6	Mucoid
HA-*cupB5*(504aa)-His-PAO1	-KNLH_6	Mucoid
HA-*cupB5*(497aa)-His-PAO1	-AQLH_6	Mucoid
HA-*cupB5*(491aa)-His-PAO1	-TVVH_6	Mucoid
HA-*cupB5*(490aa)-His-PAO1	-YTVH_6	Non-mucoid
HA-*cupB5*(489aa)-His-PAO1	-YYTH_6	Non-mucoid
HA-*cupB5*(488aa)-His-PAO1	-YYYH_6	Non-mucoid
HA-*cupB5*(483aa)-His-PAO1	-YVSH_6	Non-mucoid
HA-*cupB5*(404aa)-His-PAO1	-VNWH_6	Non-mucoid
HA-*cupB5*(353aa)-His-PAO1	-GTWH_6	Non-mucoid
HA-*cupB5*(231aa)-His-PAO1	-LNFH_6	Non-mucoid
HA-*cupB5*(176aa)-His-PAO1	-YRFH_6	Non-mucoid
HA-*cupB5*(144aa)-His-PAO1	-VLFH_6	Non-mucoid
HA-*cupB5*(135aa)-His-PAO1	-QVFH_6	Non-mucoid
HA-*cupB5*(132aa)-His-PAO1	-ANGH_6	Non-mucoid

Table 4.S2. Strains and plasmids used in this study.

Strains and plasmids	Phenotype and genotype	Source or reference
P. aeruginosa strains		
PAO1	Non-mucoid, prototroph	P. Phibbs[a]
PAO1-VE2	PAO1 TA flanked *aacC1* (Gm^R) inserted upstream of *mucE* (PA4033), mucoid	(Qiu et al., 2007)
PAO1-VE22	PAO1 TA flanked *aacC1* (Gm^R) inserted upstream of *cupB5* (PA4082), mucoid	This study
PA14	Non-mucoid, prototroph	F. Ausubel[b]
FRD2	Non-mucoid, derived from *mucA*22 strain FRD1	(Olson and Ohman, 1992)
CF3715	Non-mucoid, clinical strain	D. Speert[c]
CF4009	Non-mucoid, clinical strain	D. Speert[c]
CF2	Non-mucoid, *mucA* mutant, *algU* wild type, derived from clinical mucoid strain	(Yin et al., 2013a)
CF14	Non-mucoid, *mucA* mutant, *algU* mutant, derived from clinical mucoid strain	(Yin et al., 2013b)
CF17	Non-mucoid, *mucA* mutant, *algU* wild type, derived from clinical mucoid strain	(Yin et al., 2013b)
CF4349	Non-mucoid, *mucA* mutant, *algU* wild type, derived from clinical mucoid strain	(Yin et al., 2013b)
PAO1Δ*algW*	PAO1 *algW*::tet^R, nonmucoid	(Qiu et al., 2007)
PAO1Δ*mucP*	PAO1 *mucP*::tet^R, nonmucoid	(Qiu et al., 2007)
PAO1Δ*clpX*	PAO1 *clpX* ::Gm^R	(Qiu et al., 2008b)
PAO1Δ*clpP*	PAO1 *clpP* ::Gm^R	(Qiu et al., 2008b)
PAO1Δ*algU*	PAO1 with in-frame deletion of *algU*	(Qiu et al., 2007)
PAO1Δ*algD*	PAO1 with in-frame deletion of *algD*	This study
E. coli strains		
TOP10	DH5α derivative	Invitrogen
SM10/ l pir	*thi thr leu tonA lacY supE recA* :: RP4-2-Tc :: Mu lpirR6K Km^R	Laboratory strain
Plasmids		
pFAC	Mini-himarI mariner transposon with a selectable marker Gm^R Ap^R	(Wong and Mekalanos, 2000)
pRK2013	Km^R *Tra Mob ColE1*	(Figurski and Helinski, 1979)
pHERD 20T	pUCP20T P_{lac} replaced by fragment of *araC*–P_{BAD} cassette	(Qiu et al., 2008a)
pLP170	8.3-kb, lacZ, ApR\ multiple cloning site	Passador Lab[d]
PHERD 20T-HA-*cupB5*-His	*cupB5* (PA4082) from PAO1 in pHERD20T EcoRI/HindIII	This study

PHERD 20T- HA-*cupB5*(1015aa) -His	*cupB5* (PA4082) from PAO1 in pHERD20T EcoRI/HindIII	This study
PHERD 20T-HA-*cupB5* (585 aa) -His	*cupB5* (PA4082) from PAO1 in pHERD20T EcoRI/HindIII	This study
PHERD 20T-HA-*cupB5* (531 aa) aa)-His	*cupB5* (PA4082) from PAO1 in pHERD20T EcoRI/HindIII	This study
PHERD 20T-HA-*cupB5* (520 aa)-His	*cupB5* (PA4082) from PAO1 in pHERD20T EcoRI/HindIII	This study
PHERD 20T-HA-*cupB5* (510 aa)-His	*cupB5* (PA4082) from PAO1 in pHERD20T EcoRI/HindIII	This study
PHERD 20T-HA-*cupB5* (507 aa)-His	*cupB5* (PA4082) from PAO1 in pHERD20T EcoRI/HindIII	This study
PHERD 20T-HA-*cupB5* (504 aa)-His	*cupB5* (PA4082) from PAO1 in pHERD20T EcoRI/HindIII	This study
PHERD 20T-HA-*cupB5* (497 aa)-His	*cupB5* (PA4082) from PAO1 in pHERD20T EcoRI/HindIII	This study
PHERD 20T-HA-*cupB5* (491 aa)-His	*cupB5* (PA4082) from PAO1 in pHERD20T EcoRI/HindIII	This study
PHERD 20T-HA-*cupB5* (490 aa)-His	*cupB5* (PA4082) from PAO1 in pHERD20T EcoRI/HindIII	This study
PHERD 20T-HA-*cupB5* (489 aa)-His	*cupB5* (PA4082) from PAO1 in pHERD20T EcoRI/HindIII	This study
PHERD 20T-HA-*cupB5* (488 aa)-His	*cupB5* (PA4082) from PAO1 in pHERD20T EcoRI/HindIII	This study
PHERD 20T-HA-*cupB5* (483 aa)-His	*cupB5* (PA4082) from PAO1 in pHERD20T EcoRI/HindIII	This study
PHERD 20T-HA-*cupB5* (404 aa)-His	*cupB5* (PA4082) from PAO1 in pHERD20T EcoRI/HindIII	This study
PHERD 20T-HA-*cupB5* (353 aa)-His	*cupB5* (PA4082) from PAO1 in pHERD20T EcoRI/HindIII	This study
PHERD 20T-HA-*cupB5* (231 aa)-His	*cupB5* (PA4082) from PAO1 in pHERD20T EcoRI/HindIII	This study
PHERD 20T-HA-*cupB5* (176 aa)-His	*cupB5* (PA4082) from PAO1 in pHERD20T EcoRI/HindIII	This study
PHERD 20T-HA-*cupB5* (144 aa)-His	*cupB5* (PA4082) from PAO1 in pHERD20T EcoRI/HindIII	This study
PHERD 20T-HA-*cupB5* (135 aa)-His	*cupB5* (PA4082) from PAO1 in pHERD20T EcoRI/HindIII	This study
PHERD 20T-HA-*cupB5* (132 aa)-His	*cupB5* (PA4082) from PAO1 in pHERD20T EcoRI/HindIII	This study
pEX100-Δ*algW*	A 1.4-kb *algW*-flanked fragment with in-frame deletion of *algW* in pEX100 NotI	(Qiu et al., 2007)
pLP170-P_{algW}	Promoter of *algW* (PA4446) from PAO1 in pLP170 EcoRI/HindIII	(T. Ryan Withers et al., 2013)
pLP170-P_{algU}	Promoter of *algU* (PA0762) from PAO1 in pLP170 EcoRI/HindIII	(T. Ryan Withers et al., 2013)
pLP170-P_{algD}	Promoter of *algD* (PA3540) from PAO1 in pLP170 EcoRI/HindIII	(T. Ryan Withers et al., 2013)

[a], East Carolina University, USA; [b], Harvard Medical School, USA; [c], University of British Columbia, CA; [d]University of Rochester, USA.

Supplementary References

Figurski D.H., Helinski D.R. (1979). Replication of an origin-containing derivative of plasmid RK2 dependent on a plasmid function provided in trans. *Proc Natl Acad Sci U S A* 76: 1648-1652.

Olson J.C., Ohman D.E. (1992). Efficient production and processing of elastase and LasA by *Pseudomonas aeruginosa* require zinc and calcium ions. *J Bacteriol* 174: 4140-4147.

Qiu D., Damron F.H., Mima T., Schweizer H.P., Yu H.D. (2008a). PBAD-based shuttle vectors for functional analysis of toxic and highly regulated genes in *Pseudomonas* and *Burkholderia spp*. and other bacteria. *Appl Environ Microbiol* 74: 7422-7426.

Qiu D., Eisinger V.M., Head N.E., Pier G.B., Yu H.D. (2008b). ClpXP proteases positively regulate alginate overexpression and mucoid conversion in *Pseudomonas aeruginosa*. *Microbiology* 154: 2119-2130.

Qiu D., Eisinger V.M., Rowen D.W., Yu H.D. (2007). Regulated proteolysis controls mucoid conversion in *Pseudomonas aeruginosa*. *Proc Natl Acad Sci U S A* 104: 8107-8112.

Withers T.R., Damron F.H., Yin Y., Yu H.D. (2013). Truncation of type IV pilin induces mucoidy in *Pseudomonas aeruginosa* strain PAO579. *Microbiology Open* (accepted).

Wong S.M., Mekalanos J.J. (2000). Genetic footprinting with mariner-based transposition in *Pseudomonas aeruginosa*. *Proc Natl Acad Sci U S A* 97: 10191-10196.

Chapter 5

Conclusions, perspectives and future directions

Conclusions and persepctives

DegS is an important *E. coli* protease both for the outer-membrane stress response and for furthering our understanding of protein allostery. The two-state allosteric model is simple, stating only that the allosteric equilibrium between inactive and active DegS is controlled by the preferential binding of OMP peptide and substrate RseA to the active form. Yet the model is extremely powerful and has been employed to successfully explain a wide variety of experimental results and make important predictions for future experiments. In this thesis, I have sought to improve our understanding of the molecular basis for DegS allostery.

Before this work was presented, it had been established that a funcational oxyanion hole is necessary for a catalytically functional DegS and that OMP peptide binding relieves autoinhibitory interactions that stabilize the inactive form of the enzyme. It was unclear, however, how OMP-peptide binding breaks these inhibitory interactions and how that activation signal is propagated across the enzyme to the active site. Here, I completed this story and provided a complete mechanism of how OMP-peptide binding activates DegS (Fig. 5.1). I gave evidence that OMP-peptide binding induces a series of steric clashes that results in the rearrnagement of the L3 loop, thereby breaking inhibitory interactions. The rearranged L3 loop positions Arg^{178} to make contacts with the neighboring protease domain at the subunit interface. This residue and other residues in the conserved activation cluster form a network of hydrogen-bonding, salt-bridge and hydrophobic interactions that stabilize the active conformation of the enzyme and help facilitate intersubunit communication. This network of residues stretches from Arg^{178} on the L3 loop to the active-site loop forming the oxyanion hole. Thus, the activation

signal is propagated from OMP binding through the steric clashes and the activation cluster rearrangement to the stabilization of the oxyanion hole and a catalytically functional enzyme.

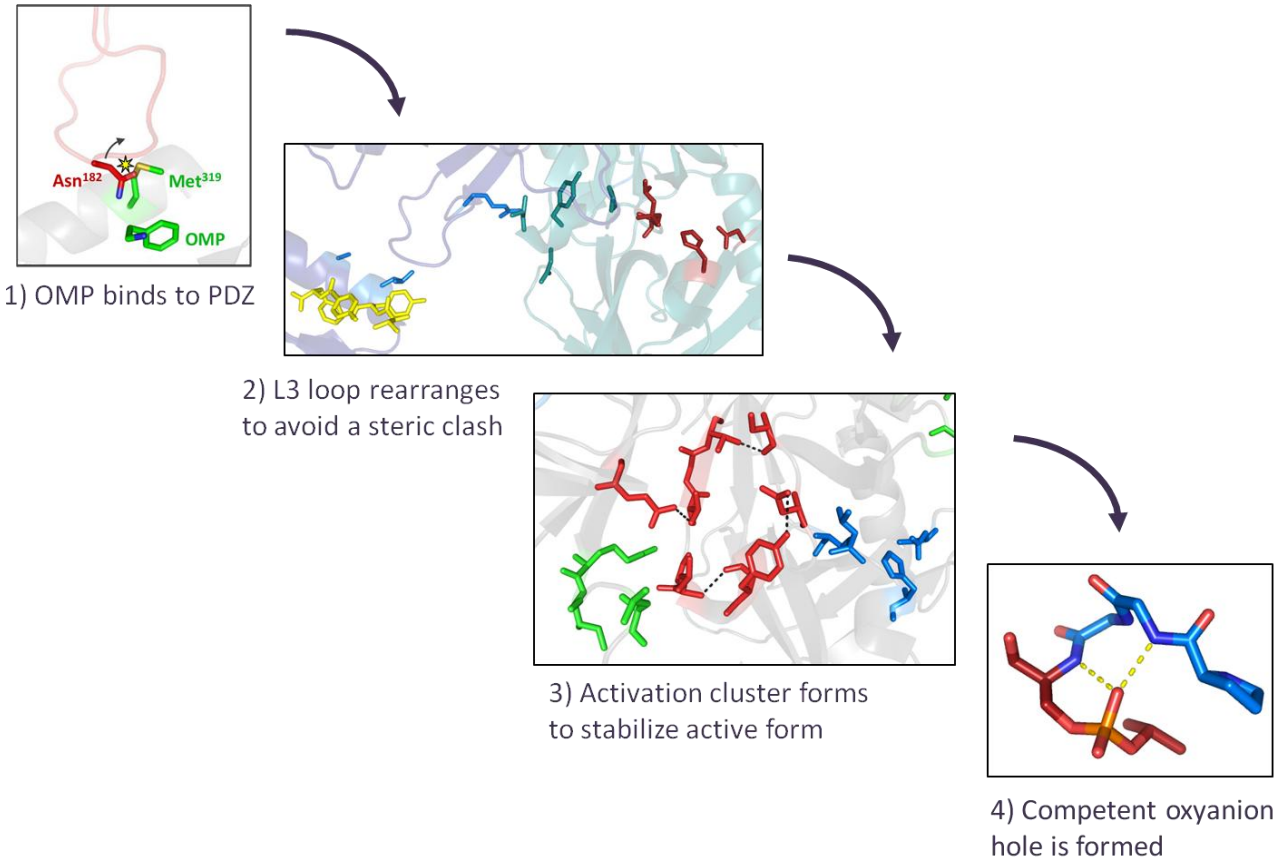

Fig. 5.1. Activation of DegS by OMP peptide. OMP peptide binds to the PDZ domain of DegS and induces a series of steric clashes between Met^{319} on the PDZ domain and Asn^{182} on the L3 loop of the protease domain, forcing the L3 loop to rearrnage. This positions Arg^{178} on the L3 loop to contact the neighboring protease domain, allowing activation cluster residues to rearrange and form a network of stabilizing interactions that stretches to the active-site loop and a functional oxyanion hole.

Future directions and unsuccessful experiments

With the work presented here, we now know how activated DegS is stabilized and how OMP-peptide binding leads to this state. A next step in understanding DegS allosteric control is to elucidate the mechanism of protease activation by RseA. Where does RseA bind on DegS? Which sequence determinants are important for this interaction? Are there structural changes that RseA binding induces in DegS? Are they the same changes that result from OMP binding, as we think, or is the two-state model too simple? We can find some clues by looking at crystal structures of homologous HtrA proteases bound to substrates, which suggest that substrates directly interact with the activation cluster to stabilize the active form (see Chapter 2), but there is little information available on RseA and DegS themselves. I spent considerable effort in pursuit of answers to these questions; unfortunately, I was mostly unsuccessful. The experiments outlined below describe my approaches.

Perhaps the simplest question is where DegS and RseA interact. It is clear that the cleavage site of RseA must contact the active site of DegS. But a decapeptide corresponding to the cleavage-site sequence of RseA is cleaved by DegS 500-fold more slowly than full-length $RseA^{peri}$ (unpublished data), suggesting that there must be exosites somewhere else on RseA that contribute to binding and/or catalysis. The most conceptually simple way to answer this question would be to co-crystallize DegS and RseA, but previous attempts to do so had failed. I hypothesized that this might be due to the flexible RseA protein (Walsh *et al.*, 2003) being unable to organize into a packed crystal or because there was not a tight-enough complex being formed, or both.

To create a less-flexible RseA and also to investigate the location of exosites, I created a minimal RseA peptide (RAMP) that bound to DegS via anisotropy with the same affinity as wild type RseA. To do this, I used conservation information and mutagenesis to design truncated RseA variants and tested which ones effectively competed with wild type RseA for degradation by DegS. I found that 15 residues could be truncated from the N-terminus of RseA and 31 from the C-terminus without significantly affecting binding. I attempted to co-crystallize DegS H198P/D320A/S201A (HPDASA), OMP peptide, and RAMP. I successfully grew crystals, but when I collected diffraction data and solved the structure, no substrate density was found.

It would not be surprising if a tight complex between DegS and RseA (or RAMP) was not being formed, as the binding affinity of these two partners for each other is quite low. Even in the presence of saturating YYF peptide, the K_M for RseA degradation by wild type DegS is 370 μM (Sohn and Sauer, 2009). I developed an anisotropy binding assay by attaching a fluorophore to $RseA^{peri}$ and binding to wild-type DegS was detected but could not be saturated at the solubility limits of the assay. Fl-$RseA^{peri}$ binding to HPDASA, which is almost 100% in the active conformation but lacks a catalytic serine, had a K_D of ~100 μM.

I embarked on a series of experiments designed to create a tighter complex of DegS and RAMP. I created a genetic fusion of DegS H198P/S201A (HPSA) and RAMP with a linker that would allow RAMP to reach the DegS active site and saw that OMP peptide bound tighter to this fusion protein than to HPSA alone. This fusion did not crystallize. I stapled the two proteins together by introducing cysteines at the P1 position of RAMP and the catalytic site of DegS (or $DegS^{\Delta PDZ}$) and creating a disulfide bond. The complex formed but did not crystallize. I combined these

tactics and created a version of the genetic fusion with the engineered cysteines and made a complex that was covalently connected both at the proteins' termini and at the DegS active site. These properly-formed complexes were difficult to purify away from variants that made incorrect disulfide bonds, but by cleaving the linker between DegS and RAMP, I was able to isolate DegS trimers that had, on average, one or two RAMP molecules disulfide-bonded to the active site(s). They did not crystallize.

Moving away from crystallography, I sought to use hydroxy-radical footprinting to identify sites of RseA interaction on DegS (protocol: Loizos, 2004). For this experiment, I used hydroxy-radicals to perform limited proteolysis on DegS S201A by itself and with RseA present. I first labeled either the N-terminus or the C-terminus of DegS with a fluorophore and then electrophoresed the cleavage reactions on an SDS gel and visualized the cleavage pattern with a fluorescence-sensitive imager (Fig. 5.2A). For each band, I evaluated the differences in intensity between the two cleavage conditions. I then mapped each band to a specific part of the DegS sequence by comparing the relative mobilities of each band to standards generated by cleaving DegS with CNBr, which cleaves after methionine residues, to map each band to a section of the DegS sequence. The bands were then divided into categories based on the observed degree of difference between cleavage in the presence of RseA and cleavage in its absence. For both the N-terminal label and C-terminal label, there was an area on the PDZ domain around the L6 loop that was cleaved less when RseA was present and there was an area on the protease domain near residue 110 that was cleaved to a greater extent when RseA was present (Fig. 5.2B). These regions are both potential candidates for contacting RseA exosites but the resolution of this experiment is too low to be conclusive on its own.

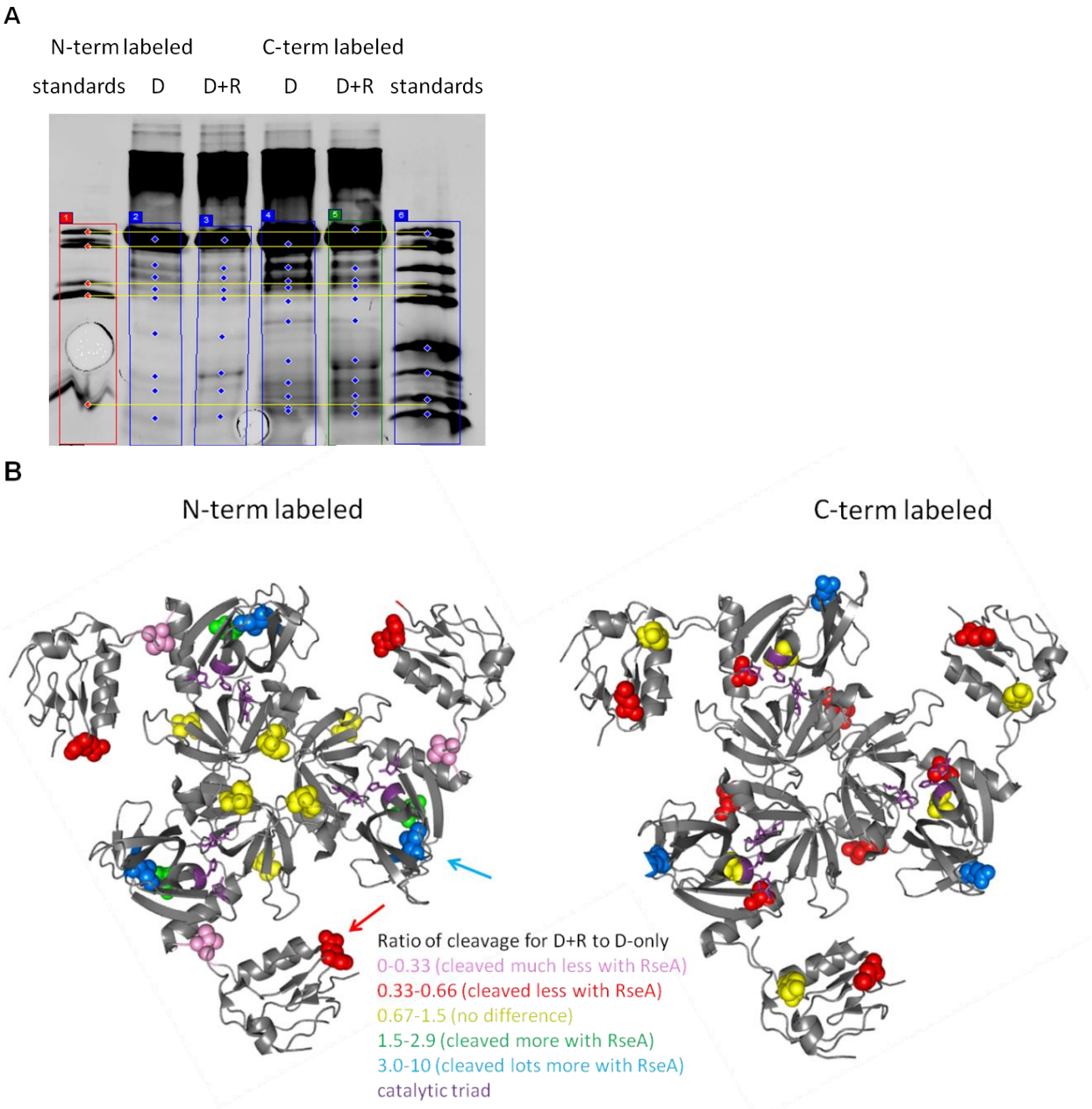

Fig. 5.2. Hydroxyl-radical cleavage of DegS. (A) DegS H198P/D320A/S201A/S33C ("N-term labeled") or H198P/D320A/S201A/T354C ("C-term labeled") was reacted with Oregon Green-maleimide and then the resulting labeled DegS (83 µM) was incubated with YYF (100 µM), either buffer or RseA (100 µM), ammonium iron (II) sulate (1 mM), EDTA (2 mM), sodium ascorbate (20 mM), hydrogen peroxide (1 mM), and regular DegS reaction buffer. For preparation of standards, DegS (83 µM) was incubated for 20 minutes at room temperature with cyanogen bromide (400 mM), sodium dodecyl sulfate (0.4%) and HCl (to pH 2) and then lyophilized and resuspended in DegS reaction buffer. All proteins were run on a 12% SDS-PAGE gel and visualized using a Typhoon imager. (B) Bands from the above gel were quantified using ImageQuant (GE Healthcare) and standard lanes used to assign DegS location for each band. Band locations were visualized using PyMol and colored according to the degree of difference between the DegS-and-RseA experiment and DegS-only experiment. Arrows indicate overlaps between the N-terminally labeled and C-terminally labeled trials.

I also sought to design a conformation-sensing assay that fluorescently reports whether DegS is inactive or active. I would have used this to monitor the effects of OMP-peptide binding and RseA binding on conformation and also examine kinetics of the allosteric switch. Different fluorophores were attatched to an engineered cysteine residue at position 179 on the L3 loop. In one variation of the assay, the fluorphore was selected to be environmentally sensitive. In another version, engineered histidines chelated a metal ion on a neighboring protease-domain alpha helix, which should quench the L3 loop-bound fluorophore only in the inactive conformation (Taraska *et al*, 2009). In both cases, the assay appeared to report somewhat on the conformation but also reacted directly to peptide binding to the nearby PDZ domain. Because of the similarity between the tertiary structure of the inactive and active forms of DegS, no additional candidates for fluophore location were apparent.

Further experimentation will be necessary to definitively establish how RseA contacts and activates DegS. It will be interesting to draw parallels and identify differences between the mechanisms of activation by RseA and OMP peptide.

References

Loizos N. (2004). Identifying protein interactions by hydroxyl-radical protein footprinting. Curr Protoc Protein Sci Chapter 19, Unit 19.9.

Sohn J, Sauer RT. (2009). OMP peptides modulate the activity of DegS protease by differential binding to active and inactive conformations. Mol Cell *33*, 64-74.

Taraska JW, Puljung MC, Olivier NB, Flynn GE, Zagotta WN. (2009). Mapping the structure and conformational movements of proteins with transition metal ion FRET. Nat Methods *6*, 532-7.

Walsh NP, Alba BM, Bose B, Gross CA, Sauer RT. (2003). OMP peptide signals initiate the envelope-stress response by activating DegS protease via relief of inhibition mediated by its PDZ domain. Cell *113*, 61-71.